RECIPROCITY AND ITS APPLICATION TO THE OBLIQUE REFLECTION OF ELECTROMAGNETIC WAVES FROM THE IONOSPHERE

A THESIS

Presented to

The Faculty of the Graduate Division

by

Thomas Dewey Shockley, Jr.

In Partial Fulfillment

of the Requirements for the Degree

Doctor of Philosophy

in the School of Electrical Engineering

Georgia Institute of Technology

June, 1963

In presenting the dissertation as a partial fulfillment of the requirements for an advanced degree from the Georgia Institute of Technology, I agree that the Library of the Institution shall make it available for inspection and circulation in accordance with its regulations governing materials of this type. I agree that permission to copy from, or to publish from, this dissertation may be granted by the professor under whose direction it was written, or, in his absence, by the dean of the Graduate Division when such copying or publication is solely for scholarly purposes and does not involve potential financial gain. It is understood that any copying from, or publication of, this dissertation which involves potential financial gain will not be allowed without written permission.

_____

_____

78
122

RECIPROCITY AND ITS APPLICATION TO THE OBLIQUE REFLECTION OF ELECTROMAGNETIC WAVES FROM THE IONOSPHERE

Approved:

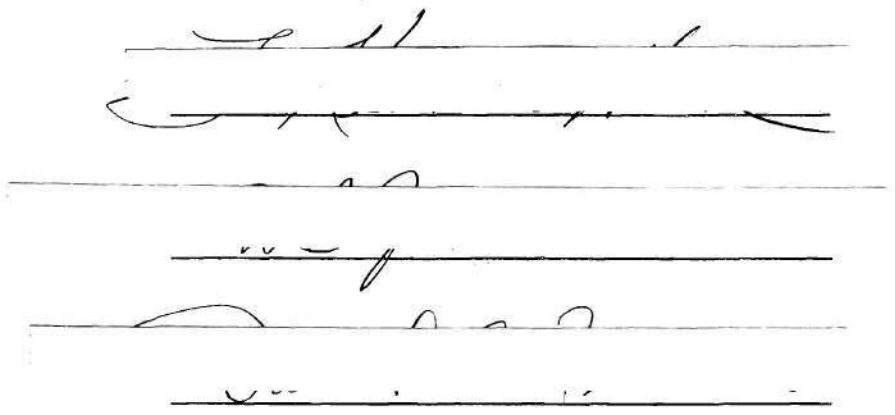

Date Approved by Chairman: May 10, 1963

ACKNOWLEDGMENTS

The author wishes to thank his thesis advisor, Dr. F. K. Hurd, for his advice, support and encouragement throughout the course of the present study. He also wishes to thank the members of his reading committee, Drs. D. C. Fielder and W. B. Jones, for their suggestions in the preparation of the final form of the manuscript. Also gratefully acknowledged is the assistance given by the Rich Electronic Computer Center in providing computing facilities for the computations involved in the study.

TABLE OF CONTENTS

LIST OF TABLES

LIST OF ILLUSTRATIONS

SUMMARY

One of the important aspects of ionospheric propagation arising in communications studies is the question of the reciprocity of signal transmission in opposite directions over a common communication link. In general existing reciprocity theorems are invalid when applied to wave propagation in the ionosphere because the tensors describing the permittivity and conductivity of the ionosphere are asymmetrical.

In this study, reciprocity is defined in a manner such that the antenna polarization characteristics are included in the ionospheric effects. Reciprocity defined in this manner is called "relative reciprocity" as contrasted to complete reciprocity. Thus complete reciprocity pertains to the propagation of electromagnetic fields between two points. Relative reciprocity pertains to the transmission and reception of electromagnetic waves between two fixed antenna systems and includes the effects of the antenna systems. Obviously, although complete reciprocity is of theoretical interest, relative reciprocity (or non-reciprocity) is the phenomena which is of practical interest and is the phenomena which is capable of experimental investigation.

Relative reciprocity, based on the inclusion of the antenna characteristics with ionospheric effects, is defined in terms of the amplitudes of the signals appearing at the output terminals of the receiving antennas through a mathematical extension of Goubau's reciprocal antenna theorem. The theorem may be stated as

> Let T_1 and T_2 be two antennas, which individually have the same field patterns when used for either the transmission or the reception of electromagnetic waves and which are located at the points S_1 and S_2 respectively. Electromagnetic waves of the same frequency are transmitted simultaneously from both S_1 and S_2 and then received at both S_1 and S_2 after oblique reflection from the ionosphere. Relative reciprocity is said to exist for the two-way transmission link during any period of time in which the magnitudes of the received signals U_1 and U_2 appearing at the output terminals of the receiving antennas T_1 and T_2 may be linearly related by a fixed constant b such that $U_1 = bU_2$, $b > 0$. For periods during which non-reciprocity exists, b will be a variable.

The specifications of an experimental test to provide adequate data for correlation with the theoretical aspects of relative reciprocity are formulated. Included in the test specifications are the selections of major equipments such as the transmitting and receiving equipment, antennas and data recording equipment. A detailed outline of a technique, based on a master and slave clock system, to provide the synchronization of two-way transmission is included in the test outline. Data reduction and interpretation techniques, which are applicable to relative reciprocity, are discussed in both a theoretical and a practical sense. In order to provide a method of cataloging and comparing relative reciprocity data, a time weighing function T_W which indicates the decimal portion of the test periods during which relative reciprocity exists is defined.

Although no experimental tests were performed during the present study, some experimental data was available to the author for reduction in terms of the relative reciprocity theorem. The computations and results of the data reduction clearly demonstrate the practical value and the versatility of the relative reciprocity theorem even though the experimental data involved was obtained under less than optimum conditions.

During the process of reducing and interpreting the experimental data, a question arose concerning factors which contributed to or possibly caused the periods of non-reciprocal transmission observed in the data. In order to provide in some measure answers to this question the magneto-ionic wave equations (Booker's equations) were programmed for solution on a digital computer for the conditions existing over the Fairburn-Ipswich experimental transmission link.

On the basis of these computations, the effects of the lateral deviation of the wave packets during their stay in the ionosphere were related to the periods of non-reciprocal transmission. These effects are discussed in terms of variations in the composition of the E layer of the ionosphere as well as in terms of the tilt of the lower boundary of the ionosphere.

The following conclusions evolved from this study.

1. The mathematical validity and practical applicability of the relative reciprocity theorem was established.

2. Test procedures were formulated which define one optimum technique for obtaining valid experimental relative reciprocity data.

3. Non-reciprocal effects of the lateral deviation of wave packets transmitted over an experimental two-way propagation link (Fairburn-Ipswich link) were established for the one-hop E-region mode of propagation.

CHAPTER I

INTRODUCTION

During the past fifty years many theoretical discussions concerning the reflection of electromagnetic waves from the ionosphere have appeared in the literature. In 1912 Eccles (1)* made the first attempt to formulate mathematically the suggestions proposed independently by Kennelly and Heaviside concerning beyond the horizon propagation of radio waves. Larmor (2) continued this theoretical attack on the problem and in 1924 published a paper in which he characterized the ionosphere in the light of a dielectric medium in which the incident electromagnetic waves could be returned to the earth by a process of gradual refraction. A number of papers were published in 1925 and 1926, but most of the results were left in the form of unsolved equations for either the refractive index or the absorption coefficient. In 1927, however, both Lassen and Appleton independently published accounts of the general case of ionospheric propagation and reflection which included the possibility of collisions between the free electrons and heavy particles. Appleton (3) published his theory in full in 1932 and his expression for the complex refractive index has been more widely utilized than any of the other published forms. Many papers appeared in the next two decades. Mitra's (4) book, The Upper Atmosphere, presents an excellent account of the theoretical progress up to 1950. The period between 1950

---

*Numbers refer to bibliography.

and 1960 is covered by Budden's (5) book, Radio Waves in the Ionosphere.

A large part of the early ionospheric work was theoretical in nature due to limitations in experimental equipments. With the advent of World War II, the communication link between English and German scientist, who were the major contributors to both theoretical and experimental ionospheric work, was cut. Although the war temporarily deterred the overall program, it provided an impetus to all phases of the work which began after the war. New developments in the fields of radar, electronic computers, and rocket vehicles extended the capabilities of both the theoretical and the experimental phases of the work which now began with renewed vigor.

The utilization of high speed digital computers provided a means of approximating solutions to the complex set of equations governing wave propagation in the ionosphere. Rocket vehicles were used to probe the ionosphere to provide valuable data to substantiate or to disprove existing theories concerning the composition of the ionosphere. Radar equipments were adapted so that the theoretical predictions concerning wave propagation in the ionosphere could be checked experimentally. A large part of the work performed in the late 1940's and early 1950's was oriented in a direction designed to establish the composition of the ionosphere, to determine the variation in the composition in a diurnal, monthly, seasonal, and yearly manner. The results of such investigations provided information on the maximum usuable frequencies for various transmission distances on a diurnal and seasonal basis. In recent years the National Bureau of Standards has been one of the major contributors to such studies. One of the important aspects of ionospheric propagation

arising in communications studies of this nature is the question of the reciprocity of transmission in opposite directions over a common communication link. This particular problem forms the basis for the investigations discussed in the following sections of the present study. A review of the literature revealed that there had apparently been little correlation between the theoretical attack on the solution of the reciprocity problem and subsequent experimental tests involving reciprocal transmission. For this reason the objectives of the present study are to define reciprocity in a sense which is applicable to the case of oblique reflections of electromagnetic waves from the ionosphere in such a manner that the definition may be correlated with the results of an experimental test and to specify the requirements of an experimental test which could be utilized to obtain reciprocity data for correlation purposes. Although no actual experimental tests were performed during the period covered by the present study, some available reciprocity test data was analyzed in light of the relative reciprocity theorem and the test procedures presented in the present study.

In order to present the theoretical background necessary to facilitate an understanding of the techniques involved in the present study, a brief summary of the factors governing the composition of the ionosphere and the wave equations governing ionospheric propagation are presented in the two succeeding chapters.

CHAPTER II

COMPOSITION OF THE IONOSPHERE

One of the most important effects of solar radiation on the upper atmosphere is the ionization of its constituent gases. This ionization becomes noticeable at a height of about 60 kilometers above the surface of the earth and extends upward to the highest limits of the atmosphere. The density of ionization is not uniform; there exists various "layers" or "regions" of maximum ionization. In general only very shallow troughs exist between the ionization peaks of the various regions. These ionized regions, known collectively as the "ionosphere," play a fundamental role in the long range propagation of electromagnetic waves above the earth's surface.

The lowest of these regions, the D-region, exists from an approximate height of 60 to 90 kilometers. An understanding of the undisturbed D-region requires a knowledge of the atmospheric constituents including minor constituents resulting from photochemical reactions of considerable complexity which are not completely understood. Several D-region models have been proposed on the basis of radio data, but none have satisfactorily explained this region. The D-region is primarily an absorbing region and will produce total reflections of electromagnetic waves only at frequencies below approximately 350 kilocycles per second.

Some D-region experimental work has been performed in the frequency range from 1 to 5 megacycles per second with high power and high resolution radar equipment. Under these conditions very weak partial

reflections of electromagnetic waves have been observed at an approximate height of 75 kilometers in the daytime and 90 kilometers at night. Gregory (6) contends that there is a direct connection between the decrease of the E-region reflection strength and the increase in the partial reflection strength in the region between 66 and 85 kilometers on winter days during which high D-region absorption characteristics are observed. This conclusion is based on the results of experimental work performed at a frequency of 1.75 megacycles per second. In view of the uncertainty of the interpretation of the experimental data, no general theory concerning the formation of this region has received acceptance.

A second type of ionized region, sporadic in nature, appears at a level of approximately 100 kilometers. This region is characterized by its random time of occurrence, an apparent partial transparency, an apparent reflection height that is seemingly independent of frequency, and a variation in penetration frequency with transmitter output power. This region is called the Sporadic E-region or E_s. The origin of the E_s-region is as yet uncertain, but extensive examinations have been made into the association between the various characteristics of E_s and meteoric activity, aurora and airglow, magnetic effects, lunar activity and lunar and solar tidal effects. Thomas and Smith (7) present an excellent review of the present knowledge of the sporadic E_s-region.

In the middle ionosphere from a height of about 100 to 125 kilometers, the ionization peak of the E-region occurs. Appleton (8) gives the approximate ionization peak height as 125 kilometers when the sun is vertical in the sky. The chief characteristic of the E-region is the regularity of its formation and behavior. It is generally assumed that

the ionizing radiation producing the normal E-region is electromagnetic in character and solar in origin. Radio soundings during solar eclipses have indicated that the majority of the radiation comes from the sun's visible disk, but that additional radiation may also come from active localized spots and possibly from the corona. Rocket soundings have demonstrated that the ionizing agency for the E-region consists of soft X-rays. Similar experiments have also provided values for the effective recombination coefficient, ψ. The experimentally determined values of ψ are in disagreement with the values predicted by quantum theory for the radiative recombination process. It is possible however that reconciliation of experiment and theory may be effected by invoking the possibility of dissociative recombination as suggested by Bates and Massey (9). Long term studies have also shown a direct connection between the electron density N for the E-region and solar activity. Appleton (8) shows this condition by a plot of the square of the critical penetration frequency f_E versus the Zurich sunspot number R.

The F-region (10) may be defined as that part of the ionosphere which lies above a height of about 150 kilometers. Ionosonde records and rocket soundings (11) have shown that there are two ionization peaks in the F-region during the daylight hours, which tend to merge into a single region during the night. The lower of these two ionized regions has been designated as the F_1-region and has an ionization peak at a height of approximately 160 kilometers at noon. The upper of these regions, the F_2-region, has an ionization peak which averages around a height of about 250 kilometers by day. Although there appears to be reason to believe, at least for sunspot minimum conditions, that both the F_1 and

F_2-regions are formed by the same solar ionizing radiation, the morphology of the two regions are different.

The F_1-region electron density profile may be approximated by a "Chapman region" (see Appendix). Although below the level of peak ionization, the F_1-region behaves substantially as a Chapman region, small deviations are found when months and years of ionosonde measurements are examined statistically. Martyn (12) has shown that these perturbations are due to local electric currents in association with solar and lunar magnetic variations.

Unfortunately, the morphology of the F_2-region is much more complex and a simple Chapman region cannot be used to describe its structure. In addition this region is subject to many anomalies and is perturbed by tidal influences, both solar and lunar, as well as by the conditions associated with magnetic storms. Some of these perturbations and anomalies arise from the electrodynamical forces associated with the flow of electric currents in the ionosphere.

The F_2-region is unsymmetrical about the geographic equator, but has symmetrical characteristics about the geomagnetic equator, which in itself is an anomaly. A second departure from the Chapman region is that there is a trough in the penetration frequency f_{F_2} at or near the magnetic equator. In moderate to high latitudes there is a gross seasonal anomaly in that winter daytime values of f_{F_2} are not smaller than the corresponding summer values. In moderate latitudes at sunspot maximum, the noon winter values are greater than the summer ones.

Variations of the height h_m of maximum electron density N_m in the F_2-region are not fully known. At moderate to high latitudes, the noon

value of h_m is about 220 kilometers at the equinoxes at sunspot minimum on magnetically quiet days. Under the same conditions in winter, h_m is about 10 kilometers lower and in summer about 20 kilometers higher. The corresponding midnight value of h_m is about 320 kilometers with no clear seasonal variation yet established. Variations in the noon values of h_m versus latitude are not yet established, but it has been established that the F_2-region at the magnetic equator is higher than at the lower latitudes.

Ionogram traces of F-region reflections occasionally become broad and diffuse near the critical penetration frequencies which indicates that the region is not uniformly stratified, but contains embedded irregularities such as clouds or columns of varying electron density. This phenomena is closely associated with geomagnetic activity; however, there appears to be a minimum of Spread F at all times at medium geomagnetic latitudes.

CHAPTER III

SUMMARY OF THE MAGNETO-IONIC EQUATIONS

The general problem of the propagation of electromagnetic waves in the ionosphere is best introduced by an examination of the derivation of the wave equations. Prior to any mathematical derivation, it should be noted that it is exceedingly difficult to state explicit results for the general case of propagation. The complexity of the general problem is apparent in view of the fact that as the wave propagates through the ionosphere, the electron density, the electron collisions with neutral particles, the earth's magnetic field and the wave angle of incidence vary along the path of propagation. In addition the presence of the earth's magnetic field in general causes the original wave to split into two components (an ordinary wave and an extra-ordinary wave) which have polarizations that are different from each other and from the original wave prior to its penetration into the ionosphere.

In the following summary of the magneto-ionic wave equations, the material presented is a supplemented summation of material from unpublished notes, "Massachusetts Institute of Technology Summer Program on Plasma Dynamics," presented in 1959 at the Massachusetts Institute of Technology by W. P. Allis and S. Buchsbaum (13). Most of this material can be derived from the general form of the Appleton-Hartree equations. The remainder of the material is taken from the Russian literature (14).

The ray approximation equations, as derived by Booker are also included because they are utilized in the discussion concerning the effect

of the lateral deviation of a wave packet from its transmission path upon periods of non-reciprocal ionospheric propagation. Since the theoretical derivation of these equations is discussed extensively in the literature (15) and (16), the results are presented with a minimum of discussion.

Wave Equations

The fundamental equations governing the propagation of electromagnetic waves in the ionosphere are Maxwell's equations coupled with the equations of motion of the free charges existing in the ionosphere. In the following derivation of the wave equations, the following assumptions are utilized.

1. The ionosphere is stratified in layers of varying electron density.

2. Free electrons, heavy positive ions and neutral molecules are distributed with statistical uniformity so that there is no resultant space charge and the only particles experiencing motion are the electrons.

3. The permeability of the ionosphere is equal to that of free space.

4. The effect of the magnetic field of the electromagnetic waves on the motion of free electrons may be neglected in comparison with the uniform magnetic field $\underline{B}_o$ of the earth.

5. The theorem of linear superposition is applicable.

6. All time variations are assumed sinusoidal steady state.

For the conditions stated above, the following equations may be written.

$$(j\omega + \nu)m\underline{v} = e\underline{E} + e(\underline{v} \times \underline{B}_o) \tag{1}$$

$$\nabla \times \underline{H} = \overline{\sigma} \cdot \underline{E} + j\omega \overline{\epsilon} \cdot \underline{E} \tag{2}$$

$$\nabla \times \underline{E} = -j\omega\mu_o \underline{H} \tag{3}$$

$$\nabla \cdot \underline{E} = 0 \tag{4}$$

$$\nabla \cdot \underline{B} = 0 \tag{5}$$

The rationalized MKS system of units is utilized in equations 1 through 5. Definition of the symbols is as follows: $\underline{E}$ is the electric field strength of the wave, $\underline{H}$ is the magnetic field strength of the wave, $\underline{B}$ is the magnetic flux density of the wave, ω is the angular frequency of the wave, ν is the average electron collisional velocity with neutral particles, m is the mass of an electron, $\underline{v}$ is the electron velocity, e is the electron charge, $\underline{B}_o$ is the magnetic flux density of the earth s magnetic field, $\overline{\sigma}$ is the conductivity of the ionosphere, $\overline{\epsilon}$ is the permittivity of the ionosphere, and μ_o is the permeability of the ionosphere (assumed to be equal to the permeability of free space). Vectors are denoted by a bar placed underneath the symbol and tensors are denoted by a bar placed over the symbol.

It is interesting to note at this point that the right-hand side of equation (2) denotes the total current density. This term is quite frequently interpreted as the sum of a conduction current density $\overline{\sigma} \cdot \underline{E}$ and a displacement current density $j\omega \overline{\epsilon} \cdot \underline{E}$. In reality it does not matter what is called the conduction and the displacement currents, provided that all of the current is taken into account.

For computational purposes, it is convenient to write $\overline{\epsilon}$ as $\overline{\epsilon}_o$ and

to define

$$\bar{\Phi}_{\epsilon} = \epsilon_o(\bar{I} + \bar{\sigma}/j\omega\epsilon_o) = \epsilon_o \bar{\Phi}_K \tag{6}$$

The general expression for the conduction current density is $\underline{J}_c = N\, e\, \underline{v} = \bar{\sigma} \cdot \underline{E}$ where N is the number density of charge carriers, e is the charge on an electron and $\underline{v}$ is the drift velocity of the electrons. Since $\underline{v} = \bar{M} \cdot \underline{E}$, $\bar{\sigma}$ may be written as

$$\bar{\sigma} = N\, e\, \bar{M} \tag{7}$$

where $\bar{M}$ (the mobility tensor) is defined below. For the case of a plane wave, whose wave normal $\underline{n}$ is arbitrarily oriented with respect to the earth's magnetic field $\underline{B}_o$ the electron velocity $\underline{v}$ may be expressed through utilization of equation (1) as

$$\begin{bmatrix} v_x \\ v_y \\ v_z \end{bmatrix} = \begin{bmatrix} M_{xx} & M_{xy} & M_{xz} \\ M_{yx} & M_{yy} & M_{yz} \\ M_{zx} & M_{zy} & M_{zz} \end{bmatrix} \begin{bmatrix} E_x \\ E_y \\ E_z \end{bmatrix} \tag{8}$$

where

$$M_{xx} = (K^2+B_{ox}^2)Q, \quad M_{xy} = (KB_{oz}+B_{oy}B_{ox})Q, \quad M_{xz} = (B_{ox}B_{oz}-KB_{oy})Q, \tag{9}$$

$$M_{yx} = (B_{ox}B_{oy}-KB_{oz})Q, \quad M_{yy} = (K^2+B_{oy}^2)Q, \quad M_{yz} = (KB_{ox}+B_{oy}B_{oz})Q,$$

$$M_{zx} = (KB_{oy}+B_{ox}B_{oz})Q, \quad M_{zy} = (B_{oy}B_{oz}-KB_{ox})Q, \quad M_{zz} = (K^2+B_{oz}^2)Q,$$

$$K = m(j\omega + \nu)/e \quad \text{and} \quad Q = e\left[(j\omega + \nu)(K^2 + B_{oz}^2)\right]/m\ .$$

Since $\bar{\Phi}_K = (\bar{I} + \bar{\sigma}/j\omega\epsilon_o)$, substitution for $\bar{\sigma}$ gives

$$\left[\Phi_K\right] = \begin{bmatrix} 1+NeM_{xx}/j\omega\epsilon_o & NeM_{xy}/j\omega\epsilon_o & NeM_{xz}/j\omega\epsilon_o \\ NeM_{yx}/j\omega\epsilon_o & 1+NeM_{yy}/j\omega\epsilon_o & NeM_{yz}/j\omega\epsilon_o \\ NeM_{zx}/j\omega\epsilon_o & NeM_{zy}/j\omega\epsilon_o & 1+NeM_{zz}/j\omega\epsilon_o \end{bmatrix} = \begin{bmatrix} \Phi_{xx} & \Phi_{xy} & \Phi_{xz} \\ \Phi_{yx} & \Phi_{yy} & \Phi_{yz} \\ \Phi_{zx} & \Phi_{zy} & \Phi_{zz} \end{bmatrix} \quad (10)$$

where the M_{ij} are defined by equation (9).

Forming $\nabla \times \nabla \times \underline{E}$ from equation (3) yields

$$\nabla \times \nabla \times \underline{E} = -j\omega\mu_o(\nabla \times \underline{H}) . \quad (11)$$

Substitution of equations (2) and (6) into equation (11) gives

$$\nabla \times \nabla \times \underline{E} = (\omega/c)^2 \bar{\Phi}_K \cdot \underline{E} . \quad (12)$$

Since $\nabla \times \nabla \times \underline{E} = -(\omega/c)^2 \underline{n} \times \underline{n} \times \underline{E}$, substitution of this expression into equation (12) yields the basic $\underline{E}$ field equation

$$\underline{n} \times \underline{n} \times \underline{E} + \bar{\Phi}_K \cdot \underline{E} = 0 . \quad (13)$$

$\underline{n}$ is a vector normal to the wave, whose magnitude n is the index of refraction.

In the following discussion, the average electron collision velocity ν with neutral particles is assumed to be zero and the earth's magnetic field $\underline{B}_o$ is directed along the positive z-axis of a right-handed orthogonal coordinate system in which the x-z plane is the wave plane of incidence. The angular displacement between $\underline{B}_o$ and $\underline{n}$ is denoted by θ. These assumptions now permit $\bar{\Phi}_K$ to be expressed in the following form.

$$\left[\phi_K\right] = \begin{bmatrix} 1 - \omega_p^2/(\omega^2 - \omega_b^2) & j\omega_b\omega_p^2/\omega(\omega^2 - \omega_b^2) & 0 \\ -j\omega_b\omega_p^2/\omega(\omega^2 - \omega_b^2) & 1 - \omega_p^2/(\omega^2 - \omega_b^2) & 0 \\ 0 & 0 & 1 - \omega_p^2/\omega^2 \end{bmatrix} \tag{14}$$

In equation (14) ω_b is the electron cyclotron frequency or the gyro frequency and is defined as

$$\omega_b^2 = (eB_o/m)^2 \tag{15}$$

and ω_p is the plasma frequency and is defined as

$$\omega_p^2 = Ne^2/\epsilon_o m \ . \tag{16}$$

In order that the set of equation (13) have a non-trivial solution the determinant of the coefficients of E_x, E_y and E_z must vanish yielding the dispersion equation for the index of refraction n.

$$\left[\phi_{xx}\sin^2\theta + \phi_{zz}\cos^2\theta\right]n^4 - \left[(\phi_{xx}^2 + \phi_{xy}^2)\sin^2\theta + \phi_{xx}\phi_{zz}(1 + \cos^2\theta)\right]n^2 + \left[\phi_{xx}^2 + \phi_{xy}^2\right]\phi_{zz} = 0 \tag{17}$$

Equation (17) is in general bi-cubic, but the sixth degree terms cancel and one root is lost. It can be shown that a wave propagating close to the speed of sound has been lost.

It is now convenient to decompose $\underline{E}$ into two circularly polarized components rotating in opposite directions. Let $\underline{E}_r$ be perpendicular to $\underline{B}_o$ and rotate right-handed about $\underline{B}_o$ and $\underline{E}_\ell$ be perpendicular to $\underline{B}_o$ and rotate left-handed about $\underline{B}_o$. The resultant of these two circularly

polarized waves is a linearly polarized plane wave. Both $\underline{E}_r$ and $\underline{E}_\ell$ will produce circular motion of the electrons in the presence of $\underline{B}_o$ with the rotation in each case in the same direction as the $\underline{E}$ vector producing the rotation.

Since $\phi_r = \phi_{xx} + j\phi_{xy}$ and $\phi_\ell = \phi_{xx} - j\phi_{xy}$, the subscripts on ϕ_r and ϕ_ℓ represent right and left-handed circular polarization with respect to $\underline{B}_o$, equation (17) may be solved for the $\tan^2\theta$ yielding

$$\tan^2\theta = -\phi_{zz}(n^2 - \phi_r)(n^2 - \phi_\ell)/(n^2 - \phi_{zz})(\phi_{xx}n^2 - \phi_r\phi_\ell) \ . \qquad (18)$$

The two principle directions of propagation are along $\underline{B}_o$ ($\theta = 0$) and perpendicular to $\underline{B}_o$ ($\theta = \pi/2$). For propagation along the magnetic meridian, θ is zero and $\tan^2\theta$ becomes zero. Setting the numerator of equation (18) equal to zero gives

$$n_r^2 = \phi_r \quad \text{and} \qquad (19)$$

$$n_\ell^2 = \phi_\ell \ .$$

The form of the plane wave may be assumed to be $\exp j\omega(t - \underline{n} \cdot \underline{r}/c)$, where $\underline{n}$ is a vector whose magnitude n is equal to the index of refraction and whose direction is normal to the wave. The wave phase velocity u may be expressed as the ratio of the free space velocity c and the index of refraction n($u = c/n$). If n is real (i.e., $n^2 > 0$), the wave function will oscillate in space and the wave will be propagated. On the other hand, the wave function will decay exponentially in space with increasing $\underline{r}$ and will be attenuated if n is imaginary (i.e. $n^2 < 0$). In the present discussion the fields involved with $n^2 < 0$ represent reactive or evanescent

fields. Because of the reactive nature of the fields, the ratio of $\underline{E}$ to $\underline{H}$ produces a characteristic impedance and a phase velocity which are imaginary in the direction of $\underline{n}$. This type of attenuation is not to be confused with the attenuation occurring due to an absorption loss for the case where the average election collisional velocity ν is not assumed to be zero. Reference to equation (19) reveals that the waves will be propagated when ϕ_r and ϕ_ℓ are positive and will be attenuated when they are negative.

For propagation at right angles to $\underline{B}_o$, θ is equal to $\pi/2$ and $\tan^2 \theta$ tends to infinity. This condition yields two waves whose indices of refraction are

$$n_p^2 = \phi_{zz} \quad \text{and} \tag{20}$$

$$n_t^2 = \phi_r \phi_\ell / \phi_{xx} \, .$$

The wave defined by the index of refraction n_p has its $\underline{E}$ vector parallel to $\underline{B}_o$ and transverse to $\underline{n}_p$ so it is unaffected by the presence of the earth's magnetic field. The second wave, defined by the index of refraction n_t, has its $\underline{E}$ vector in a plane traverse to $\underline{B}_o$.

Equations (19) and (20) describe the principle waves and their corresponding indices of refraction. Figure 1 shows the polarization and direction of propagation for these waves relative to the earth's magnetic field $\underline{B}_o$.

In the investigation of the conditions governing attenuation ($n^2 < 0$) and propagation ($n^2 > 0$), it may be noted that the square of the index of refraction changes sign whenever it passes through zero or infinity. The lines along which n^2 is equal to zero or infinity

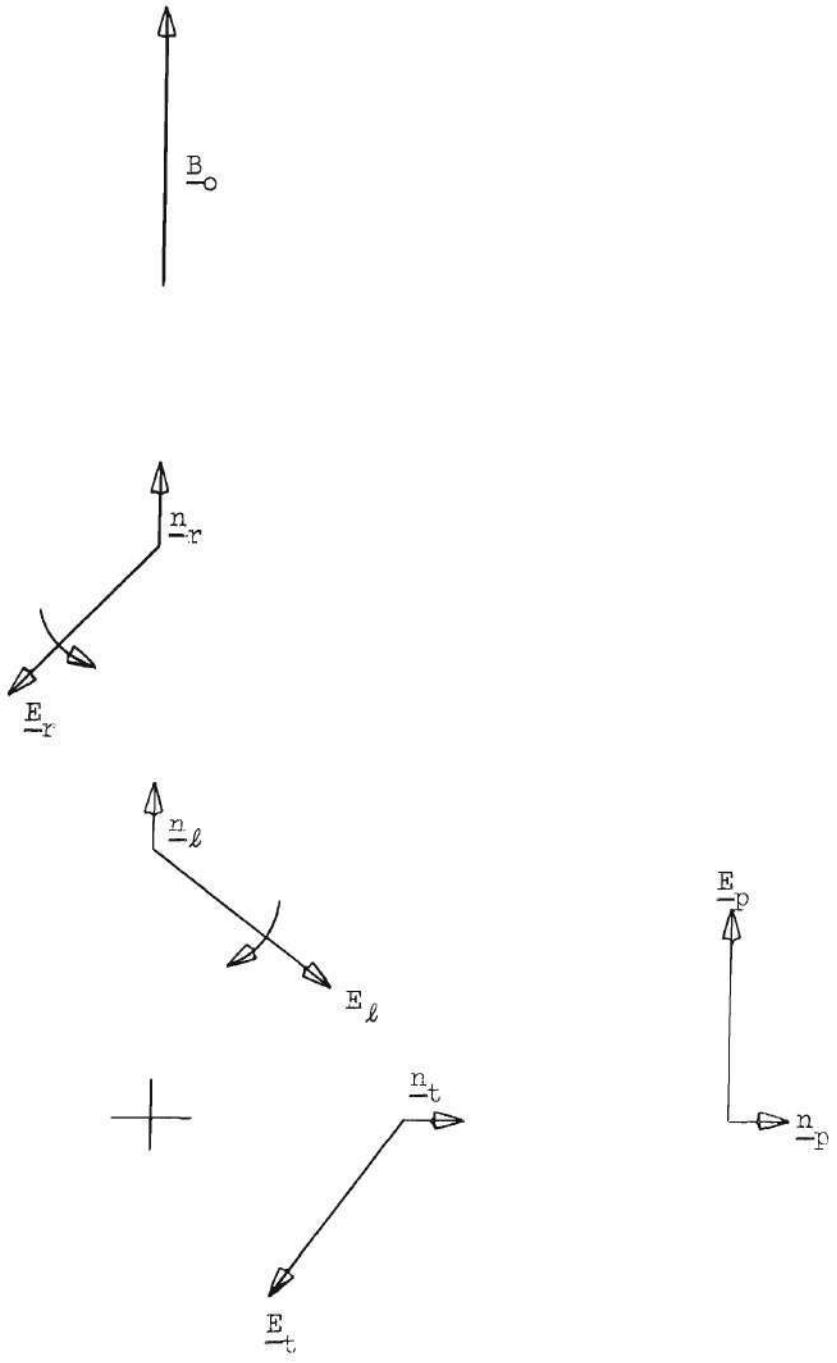

Figure 1. Principal Wave Polarizations.

divide the regions of wave propagation and attenuation (see Figure 2). Lines along which n^2 is infinite are generally referred to as resonances because of the form of the solutions for $\omega = f(\omega_b, \omega_p)$. Lines along which n^2 is zero are called cut-offs. Whenever $\theta = 0$ (propagation along $\underline{B}_o$) or $\theta = \pi/2$ (propagation perpendicular to $\underline{B}_o$), the term principle resonance or cut-off is used. The principle resonances occur for propagation along and perpendicular to $\underline{B}_o$ when n^2 becomes infinite. For propagation along $\underline{B}_o (\theta = 0)$, a single principle resonance occurs when n_r^2 becomes infinite at $\omega = \omega_b$. For propagation perpendicular to $\underline{B}_o$ $(\theta = \pi/2) n_t$ becomes infinite when $\omega^2 = \omega_p^2 + \omega_b^2$ producing a principle resonance for this propagation condition. The principle cut-offs occur for propagation along and perpendicular to $\underline{B}_o$ when n^2 becomes zero. Two principle cut-offs occur for propagation along $\underline{B}_o$ $(\theta = 0)$ since n_r^2 becomes zero when $\omega_p^2 = \omega^2 - \omega\omega_b$ and n_ℓ^2 becomes zero when $\omega_p^2 = \omega^2 + \omega\omega_b$. For propagation perpendicular to $\underline{B}_o (\theta = \pi/2)$, principle cut-offs occur when $\omega = \omega_p (n_p^2 = 0)$ and when $\omega_p^2 = \omega^2 \pm \omega\omega_b (n_t^2 = 0)$.

Since ν has been assumed to be zero, our mathematical model does not allow for energy absorption. Under these conditions the plasma model of the ionosphere is either transparent or opaque. Interpretation of the conditions of resonance and cut-off may be facilitated by a plot, on the normalized ω_b/ω versus ω_p/ω plane, of the equations governing these conditions. Figure 2 is a plot of the equations of the preceding paragraph on this normalized plane. Inspection of Figure 2 reveals that the normalized plane is divided into eight regions by the principle resonance and cut-off lines. In region 1 all four waves may propagate. In order to move into region 2, the principle cut-off line $(n_r = n_t = 0)$ must be crossed. Therefore in region 2 the ℓ and p waves propagate. The t wave

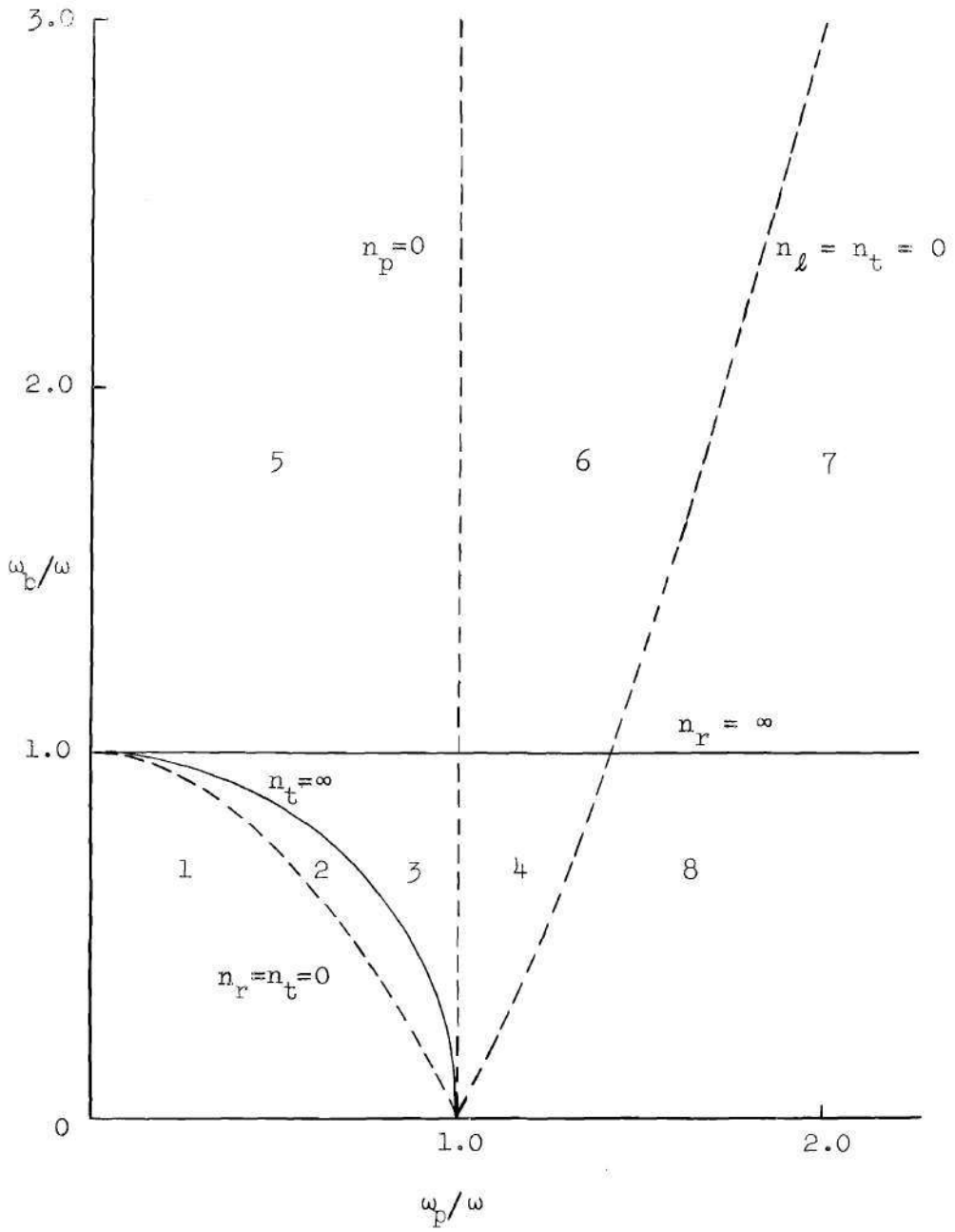

Figure 2. Regions of Wave Propagation and Attenuation.

reappears in region 3 due to presence of the resonance $n_t = \infty$ between regions 2 and 3. In region 4 only the ℓ and t waves propagate. All four waves may propagate in region 5 whereas the p wave is evanescent in region 6. The only wave not evanescent in region 7 is the r wave. All waves are evanescent in region 8. Allis (17) presents these same eight regions and the resulting wave surfaces in terms of a normalized $(\omega_b/\omega)^2$ versus $(\omega_p/\omega)^2$ plane plot.

It is possible that both resonances and cut-offs may occur for directions other than the principle directions. Taking the limit of equation (18) as n^2 tends to infinity yields

$$\lim_{n^2 \to \infty} \tan^2 \theta = -\phi_{zz}/\phi_{xx} \quad . \tag{21}$$

Since $\tan^2 \theta \geq 0$, a resonance will occur whenever ϕ_{zz} and ϕ_{xx} have opposite signs. In order to determine the existence of any cut-offs besides the principle cut-offs, the limit of equation (18) is taken as n^2 tends to zero. Since this limit yields $\tan^2 \theta = -1$, no other cut-offs occur.

If ν is not negligible, then the relative dielectric tensor Φ_k is given by equation (10). The resonances and cut-offs are difficult to define explicitly because of the couplings between the various wave surfaces. In addition the mechanics for providing absorption is included in the mathematical model of the ionosphere. There are now three wave surfaces and the regions of propagation and attenuation increase to 13. Two of the waves are essentially the same as for the preceding case. The third wave is called the "plasma electron" wave (17).

Ray Approximation

The ray approximation form of solution of the magneto-ionic equations is based on the assumption that any change in the index of refraction over one wave length of the propagating frequency is negligible when compared with the index itself. This condition is generally satisfied for the case of high frequency propagation for a normal composition of the ionosphere. A brief summary of the theory of magneto-ionic wave-packet propagation, as developed by Booker (15) and (16), is presented in the succeeding paragraphs.

Figure 3 illustrates the orientation of a three-dimensional orthogonal rectangular coordinate system relative to a flat earth. A plane harmonic wave of frequency f is shown at oblique incidence upon a horizontally stratified ionosphere, the x, y plane, at an angle θ to the vertical z-axis. The wave plane of incidence makes an angle Ω with the positive x-axis. In the neighborhood of a point in the ionosphere, the phase propagation can be described by a vector whose components parallel to the three coordinate axes are $\sin\theta\cos\Omega$, $\sin\theta\sin\Omega$, and q. The coordinates $\sin\theta\cos\Omega$ and $\sin\theta\sin\Omega$ depend only on the prescribed direction of incidence. The vertical component q varies with height as the wave propagates through the ionosphere. The wave function may be expressed as

$$\exp\left\{ j2\pi/\lambda \left[ct - (\sin\theta\cos\Omega)x - (\sin\theta\sin\Omega)y - \int_0^z q\,dz \right] \right\}. \qquad (22)$$

In this expression the velocity of light in free space is denoted by c and the wave length in free space by λ. Substitution of equation (22)

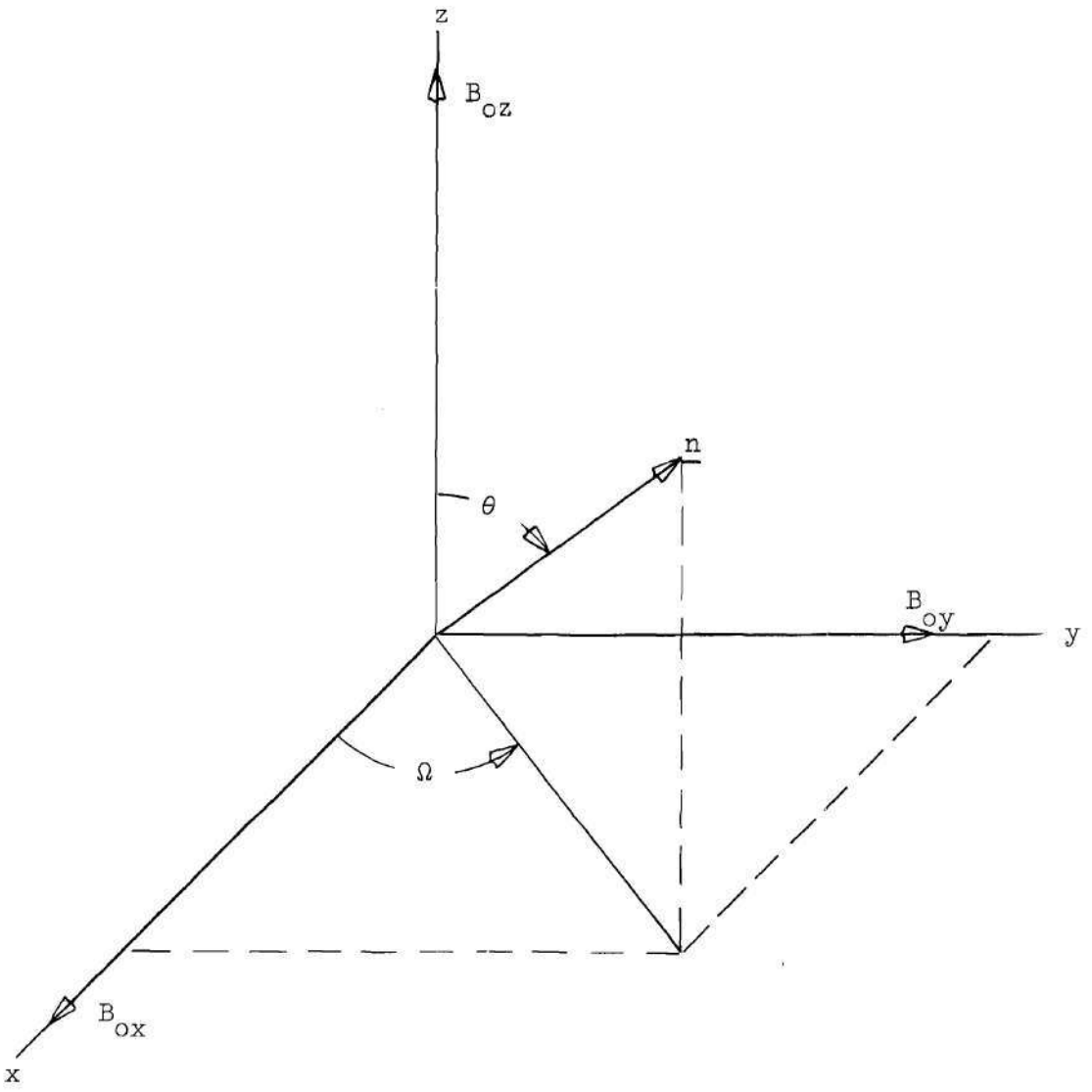

Figure 3. Coordinate System for the Ray Equations.

into equations (2) thru (6) yields the following quartic equation in q after elimination of the field quantities.

$$a_4 q^4 + a_3 q^3 + a_2 q^2 + a_1 q^1 + a_0 q^0 = 0 \qquad (23)$$

The coefficients in the preceding quartic equation in q become

$$a_0 = \left[(1-j\nu/\omega)\cos^2\theta - \alpha\right]\left\{\left[\cos^2\theta\,(1-j\nu/\omega)-\alpha\right]\left[(1-j\nu/\omega)-\alpha\right] - \beta^2\cos^2\theta\right\} - \cos^2\theta\,(\beta_x \sin\theta\cos\Omega + \beta_y \sin\theta\sin\Omega)^2\alpha, \qquad (24)$$

$$a_1 = -2\cos^2\theta\,(\beta_x \sin\theta\cos\Omega + \beta_y \sin\theta\sin\Omega)\,\beta_z\,\alpha,$$

$$a_2 = -2(1-j\nu/\omega)\left\{\left[(1-j\nu/\omega)\cos^2\theta - \alpha\right]\left[(1-j\nu/\omega)-\alpha\right] - \beta^2\cos^2\theta\right\} + \alpha\left\{(\beta_x \sin\theta\cos\Omega + \beta_y \sin\theta\sin\Omega)^2 - \beta_z^2\cos^2\theta - \beta^2\right\},$$

$$a_3 = 2\alpha\beta_z(\beta_x \sin\theta\cos\Omega + \beta_y \sin\theta\sin\Omega), \text{ and}$$

$$a_4 = (1-j\nu/\omega)\left[(1-j\nu/\omega)^2 - \beta^2\right] - \alpha\left[(1-j\nu/\omega)^2 - \beta_z^2\right]$$

where $\beta_x = \omega_{bx}/\omega$, $\beta_y = \omega_{by}/\omega$, $\beta_z = \omega_{bz}/\omega$, $\beta = \omega_b/\omega$ and $\alpha = \omega_p^2/\omega^2$. The roots of equation (23) describe the upgoing and downcoming magneto-ionic wave components. Whenever there are four distinct roots of this equation, two of the roots describe the upgoing and downcoming wave components designated as the ordinary wave and the other two roots describe the upgoing and downcoming wave components designated as the extraordinary wave.

However Booker (16) has shown that some simplification of calculation may be effected if α is expressed as a function of q. If equations (24) are rearranged in terms of powers of α and then substituted into

equation (23), equation (25) follows in the form

$$\alpha^3 + a_7\alpha^2 + a_6\alpha^1 + a_5\alpha^0 = 0 \qquad (25)$$

where

$$a_5 = (j\nu/\omega - 1)\left[(1-j\nu/\omega)^2 - \beta^2\right]\left[\cos^2\theta - q^2\right]^2 , \qquad (26)$$

$$a_6 = (\cos^2\theta - q^2)\left\{\left[2(1-j\nu/\omega)^2 - \beta^2\right] + (1-j\nu/\omega)^2(\cos^2\theta - q^2) + (\sin\theta\cos\Omega\,\beta_x + \sin\theta\sin\Omega\,\beta_y + q\,\beta_z)^2\right\} \text{ and}$$

$$a_7 = (j\nu/\omega - 1)\left[1 + 2(\cos^2\theta - q^2)\right] .$$

The solution to either equation (23) or (25) is generally presented in the form of the locus of the variation of q versus α for a fixed orientation of the earth's magnetic field. Figure 4 shows this form of graphical presentation of the solution to Booker's equation. The dashed curves represent the two solutions of equation (25) for the extra-ordinary wave and the solid curve the solution for the ordinary wave. In general only one of the two extra-ordinary wave solutions is of interest in a given problem. Points R_1, R_2 and R_3 indicate the values of α at which total reflection occurs. Since phase propagation is not usually affected by the presence of damping ($\nu \neq 0$), ν is normally assumed to be negligibly small and omitted from consideration in obtaining q, α plots of the type shown in Figure 4.

The ray approximation technique may also be utilized to describe the "lateral deviation" of the wave-packet. This is the deviation in a direction perpendicular to the vertical plane containing the straight line

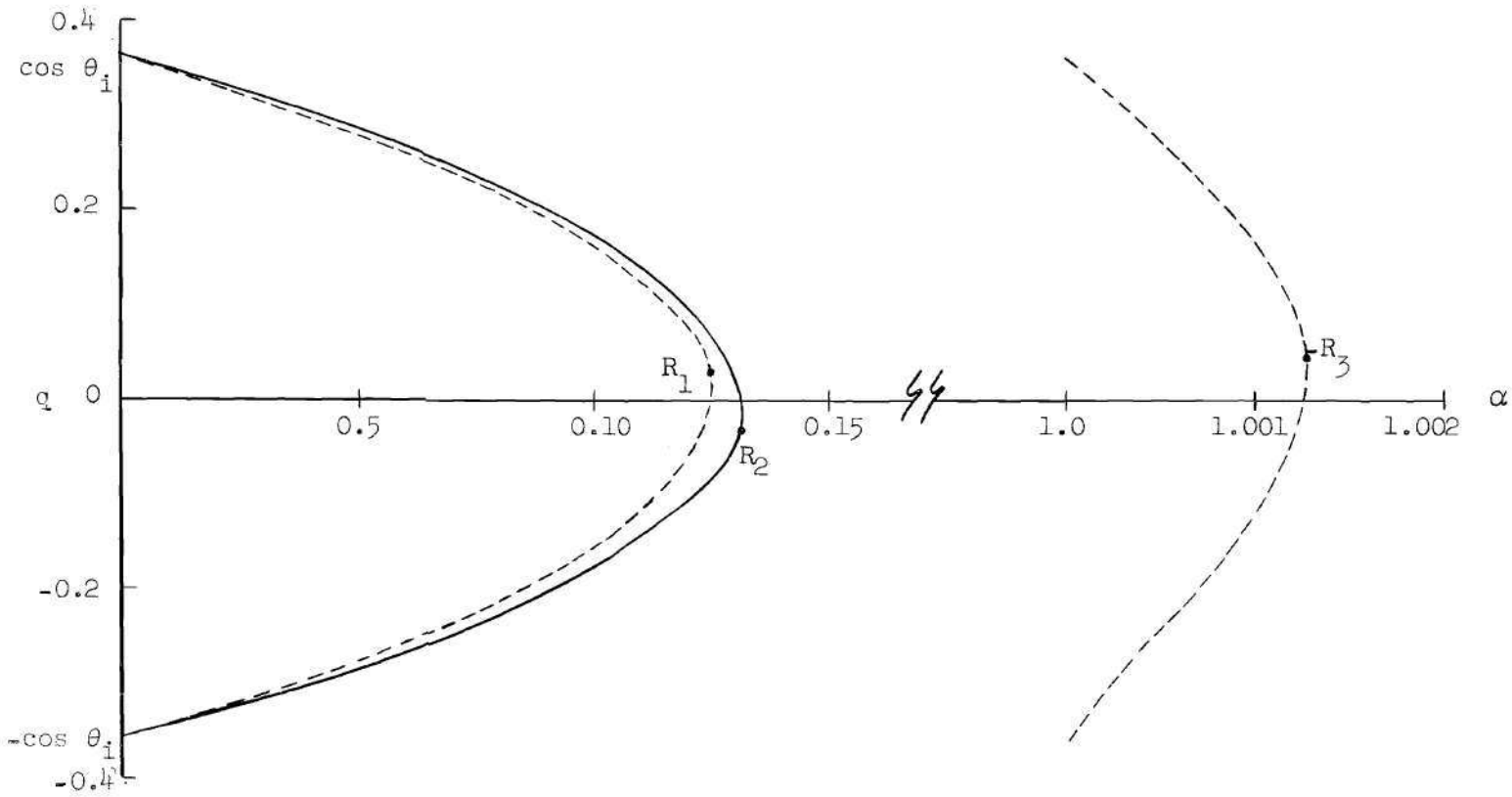

Figure 4. q, α Curves.

path connecting the transmitting and receiving stations. Below the ionosphere the wave-packet may be regarded as a large number of plane waves propagating at different frequencies and in different directions. These waves interfere constructively at the instantaneous location of the wave-packet and interfere destructively elsewhere. Each of these plane waves gives rise to a wave of the type described by equation (22). The wave-packet path is given by following the point of constructive interference of these plane waves. This is accomplished by the method of Booker (16) by determining the time and location at which first-order variations in wave frequency f and in the direction of incidence ($\sin\theta\cos\Omega$, $\sin\theta\sin\Omega$, q) produce no first order variations in the phase of the wave function. The partial derivatives of equation (22) with respect to $(2\pi/\lambda)$, $\sin\theta\cos\Omega$, and $\sin\theta\sin\Omega$ of the phase expression are equated to zero to produce the desired results.

Taking the indicated partial derivatives of the phase expression $(2\pi/\lambda)(ct - [\sin\theta\cos\Omega]x - [\sin\theta\sin\Omega]\,y - \int_o^z q\,dz)$ and equating them to zero yields

$$ct - I_1 x - I_2 y - \int_o^z \left[\frac{\partial(2\pi q/\lambda)}{\partial q}\right] dz = 0 , \qquad (27)$$

$$x + \int_o^z \left[\partial q/\partial I_1\right] dz = 0 \quad \text{and} \qquad (28)$$

$$y + \int_o^z \left[\partial q/\partial I_2\right] dz = 0 , \qquad (29)$$

where $I_1 = \sin\theta\cos\Omega$, and $I_2 = \sin\theta\sin\Omega$. The total lateral deviation perpendicular to the original plane of incidence is given by equation (28). This equation together with equation (29) will then give the

projection of the curved path of the wave-packet during propagation through the ionosphere upon the x-y plane.

For the purposes of this study, the path deviation of interest is the lateral deviation perpendicular to the plane of incidence. Differentiating equation (25) with respect to I_1 yields

$$\left[\frac{\partial a_7}{\partial q}\frac{\partial q}{\partial I_1} + \frac{\partial a_7}{\partial I_1}\right]\alpha^2 + \left[\frac{\partial a_6}{\partial q}\frac{\partial q}{\partial I_1} + \frac{\partial a_6}{\partial I_1}\right]\alpha + \left[\frac{\partial a_5}{\partial q}\frac{\partial q}{\partial I_1} + \frac{\partial a_5}{\partial I_1}\right] = 0 \quad (30)$$

so

$$-\frac{\partial q}{\partial I_1} = \frac{(\partial a_7/\partial I_1)\alpha^2 + (\partial a_6/\partial I_1)\alpha + (\partial a_5/\partial I_1)}{(\partial a_7/\partial q)\alpha^2 + (\partial a_6/\partial q)\alpha + (\partial a_5/\partial q)} \quad . \quad (31)$$

Neglecting attenuation by setting $\nu = 0$ and then differentiating equation (26) gives the partial derivatives needed to evaluate the right-hand side of equation (31).

$$\partial a_5/\partial I_1 = 4I_1(1 - \beta^2)(\cos^2\theta - q^2) \quad , \quad (32)$$

$$\partial a_6/\partial I_1 = -2I_1\left\{(2 - \beta^2) + (I_1\beta_x + I_2\beta_y + q\beta_z)^2 + 2(\cos^2\theta - q^2)\right\} + (\cos^2\theta - q^2)\left\{2\beta_x(I_1\beta_x + I_2\beta_y + q\beta_z)\right\},$$

$$\partial a_7/\partial I_1 = 4I_1 \quad ,$$

$$\partial a_5/\partial q = 4q(1 - \beta^2)(\cos^2\theta - q^2) \quad ,$$

$$\partial a_6/\partial q = -2q\left\{(2 - \beta^2) + (I_1\beta_x + I_2\beta_y + q\beta_z)^2 + 2(\cos^2\theta - q^2) + (\cos^2\theta - q^2)\left\{2\beta_z(I_1\beta_x + I_2\beta_y + q\beta_z)\right\}\right., \text{ and}$$

$$\partial a_7/\partial q = 4q \quad .$$

Differentiating equation (28) gives

$$dx/dz = -\partial q/\partial I_1 \qquad (33)$$

where $-\partial q/\partial I_1$ is defined by equations (31) and (32). The solution to equation (33) is presented in graphical form and is discussed in Chapter VI.

CHAPTER IV

RECIPROCITY

Any problem concerning the reciprocity of oblique reflection of electromagnetic waves from the ionosphere is complicated because of the nature of the equations governing propagation in this medium. Exact solutions for these equations may be derived for only a few special cases, which unfortunately are not applicable for most practical propagation problems. Therefore it is expedient to inquire into the meaning of the term "reciprocity" in light of the complexity of the general problem. A number of reciprocity theorems appear in the literature and an examination of several of these theorems will provide additional insight into the present problem.

Carson (18) in 1924 developed a generalization of the "Rayleigh Reciprocity Theorem," which was stated by Rayleigh (19) in the language of electric circuit theory as:

> Let there be two circuits of insulated wire A and B, and in their neighborhood any combination of wire circuits or solid conductors in communication with condensers. A periodic electromotive force in the circuit A will give rise to the same current in B as would be excited in A if the electromotive force operated in B.

The proof of this theorem depended on the assumptions: 1. the network could be described in terms of a set of simultaneous equations with constant coefficients, 2. the network was excited with applied electromotive forces of the same frequency and 3. any existing mutual impedances satisfied the reciprocal condition that $Z_{ik} = Z_{ki}$. Carson notes that such a theorem is not necessarily valid when applied to the general case

of the conduction of currents in a continuous media if there is any radiation of energy. Carson then proceeds to generalize Rayleigh's theorem by stating:

> Let a distribution of impressed periodic electric intensity $F' = F'(x, y, z)$ produce a corresponding distribution of current intensity $U' = U'(x, y, z)$, and let a second distribution of equi-periodic impressed electric intensity $F'' = F''(x, y, z)$ produce a second distribution of current intensity $U'' = U''(x,y,z)$ then
>
> $$\iiint_V (F' \cdot U'')dV = \iiint_V (F'' - U') \, dV$$
>
> the volume integration being extended over all conducting and dielectric media.

In Carson's proof of his generalized reciprocity theorem, he assumed that the permeability of free space prevailed and noted that the theorem was not valid in any ionized medium in which the earth's magnetic field had any appreciable effect on the conduction currents.

In 1925 Sommerfeld (20) published a reciprocity theorem, commonly called the Sommerfeld-Pfrang theorem, based on a reciprocity theorem contributed by Lorentz. His theorem stated

> If A_1 and A_2 are two antennas located at O_1 and O_2 respectively, and arbitrary orientations, and signals are first sent from A_1 and received by A_2 and then sent with the same average power from A_2 and received by A_1, then the intensity and phase of the electric field at the receiver A_1 will be equal to that previously produced at A_2, regardless of the electric properties and geometry of the intervening media and the form of the antennas.

Sommerfeld's proof of the validity of his theorem was predicated on the basis that the permeability, permittivity and conductivity of the media involved could be represented by symmetrical tensors.

All of the preceding theorems are invalid when applied to wave propagation in the ionosphere since the tensors describing the permittivity and conductivity of the ionosphere are not symmetrical. Prior to an

extension of the concept of reciprocity to include propagation through the ionosphere, the derivation of the Lorentz reciprocity theorem will provide additional insight into the problem.

For this purpose let us consider two independent fields ($\underline{E}_1$, $\underline{H}_1$ and $\underline{E}_2$, $\underline{H}_2$) propagated at the same sinusoidal frequency in any isotropic or non-isotropic medium. These two fields are constrained to obey Maxwell's equations and the law of superposition so that

$$\nabla \times \underline{H}_1 = j\omega\overline{\Phi}_\epsilon \cdot \underline{E}_1 \,, \tag{34}$$

$$\nabla \times \underline{E}_1 = -j\omega\overline{\Phi}_\mu \cdot \underline{H}_1 \,,$$

$$\nabla \times \underline{H}_2 = j\omega\overline{\Phi}_\epsilon \cdot \underline{E}_2 \quad \text{and}$$

$$\nabla \times \underline{E}_2 = -j\omega\overline{\Phi}_\mu \cdot \underline{H}_2 \,.$$

Forming the divergence of the cross-product $\nabla \cdot (\underline{E}_1 \times \underline{H}_2 - \underline{E}_2 \times \underline{H}_1)$ yields

$$\nabla \cdot (\underline{E}_1 \times \underline{H}_2 - \underline{E}_2 \times \underline{H}_1) = \underline{H}_2 \cdot (\nabla \times \underline{E}_1) - \underline{E}_1 \cdot (\nabla \times \underline{H}_2) - \underline{H}_1 \cdot (\nabla \times \underline{E}_2) + \underline{E}_2 \cdot (\nabla \times \underline{H}_1). \tag{35}$$

Substitution of equation (34) into equation (35) gives after expansion:

$$\nabla \cdot (\underline{E}_1 \times \underline{H}_2 - \underline{E}_2 \times \underline{H}_1) = j\omega \left[\underline{E}_2 \cdot (\overline{\Phi}_\epsilon \cdot \underline{E}_1) - \underline{E}_1 \cdot (\overline{\Phi}_\epsilon \cdot \underline{E}_2)\right] - j\omega \left[\underline{H}_2 \cdot (\overline{\Phi}_\mu \cdot \underline{H}_1) - \underline{H}_1 \cdot (\overline{\Phi}_\mu \cdot \underline{H}_2)\right]. \tag{36}$$

Integrating both sides of equation (36) over the volume V bounded by the surface A which encloses no sources yields upon application of Gauss'' theorem

$$\iint_A (\underline{E}_1 \times \underline{H}_2 - \underline{E}_2 \times \underline{H}_1) \cdot d\underline{A} = j\omega \iiint_V \left[\underline{E}_2 \cdot (\overline{\phi}_\epsilon \cdot \underline{E}_1) - \underline{E}_1 \cdot (\overline{\phi}_\epsilon \cdot \underline{E}_2)\right] dV - j\omega \iiint_V \left[\underline{H}_2 \cdot (\overline{\phi}_\mu \cdot \underline{H}_1) - \underline{H}_1 \cdot (\overline{\phi}_\mu \cdot \underline{H}_2)\right] dV . \tag{37}$$

If the tensors $\overline{\phi}_\epsilon$ and $\overline{\phi}_\mu$ are symmetrical, the right side of equation (37) vanishes defining Lorentz's reciprocity theorem in a mathematical sense.

Since the tensors describing the electro-magnetic characteristics of the ionosphere are not symmetrical, the Lorentz reciprocity theorem as stated is not applicable. However, the question of the validity of the theorem is in reality a question of the radiation properties of the sources of the two fields as will be shown. Following the method of Goubau (21), a reciprocity condition will be considered in which the source radiation characteristics are included and for which the theorem of equation (37) is valid. The tensors $\overline{\phi}_\epsilon$ and $\overline{\phi}_\mu$ are divided into two component tensors, one which is symmetrical and one which is asymetrical so that:

$$\overline{\phi}_\epsilon = \overline{\phi}^s_\epsilon + \overline{\phi}^a_\epsilon \quad \text{and} \tag{38}$$

$$\overline{\phi}_\mu = \overline{\phi}^s_\mu + \overline{\phi}^a_\mu .$$

The superscripts s and a denote the symmetrical and asymmetrical component tensors. The vectors $\underline{C}_\epsilon$ and $\underline{C}_\mu$ are now defined as follows:

$$\underline{E}_2 \cdot (\overline{\phi}^a_\epsilon \cdot \underline{E}_1) = -\underline{E}_1 \cdot (\overline{\phi}^a_\epsilon \cdot \underline{E}_2) = \underline{C}_\epsilon \cdot (\underline{E}_1 \times \underline{E}_2) \quad \text{and} \tag{39}$$

$$\underline{H}_2 \cdot (\overline{\phi}^a_\mu \cdot \underline{H}_1) = \underline{H}_1 \cdot (\overline{\phi}^a_\mu \cdot \underline{H}_2) = \underline{C}_\mu \cdot (\underline{H}_1 \times \underline{H}_2) .$$

Introduction of equation (39) into equation (37) produces equation (40).

$$\iint_A (\underline{E}_1 \times \underline{H}_2 - \underline{E}_2 \times \underline{H}_1) \cdot d\underline{A} = 2j\omega \iiint_V \left[\underline{C}_\epsilon \cdot (\underline{E}_1 \times \underline{E}_2) - \underline{C}_\mu \cdot (\underline{H}_1 \times \underline{H}_2)\right] dV \qquad (40)$$

The validity of the Lorentz theorem was not established for the general case of ionospheric wave propagation because of the presence of the earth's magnetic field and its effect on wave propagation. This condition is easily recognizable by considering the forces involved. The force exerted on electrons in a plasma is oppositely directed for waves traveling in opposite directions, but the orbital motion of the electrons about the imposed steady magnetic field is in the same direction regardless of the direction of wave propagation. One possible consequence of this condition is that the wave polarization may not be the same for transmission in both directions; therefore, the antenna characteristics must also be considered in the integrations involved in equation (40). The following discussion illustrates the role played by the antenna polarization in fulfilling the Lorentz reciprocity theorem.

Assume that the field $\underline{E}_1$, $\underline{H}_1$ is radiated from an antenna T_1 and received at an antenna T_2 and that the field $\underline{E}_2$, $\underline{H}_2$ is radiated from T_2 and received at T_1. Now let $\underline{E}_2$ and $\underline{H}_2$ be radiated by an antenna system so that

$$\underline{E}_2 = \underline{E}_2' + p\,\underline{E}_2'' \quad \text{and} \qquad (41)$$

$$\underline{H}_2 = \underline{H}_2' + p\,\underline{H}_2'' \ .$$

Here p is an arbitrary adjustable complex quantity which characterizes

the amplitude and phase of the antenna currents. Substitution of equation (41) into equation (40) yields

$$\iint_A (\underline{E}_1 \times \underline{H}_2 - \underline{E}_2 \times \underline{H}_1) \cdot d\underline{A} = 2j\omega \iiint_V \left[\underline{C}_\epsilon \cdot (\underline{E}_1 \times \underline{E}_2') - \underline{C}_\mu \cdot (\underline{H}_1 \times \underline{H}_2')\right] dV + 2pj\omega \iiint_V \left[\underline{C}_\epsilon \cdot (\underline{E}_1 \times \underline{E}_2'') - \underline{C}_\mu \cdot (\underline{H}_1 \times \underline{H}_2'')\right] dV . \quad (42)$$

By a suitable choice of antenna polarization through the variation of the complex quantity p, the right-hand side of equation (42) may be reduced to zero, thus fulfilling Lorentz's theorem. The conclusion which necessarily follows is that for each antenna system there is a reciprocal antenna system such that the two systems utilized together fulfill "Lorentz's Reciprocity Theorem" for a given set of ionospheric propagation conditions. Since the ionospheric propagation conditions vary with time, the complex quantity p must also be varied if the conditions for reciprocal transmission are to remain satisfied. This means that the polarizations of the antennas in the theoretical antenna system will also be functions of time. If for any particular set of ionospheric propagation conditions p must be equated to zero to reduce the right-hand side of equation (42) to zero, complete reciprocity in the Lorentz sense is said to exist.

In an effort to define reciprocity in a sense which is applicable to an interpretation of experimental data, the following interpretation of the preceding theoretical discussions represents a departure from the conventional approach to this problem. As a result of this departure,

two facts which contribute significantly to the relative reciprocity theorem, stated later in this chapter, may be noted at this point.

1. All of the reciprocity theorems discussed involve the concept of power density integrated over a closed surface. For this reason it does not appear that any comments regarding complete reciprocity can be derived from any theorem predicated on such a basis since the integrals involved are not unique. This statement may be justified in the following manner. An examination of the left-hand side of equation (42) reveals that the integrand is the difference of two vectors which may be interpreted as Poynting vectors. It is permissible to rewrite this surface integral as

$$\iint_A (\underline{E}_1 \times \underline{H}_2 - \underline{E}_2 \times \underline{H}_1) \cdot d\underline{A} = \iint_A \underline{S}_{12} \cdot d\underline{A} - \iint_A \underline{S}_{21} \cdot d\underline{A} \quad . \quad (43)$$

It may be shown that the integrals involved are not unique since any arbitrary vector $\underline{S}_{jk} = \nabla \times \underline{P}_i$ (where $\underline{P}_i$ is a second vector) may be added to the integrand without changing the value of the integral. To show the validity of this statement, add $\underline{S}_{jk}$ to each of the integrals on the right-hand side of equation (43).

$$\iint_A (\underline{S}_{12} + \underline{S}_{jk}) \cdot d\underline{A} - \iint_A (\underline{S}_{21} - \underline{S}_{kj}) \cdot d\underline{A} = \iint_A (\underline{S}_{12} \cdot d\underline{A} \quad (44)$$

$$- \iint_A \underline{S}_{21} \cdot d\underline{A} + \iint_A \underline{S}_{jk} \cdot d\underline{A} + \iint_A \underline{S}_{kj} \cdot d\underline{A} \quad .$$

Application of the Divergence theorem to the right-hand side of equation (44) yields

$$\iint_A \underline{S}_{12} \cdot d\underline{A} - \iint_A \underline{S}_{21} \cdot d\underline{A} + \iint_A \underline{S}_{jk} \cdot d\underline{A} + \iint \underline{S}_{kj} \cdot d\underline{A} = \quad (45)$$

$$\iint_A \underline{S}_{12} \cdot d\underline{A} - \iint_A \underline{S}_{21} \cdot d\underline{A} + \iiint_V (\nabla \cdot \underline{S}_{jk}) dV + \iiint_V (\nabla \cdot \underline{S}_{kj}) dV$$

where the volume V is bounded by the surface A.

Since $\nabla \cdot \underline{S}_{jk} = \nabla \cdot \underline{S}_{kj} = \nabla \cdot \nabla \times \underline{P}_1 = \nabla \cdot \nabla \times \underline{P}_2 = 0$,

equation (45) reduces to

$$\iint_A \underline{S}_{12} \cdot d\underline{A} - \iint_A \underline{S}_{21} \cdot d\underline{A} + \iiint_V (\nabla \cdot \underline{S}_{jk}) dV + \iiint_V (\nabla \cdot \underline{S}_{kj}) dV = \quad (46)$$

$$\iint_A \underline{S}_{12} \cdot d\underline{A} - \iint_A \underline{S}_{21} \cdot d\underline{A} \ .$$

Similar comments may also be made regarding Carson's integral statement of his reciprocity theorem and the Sommerfeld-Phrang reciprocity theorem.

2. The polarization characteristics of the antennas play a fundamental role in any theoretical or experimental interpretation of the reciprocal transmission of electromagnetic waves via the ionosphere. Goubau's reciprocal antenna theorem clearly points up this condition, which in turn is further enhanced by Budden's investigation of reciprocal transmission via the ionosphere. Budden (22) approached the problem of reciprocity in terms of a full wave treatment in which he excluded the antenna characteristics and examined the polarization of the free space wave components at the reception site. Because of the complexity of the equations, he was unable to derive a solution for the general case of oblique incidence for the ionosphere. However, he did obtain solutions for two special cases through utilization of a digital computer

facility employing approximation techniques. Based on these special results, he concluded that Goubau's reciprocity theorem was satisfied, but that complete reciprocity could not be expected to exist in the general case even though Goubau's theorem would still be valid.

In light of these conclusions, it appears logical to define reciprocity in such a manner that the antenna polarization characteristics are included in the ionospheric effects. Reciprocity defined in this manner will be called "relative reciprocity" as contrasted to complete reciprocity. Thus complete reciprocity pertains to the propagation of electromagnetic fields between two points. Relative reciprocity pertains to the transmission and reception of electromagnetic waves between two fixed antenna systems and includes the effects of the antenna systems. Obviously, although complete reciprocity is of theoretical interest, relative reciprocity (or non-reciprocity) is the phenomena which is of practical interest and is the phenomena which is capable of experimental investigation. Noting that $\overline{\phi}_{\mu}$ is symmetrical for ionospheric propagation, the right-hand side of equation (42) may be rewritten as

$$2j\omega \iiint_V \left[\underline{C}_{\epsilon} \cdot (\underline{E}_1 \times \underline{E}_2') + p\, \underline{C}_{\epsilon} \cdot (\underline{E}_1 \times \underline{E}_2'') \right] dV. \quad (47)$$

In order to satisfy Goubau's theorem, the complex parameter p is adjusted so that the integral is zero. The mathematical adjustment of the parameter p corresponds experimentally to an optimum polarization of the antenna system involved. If the parameter p assumes any non-zero value to reduce the integral to zero, complete reciprocity for an antenna system of fixed polarization does not exist. The lack of complete reciprocity

occurs because of a change in wave polarization, due to ionospheric propagation effects, which is detected by the fixed polarization characteristics of the antenna system. In order to provide a new and a more practical reciprocity theorem, relative reciprocity, based on the inclusion of the antenna characteristics with ionospheric bearing and polarization effects, may be defined in terms of the amplitudes of the signals appearing at the output terminals of the receiving antennas as

> Let T_1 and T_2 be two antennas, which individually have the same field patterns when used for either the transmission or the reception of electromagnetic waves and which are located at the points S_1 and S_2 respectively. Electromagnetic waves of the same frequency are transmitted simultaneously from both S_1 and S_2 and then received at both S_1 and S_2 after oblique reflection from the ionosphere. Relative reciprocity is said to exist for the two-way transmission link during any period of time in which the magnitudes of the received signals U_1 and U_2 appearing at the output terminals of the receiving antennas T_1 and T_2 may be linearly related by a fixed constant b such that $U_1 = bU_2$, $b > 0$. For periods during which non-reciprocity exists, b will be a variable.

One particular special case of the general relative reciprocity theorem is of great practical interest. This case arises when the polarizations of antennas T_1 and T_2 are identical and when the transmitter power levels are the same.

One of the major factors involved in the application of the relative reciprocity theorem is the determination of the minimum applicable time period. If two instantaneous signals U_1 and U_2 are compared after simultaneous transmission and reception at sites S_1 and S_2, it is apparent that they may be related by a constant b ($U_1 = bU_2$). In the event that b is not equal to zero, it is conceivable that this condition could be interpreted as constituting a condition which might be referred to as instantaneous relative reciprocity. Unfortunately this interpretation

provides no practical information insofar as relative ionospheric propagation characteristics are concerned. On the other hand when two successive sets or pairs of signals, received in two successive instants of time, are compared, the data provides information about the value of the constant b for the two consecutive sets of propagation conditions. If b is the same for both sets of signals, the relative reciprocity theorem indicates that relative reciprocity exists. This condition has practical applications in that it shows that the two-way transmission link now exhibits the same propagation characteristics for the period of time required to transmit and receive the two successive sets of signals. The associated transmit-receive time period represents the minimum period during which application of the theorem provides useful information.

Since the relationship between U_1 and U_2 for relative reciprocity is linear, a plot of successive sets of signal data on the U_1 versus U_2 plane will form a straight line with slope b during periods in which relative reciprocity exists. During periods of non-reciprocity, b will be a function of time. Application of the relative reciprocity theorem to a specific problem eliminates the difficult problem of converting the receiving antenna output signal into an equivalent free space antenna signal as required by existing ionospheric propagation reciprocity theorems. This reduction in the complexity of the interpretation of reciprocity does not detract from the general nature of the relative reciprocity theorem. The theorem simply recognizes and includes the prominent role played by the antenna characteristics in any practical investigation of reciprocity.

CHAPTER V

DEVELOPMENT OF THEORETICAL TEST SPECIFICATIONS

There have been several recent experimental investigations (24) and (25) concerning the reciprocal transmission of electromagnetic waves via oblique reflection from the ionosphere. Although both of these tests yielded useful information, neither produced conclusive results insofar as reciprocal transmission was concerned. Meadow's (24) investigations produced less than optimum results because he did not clearly define what he considered to be reciprocal transmission. Falcon (25) attempted to interpret reciprocity in terms of computed sample correlation coefficients which were associated with the receiver output signals. The utilization of the mathematical theory of linear regression as a basis for the computation of these correlation coefficients produced results which were difficult, if not impossible, to interpret. This condition prevailed because of the doubtful application of the mathematical theory to the receiver output signals which were non-linearly related to the receiver input signals (the signals of interest). This procedure was followed since it was impossible to compute correlation coefficients for the receiver input signals because the receiver gains had not been recorded during the experimental tests.

In view of the preceding discussion it is deemed desirable to set down the specifications of an experimental test which will provide adequate data for correlation with the theoretical aspects of reciprocity defined earlier in this study. Each of the following test specifications

has been formulated on the basis of correlating experimental data with the relative reciprocity theorem. Table 1 outlines the basic test specifications which are discussed individually in succeeding sections of this chapter.

Table 1. Test Specifications

Orientation of the Data Transmission Link	Arbitrary
Stations Comprising the Data Transmission Link	Signal Transmission and Reception Stations - 2
	Ionosonde Data Station - 1
Station Great Circles Separation Distances	500 - 1800 Kilometers for Signal Transmitting and Receiving Stations
	Path Midpoint - Ionosonde Data Station
Two-Way Transmission Synchronization Technique	Master-Slave Clocks
Transmission Technique	Pulse
Transmission Frequencies	5 - 63 Megacycles for Two-Way Synchronized Transmission
	1 - 25 Megacycles for Obtaining Ionosonde Data

Test procedures, data reduction and data analysis techniques have also been formulated since they are an integral part of the overall test specifications. The following discussions are presented under a number of sub-headings so that the various aspects of the overall test are grouped together in as logical a manner as possible.

The Data Transmission Link

In order to obtain oblique reflection relative reciprocity test data, two transmitting-receiving stations must be established. The function of these two stations, which comprise the data transmission link, is to provide time synchronized, two-way signal transmission and reception capabilities. Orientation of the signal transmission path relative to the direction of the earth's magnetic field is not important since the relative reciprocity theorem is applicable for any orientation.

Although the multiple hop mode of propagation is not excluded by the statement of the relative reciprocity theorem, the one-hop mode of propagation has been selected for the purposes of this study. For the one-hop mode, the minimum and maximum separation distances between the two stations are determined by the maximum range of ground wave propagation and the height of the lowest reflecting ionospheric region (the E-region) and the earth's curvature respectively. The minimum station-to-station separation distance is approximately 500 kilometers, and the selection of this distance is based on the maximum ground wave propagation distance which is anticipated at the lowest frequency range of interest. On the other hand, the selection of a maximum station separation distance of 1800 kilometers is based on the anticipated average height of the E-region of the ionosphere, approximately 110 kilometers, and the tangency of the wave path to the curvature of the earth's surface. At this point it should be noted that distinct ionosonde traces representing the one-hop E mode of propagation have been observed in tests over longer path lengths than 1800 kilometers. Moller (23) obtained a distinct one-hop E trace over a path length of 1965 kilometers

for an E-region height of 110 kilometers. It has not been established whether or not some additional atmospheric refraction effect produced some additional downward bending of the wave and was responsible for the extended range effect. This case represents the exception rather than the rule for transmission distances.

Selection of a pulse transmission technique for the data transmission link is motivated by the effect of the earth's magnetic field upon the transmitted signal pulse as it enters the ionosphere. This effect, which was pointed out in Chapter III, produces a separation of the original pulse into magneto-ionic components. The selected pulse technique permits a comparison of the different magneto-ionic components on a relative basis, which facilitates an understanding of the possible causes of periods of non-reciprocity.

A transmitting and receiving station is required at the midpoint of the great circle path connecting the two stations comprising the data transmission link. The purpose of this station is to provide vertical ionosonde data which describes the composition of the ionosphere in the vicinity of the reflecting region of the obliquely incident signal pulses. This type of data provides information for utilization in the reduction and analysis of the signal data.

In previous test work discussed in the literature, the synchronization of transmitted signals was classified as a transmission link specification. For the present test specifications a technique based on a master-slave clock synchronization technique is utilized and for this reason, the technique is discussed in detail under a separate subheading.

Synchronization of Two-Way Transmission

Simultaneity is the fundamental foundation of any theoretical or experimental discussion of reciprocity as applied to the two-way oblique incidence transmission of electromagnetic waves via the ionosphere. Ideally the signal transmission from all of the stations comprising the signal transmission link should be initiated at the same instant of time. This ideal condition cannot be met under experimental conditions, but the synchronization technique proposed approaches this ideal condition and is predicated in such a manner that simultaneity is maintained as nearly as possible throughout the test periods.

The time synchronization technique relies on a comparison method between time signals transmitted at precise time intervals (such as the one-second pulses transmitted from Naval Radio Station NBA at 18 kilocycles or from WWV and WWVH at radio frequencies) from a standard station and time signals derived from a local standard oscillator. The Hewlett-Packard Company (26) has developed a combination frequency divider and clock instrument which can be used in conjunction with a local frequency standard to provide a local time standard which may be time synchronized to within a millisecond or less with a standard master clock or station located several thousand kilometers away. Figure 5 shows a block diagram of a typical time comparison test set-up. When the time comparison arrangement of Figure 5 is put into operation, the sharp one-second pulses derived from the local standard oscillator trigger the sweep circuit of the oscilloscope at precise one-second intervals. This means that the one-second trigger pulses are within one-half second of the closest time tick from the standard station. The Model 113AR instrument contains a continuously variable calibrated phase shifter which may be utilized to shift the phase of the 100

kilocycle signal from which the one-second trigger pulses are derived. The phase shifter now permits a shift of the one-second trigger pulses so that the oscilloscope sweep is triggered one to two milliseconds prior to the arrival of a standard time tick. The dial reading of the phase shifter is recorded as a reference point for calibration of the local time standard. Two factors are involved in the calibration of the local time standard.

If low frequency ground wave propagation is utilized, the following mode information is not necessary. First the transmission time delay between the standard and local stations must be computed. Although the basic concept of such a calculation is simple, the calculation itself is tedious. The National Bureau of Standards (27) has computed a number of curves which may be used to reduce the time required to compute the transmission time delay. In order to utilize these curves the great circle distance between the local and standard stations must be accurately computed from a knowledge of the latitude and longitude of the stations involved. The mode of ionospheric propagation must also be determined for high frequency transmission of the standard time signal. Once these factors are known, the curves previously noted may be utilized to determine the transmission time correction factor to be applied to the local time standard. Although ionospheric effects may cause variations in the computed transmission time delay, the overall deviation averaged over a number of days is very small. Accuracies to one part in 10^8 may be expected over a twenty-four hour period whereas accuracies of a few parts in 10^{10} may result for a comparison period of several days.

After initial calibration of the local time standard, the position

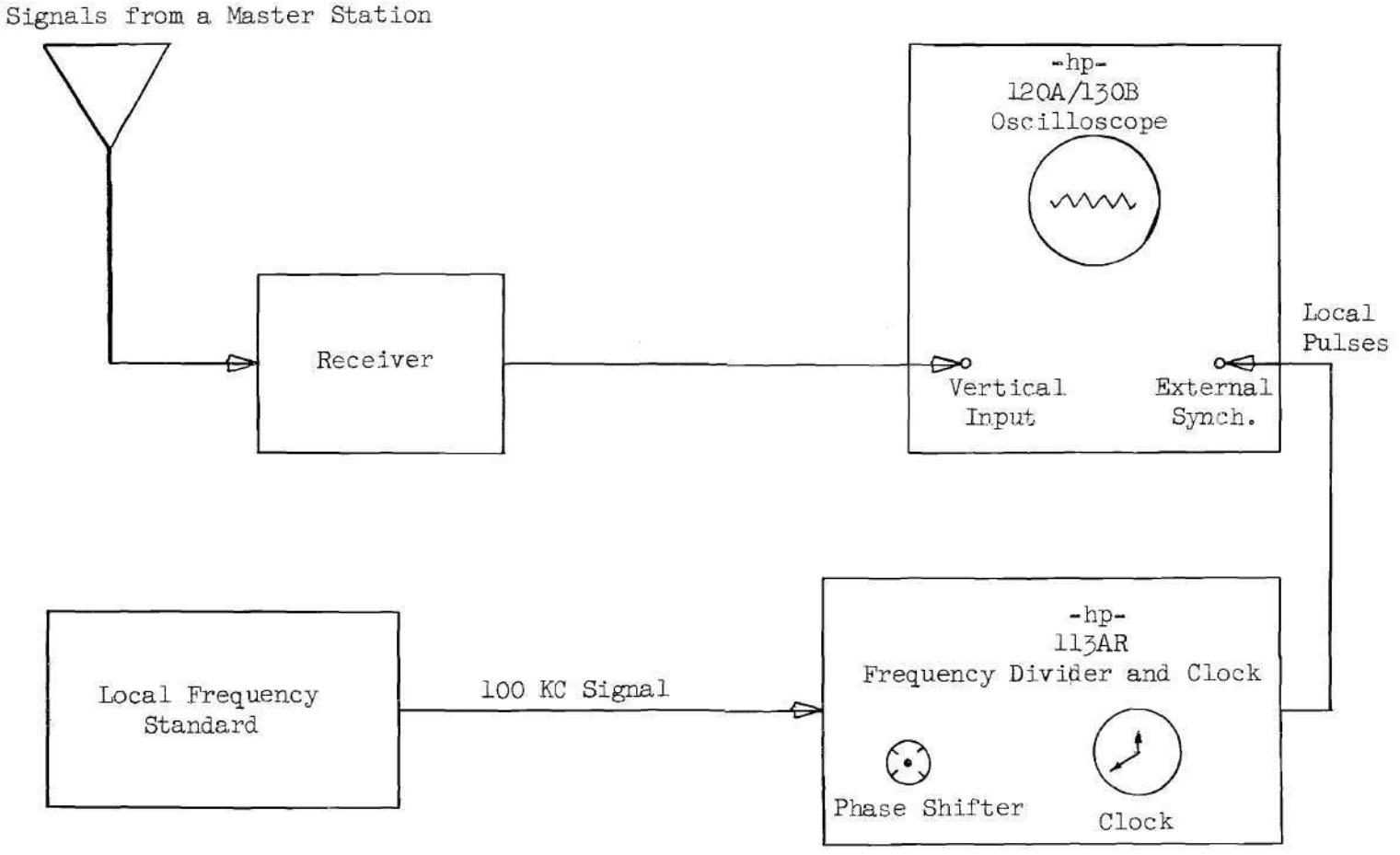

Figure 5. Time Comparison Test Set-Up Block Diagram.

of the standard time tick on the oscilloscope sweep must be monitored since any error or drift in the local frequency standard will cause a shift in this position. A log is kept indicating such variations in the local frequency standard. When such deviations are noted, the phase shifter is used to reposition the trigger pulses so that the standard time tick appears at its original position on the oscilloscope trace. In order to measure these deviations as accurately as possible, a camera is attached to the oscilloscope and pictures are made of the time tick sweep position. This provides a permanent record and minimizes the human error involved in sweep position determinations. The reading from such a trace can usually be made to a resolution of about 100 microseconds. This enables a comparison accuracy to about two parts in 10^9 to be achieved for a twenty-four hour period.

The local time standard located at each site comprising the data transmission link is independently synchronized with the same standard time station placing each site in time synchronization with the other sites. The trigger pulses provided by the site local time standards are then utilized to initiate and maintain the time synchronization of all test signals in oblique incidence ionospheric test work.

Transmitting and Receiving Equipment

The transmitting and receiving equipments located at both of the data transmission link sites must be identical. The transmitter characteristics should exhibit high stability with regard to frequency stability, transmitted pulse shape, and output power. They are therefore considered to be calibrated test equipments insofar as the tests are concerned. They must also be capable of both a fixed frequency and a swept frequency mode

of operation. The receiver characteristics should reflect a low noise figure, wide dynamic range and good stability. Their bandwidths must be such that they are capable of accepting the transmitted signal pulse with a minimum of distortion. For this reason it is important that the transmitter and receiver characteristics be mated. Selection of an antenna is predicated on the basis of both frequency and pattern considerations. Antenna patterns should be as constant as possible over the frequency band of interest and the patterns themselves should be such that data from all levels of the ionosphere may be obtained. A survey of the literature covering commercially available ionosonde equipment of this type indicated that the Granger Associates Model 902 Ionosphere Sounder (28) would satisfactorily meet the preceding requirements of a site transmitter and receiver. The model 902 characteristics are outlined in Table 2.

Table 2. Specifications of the Model 902 Transmitter/Receiver

Frequency range	4.05 to 63.6 Mc	fixed or swept
Number of channels	40, 80, 120, 160	selective
Pulses per channel	1, 2, 5, or 10	selective
Pulse repetition rate	2, 5, 10, 20, or 50 pps	selective
Pulse width	50, 100, 200, 500 or 1000 μ sec	selective
Duty cycle	2 per cent	maximum
Receiver bandwidth	6 or 16 kc	selective
Receiver Sensitivity	0.5 μvolts for $(s + n)/n = 2.1$	
Receiver dynamic range	greater than 30 db.	variable
Power output	500 watts	maximum

A suitable antenna for utilization with the model 902 Sounder is the Granger Associates Model 748 Double-Bay Fixed Log-Periodic Antenna (28) whose characteristics are shown in Table 3.

Table 3. Model 748 Antenna Characteristics

Frequency	4 to 64 Mc
Gain	13.5 db.
Azimuth Beam Width	60 degrees
Elevation Beam Width	25 degrees
Polarization	horizontal
VSWR	2 : 1
Power Capability	10 kw

The Model 902 utilizes a Hewlett-Packard Model 100ER frequency standard which can be used in conjunction with the Hewlett-Packard Model 113AR clock to provide the time synchronization necessary for conducting reciprocity tests.

Although two simultaneous outputs are provided by the model 902 Sounder, no display and recording equipment are included. In addition to the video output signals, adequate synchronization and control pulses are provided to coordinate the external recording equipment with the sounder's video output. Table 4 lists these pulses. The advantage of the two video outputs may be utilized by feeding one video signal to any oscilloscope with a frequency response of 500 kilocycles or higher, to which a 35 millimeter camera system is attached. One suitable camera system is the Beattie-Coleman Model KD-5 oscillotron recording system.

Table 4. Model 902 Output Pulses

Two Video Outputs
Start Pulse
Transmit Pulse
Synchronizing Pulse
Frequency Markers

This camera is equipped with an oscilloscope mount, and a clock and counter for continuous data recording. The other video output may be fed to a second oscilloscope for operator monitoring of data or for taking Polaroid pictures when desired.

Since the function of the third site is to obtain vertical incidence ionosonde data to aid in determining the composition of the ionosphere in the vicinity of the region of the oblique incidence reflections, the characteristic requirements of the transmitting and receiving equipments will differ from the equipments located at the data transmission link sites. The frequency requirements of the equipments located at this site are based on the frequencies utilized by the data transmission link and theorems by Briet and Tuve (29) and Martyn (30).

Briet and Tuve's theorem states that the transmission time of a ray traveling at the velocity of light over the fictitious triangular path shown in Figure 6 is the same as that of a ray traveling at its real velocity over the curved path through the ionosphere, if the earth's magnetic field and electron collisions are neglected and a flat earth and ionosphere are assumed. The neglection of electron collisions is a

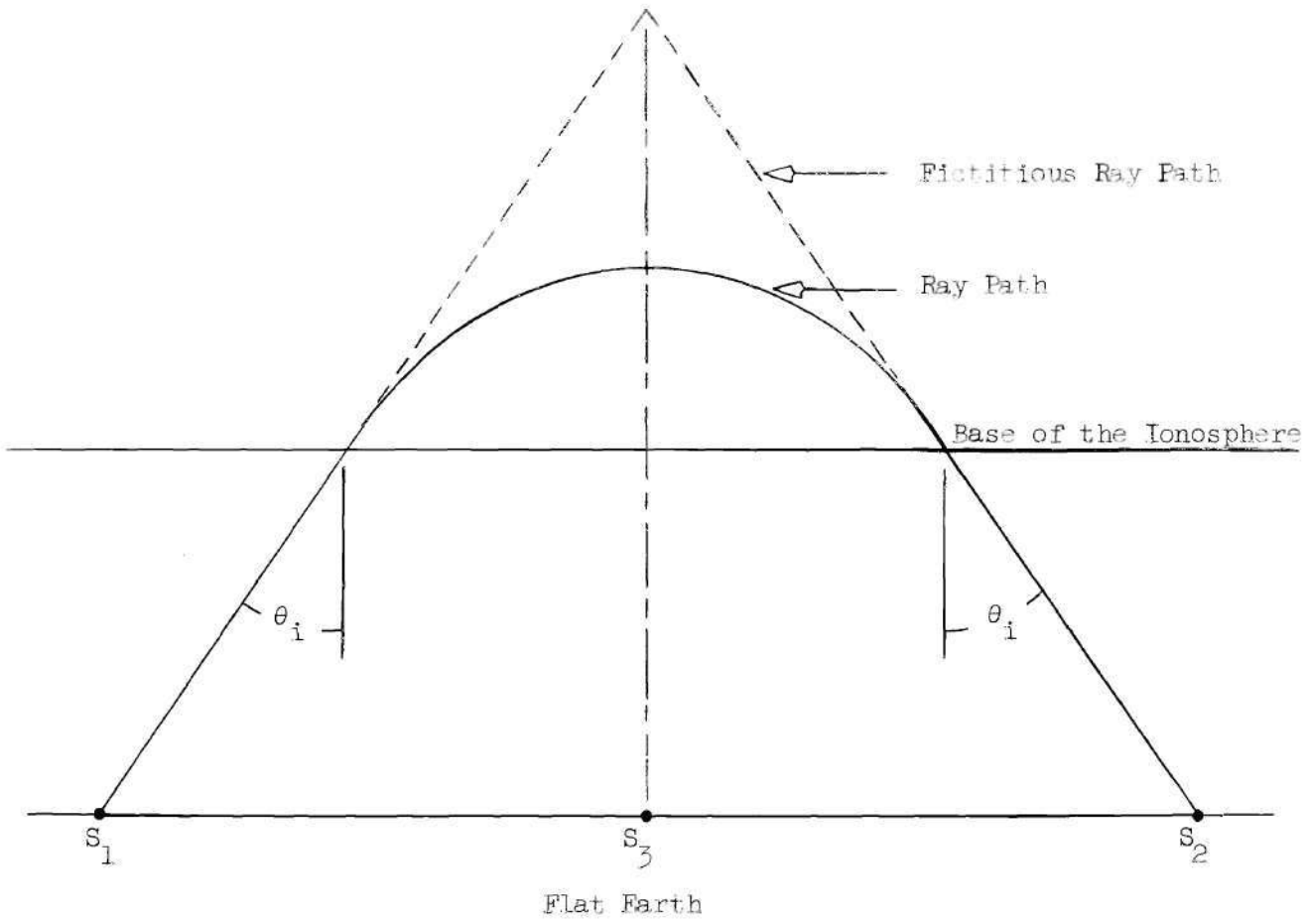

Figure 6. Flat Earth Approximation of the Equivalent Ray Path Neglecting $\underline{B}_o$.

very good approximation for the high frequency case considered in this study. Neglection of the earth's magnetic field infers that the results will apply approximately to the case of ordinary wave propagation. Appleton (31) and Beynon (32) extended the flat earth case to include the curvature of both the earth and the ionosphere, but the increased accuracy obtained by this extension was not sufficient to justify the use of the more complicated formula in view of the omission of the effects of the earth's magnetic field. Martyn has shown that the virtual height of reflection for frequency $f_v = f \cos \theta_i$ at vertical incidence is the vertical projection of the triangular path for a frequency f obliquely incident on the ionosphere at an angle θ_i. This means that the swept frequency operation of site S_3 may be centered in a narrow frequency band around $f \cos \theta_i$ during reciprocity runs.

The ionosonde data obtained at S_3 would also provide information which would be an aid in the identification of the reflecting ionospheric layers for the oblique case as well as contributing information about the maximum usable frequency for reciprocity runs. This data would also provide a means of correlating the theory of virtual and real heights of reflection for the oblique and vertical incidence cases.

The improved sweep-frequency ionosonde recorder Model C-4 discussed in reference (33) will provide the third station with adequate facilities for obtaining the necessary vertical incidence ionosonde data when used in conjunction with an antenna of suitable polarization and pattern and the local time standard described earlier in this chapter. This equipment is provided with an elaborate control system for unattended automatic operation which includes a provision for variation of the receiver

gain. A minor modification to the equipment is necessary since the clock associated with the unit has a stability of only one-half second per day. Replacement of this clock with the master-slave clock arrangement will provide the necessary time accuracy required by the theoretical test specifications.

Test Procedures

Several pre-test procedures are necessary prior to initiation of any experimental tests.

1. Local Time Standards. All three local time standards must be calibrated against the same standard station for a minimum of seven days. The comparison technique outlined earlier in this chapter must be utilized during this period and periodically thereafter to assure that the local standards maintain synchronization with the standard station.

2. Receiver Calibration. Each of the receivers utilized must be calibrated for gain and sensitivity prior to each period of testing.

3. Transmitters. Each of the two transmitters involved in the oblique reflection data transmission link must be checked to assure conformity of output pulse shapes, frequency, and power. The same procedure should be followed with the transmitter located at the third site.

4. Antennas. After installation of the two transmission link antennas at their respective sites, their radiation patterns must be measured. In the event the individual antenna radiation patterns are not identical, one of the patterns must be adjusted until both patterns are made as nearly identical as is practically possible. The third site antenna pattern should be checked to make sure that it is adequate for vertical incidence soundings.

In order to obtain reciprocity data, two general types of runs should be made. To check the short term reciprocity, a time run of three minutes may be utilized. For long term reciprocity runs, a time run of thirty minutes may be utilized. The mechanical sequence of the experimental procedure is listed below in order of time sequence.

1. All three receivers should be calibrated for gain and sensitivity and the results recorded.

2. On a pre-set instant of time all sites should begin operation in the swept frequency mode of operation, sweeping over the entire frequency range to obtain ionograms indicating the reflecting characteristics of the ionosphere. A Polaroid picture should be taken, at each of the three sites, on which the horizontal axis designates frequency and the vertical axis designates the virtual or apparent height of the reflecting region.

3. At the conclusion of the preceding step, the two stations comprising the data transmission link should switch to a fixed frequency mode of operation at a predetermined frequency f. Receiver gain settings should be recorded and at a pre-set instant of time, both of the stations should begin simultaneous transmission and reception of reciprocity signals for either three or thirty minute periods. The selection of these particular test periods is arbitrary. They may be adjusted if they are not suitable for a particular selection of a transmission link. During the test periods the data should be recorded on a time synchronized basis by the 35 millimeter camera system which would automatically place the necessary sweep and timing marks on each frame of film. It will also be necessary to record the sweep rate and calibrated gain of the scope used

in the camera system. The third station should remain in the swept frequency mode of operation during reciprocity runs and obtain vertical incidence ionosonde data in a frequency band Δf, centered about the frequency $f \cos \theta_i$. The width of the frequency band Δf is determined by the magnitude of $f \cos \theta_i$.

4. At the end of the test run, both of the link stations should return to the swept frequency mode of operation and obtain, on a synchronized basis, an ionogram indicating the regions of reflections at the end of the test runs.

5. Each time a test run is to be performed, steps 1-4 should be followed. Note: If voice communication is present at all of the sites, it will be possible to determine f and Δf at the time a test run is to be made. However if voice communication between the stations is not in operation at the time of the tests, the tests may still be performed on the basis of a pre-arranged time schedule since each site is equipped with a local time standard.

Data Reduction and Analysis

The first step in the reduction of the experimental data is the classification of the data according to the level or region of reflection, the mode of propagation (one-hop, two-hop, etc.) and to identify the magneto-ionic wave components. One of the first steps to be taken in completing this propagation classification is to reduce the swept frequency versus virtual height data recorded in photographic form (ionograms) since this data provides a source of information about the real or true height of reflection h and the distribution of the electron density N. Mathematically the relationship between the virtual height of

reflection h' and the group index of refraction n' is given by

$$h' = \int_{o}^{h_o} n' dz \tag{48}$$

where n' is a function of the electron density N, of the electromagnetic wave frequency f, of the direction and the magnitude of the earth's magnetic field $\underline{B}_o$ relative to the direction of propagation for the wave. There are many papers in the literature which describe techniques to effect the solution of equation (48) for the vertical incidence case. These techniques may be classified into two general categories, the comparison method and the inversion method.

In the comparison method a distribution of the electron density with height h is assumed and substituted into equation (48). Evaluation of the integral by numerical techniques then yields a curve of the variation of the virtual height h' with frequency f. This procedure is followed for a number of assumed distributions of N with height h yielding a number of computed curves which may be compared with experimental h'-f curves. Beynon and Thomas (34) present an excellent discussion of the comparison method for the case of vertical incidence where the effect of the earth's magnetic field has been neglected. Becker (35) extended this analysis to include the effects of the earth's magnetic field. This method has the disadvantage that an a priori assumption is made about the complete layer shape.

In the integral inversion method, two general techniques may be followed. If the earth's magnetic field and the collisions of electrons with heavy particles are neglected, equation (48) reduces to an Abelian integral equation which may be directly inverted to yield an analytical solution. For this case $h(f_p)$ may be expressed as

$$h(f_p) = \frac{2}{\pi} \int_0^{f_p} \frac{h'(f)\, df}{\sqrt{f_p^2 - f^2}} = \frac{2}{\pi} \int_0^{\pi/2} h'(f_p \sin \gamma)\, d\gamma \quad (49)$$

where $\gamma = \sin^{-1} (f/f_p)$ and f_p is the plasma frequency at the height $h(f_p)$ where the electron density is N. Kelso (36), (37) and (38) performed the integration by numerical techniques and extended the method to include the effects of the earth's magnetic field. A second approach to the integration inversion problem is by the method of laminations. Titheridge (39) describes a lamination technique based on the change in the height at successive frequencies and in the changes in the group retardation due to a given segment of ionization as the wave frequency is increased. This technique is applicable to both the ordinary and extraordinary wave traces on the ionogram. Although this technique is not as accurate as some methods now in use utilizing digital computers, its use is justified by the speed with which the ionogram data may be reduced with a minimum of manual aids.

The principle of the technique is as follows. The N(h) curve is divided into a series of heights h_m (see Figure 7) corresponding to the virtual heights of reflection h'_r at the frequencies f_r. If it is assumed that n'_{rm} is the mean value of n' over the lamination h_{r-1} to h_r for a wave frequency f_r, n'_{rh} may be expressed as

$$n'_{rm} = \left[\frac{1}{h_r - h_{r-1}}\right] \int_{h_{r-1}}^{h_r} n'\, dh \quad (50)$$

It is necessary to assume a shape for the N(h) curve within a particular lamination to evaluate equation (50). If the laminations are very small,

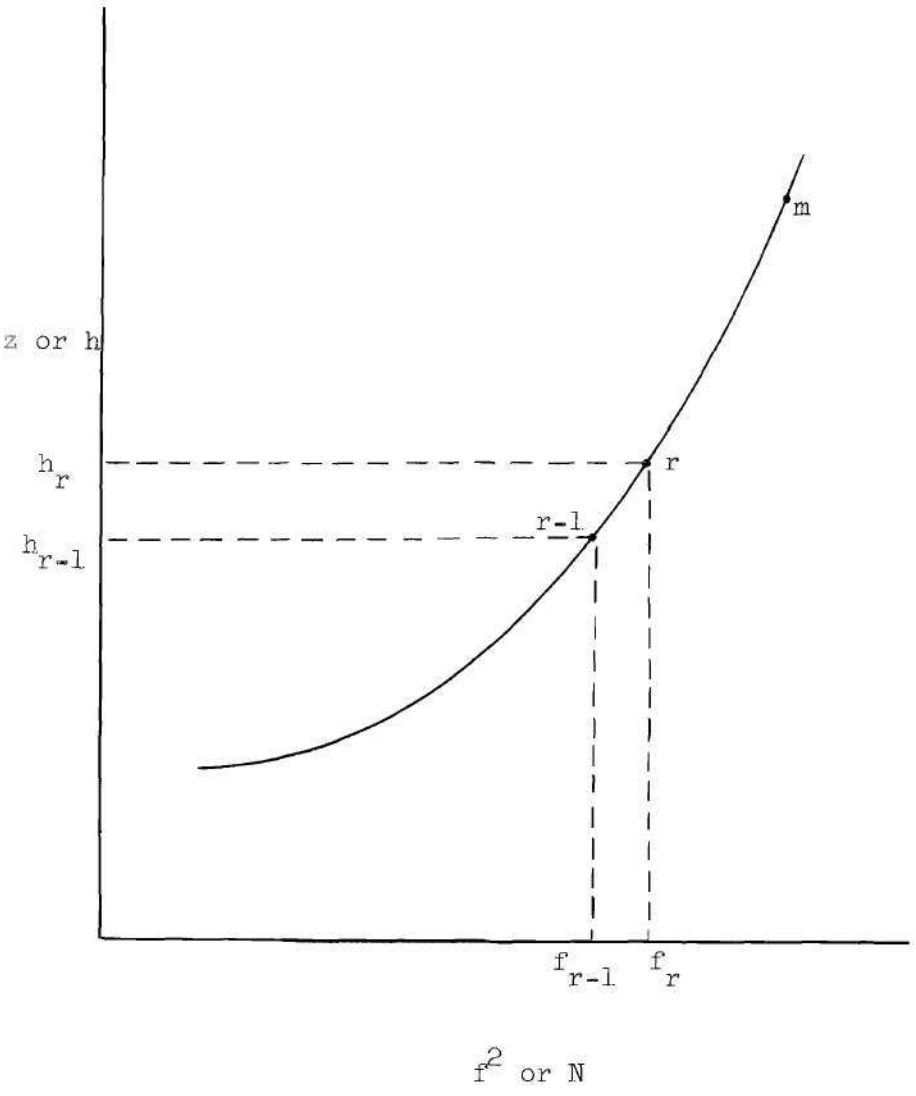

Figure 7. Subdivision of the N(h) Curve.

h may be assumed to vary linearly with N or f. Since the virtual height at any frequency is equal to the real height at that frequency plus the sum of the group retardations produced by each of the underlying laminations, the virtual heights may be written as

$$h_o' = h_o \,, \tag{51}$$

$$h_1' = h_1 + (n_{11}' - 1)(h_1 - h_o), \text{ and}$$

$$h_2' = h_2 + (n_{22}' - 1)(h_2 - h_1) + (n_{12}' - 1)(h_1 - h_o), \text{ etc.}$$

Substitution of $\Delta h_m = h_m - h_{m-1}$ and successive solution of equation (51) yields

$$\Delta h_m = \frac{1}{C_{mm}} \left\{ \Delta h_m' + \sum_{r=1}^{m-1} C_{rm} \Delta h_r \right\} \tag{52}$$

where $C_{rm} = n_{r,m-1}' - n_{r,m}'$ where $r < m$ and $C_{mm} = n_{mm}$. An accurate N(h) curve can now be computed through utilization of a vertical incidence ionogram and equation (52). Application of Titheridge's method to deduce N(h) profiles from the vertical incidence ionograms obtained at the mid-point station will provide a description of the structure of the ionosphere in the vicinity of the region of the oblique reflections. The ionograms obtained via the obliquely oriented transmission path may also be reduced and compared to the vertical incidence data for correlation purposes. The q, α curves (see Figure 4, p. 25) must be computed using equations (25) and (26). Identification of the magneto-ionic wave components may be made through utilization of the N(h) profiles and the q,α curves. In addition the layer or region of reflection of the wave

components may be ascertained from a correlation of the N(h) profiles, the q,α curves and the ionograms recorded at each receiving site.

In order to determine the modes of propagation of the reciprocity data, the signal transmission time delays must be determined. The received pulse data from each of the two data transmission link sites must be reduced to composite form on a time synchronized basis in terms of test initiation time and individual transmission times. At the beginning of each test run, time synchronization codes will appear on successive frames of filmed data. The two film rolls can be matched so that these synchronization marks are aligned. On each frame in the roll, a transmission timing mark appears. These must be aligned by frame so that the transmission time delays from transmitter to receiver may be determined. Coupled with a knowledge of the great circle path between stations, the height or layer of reflection, and the computed time delays for the various modes of propagation (one-hop E, two-hop E, one-hop F_1, etc.) over the existing data transmission link; the above information will provide a mode of propagation classification of the data. Data reduction is then completed by converting the recorded data to receiver input signal form by utilizing the receiver gain settings.

Any experimental wave propagation data, even though obtained under ideal test conditions, will exhibit some random amplitude fluctuations. In view of this condition, it would appear that a statistical interpretation of the experimental data might yield useable results. However by interpreting the reciprocity data in a statistical sense, the time dependence aspect of the problem is lost. Computation of a correlation coefficient and the subsequent interpretation of this computed coefficient

does not give sufficient information about the existence of reciprocity. It is apparent that at any time that relative reciprocity exists, a computed correlation coefficient would be approximately equal to one. Unfortunately the converse is certainly not true. A computed correlation coefficient approximately equal to one does not imply the existence of reciprocity, it only implies that a set of points plotted on a scattergram approximate the locus of a straight line. This condition is illustrated and discussed in Chapter VI.

Although an interpretation of the data in terms of the relative reciprocity theorem is presented in terms of a manual procedure, the technique provides additional insight into the general problem. A graphical interpretation of the experimental data requires that two basic plots be made. In the first plot (Figure 8) the two receiver input signal amplitudes are plotted versus one another. During periods in which relative reciprocity exists, the loci of these corresponding sets of points may be approximated by a straight line. To provide a time correlation basis for the data, a second graphical plot is necessary. The amplitudes of both signals are plotted versus time (Figure 9) and the corresponding periods during which relative reciprocity exists are designated.

To determine the periods during which relative reciprocity exists, the signal data from both stations is plotted on the relative plot of Figure 8 where each pair of points is associated with a time order of occurrence. As the points are plotted, it will be observed that they can be approximated by a straight line during the periods of time in which relative reciprocity exists. As soon as the points depart from this straight line approximation the corresponding time period is designated

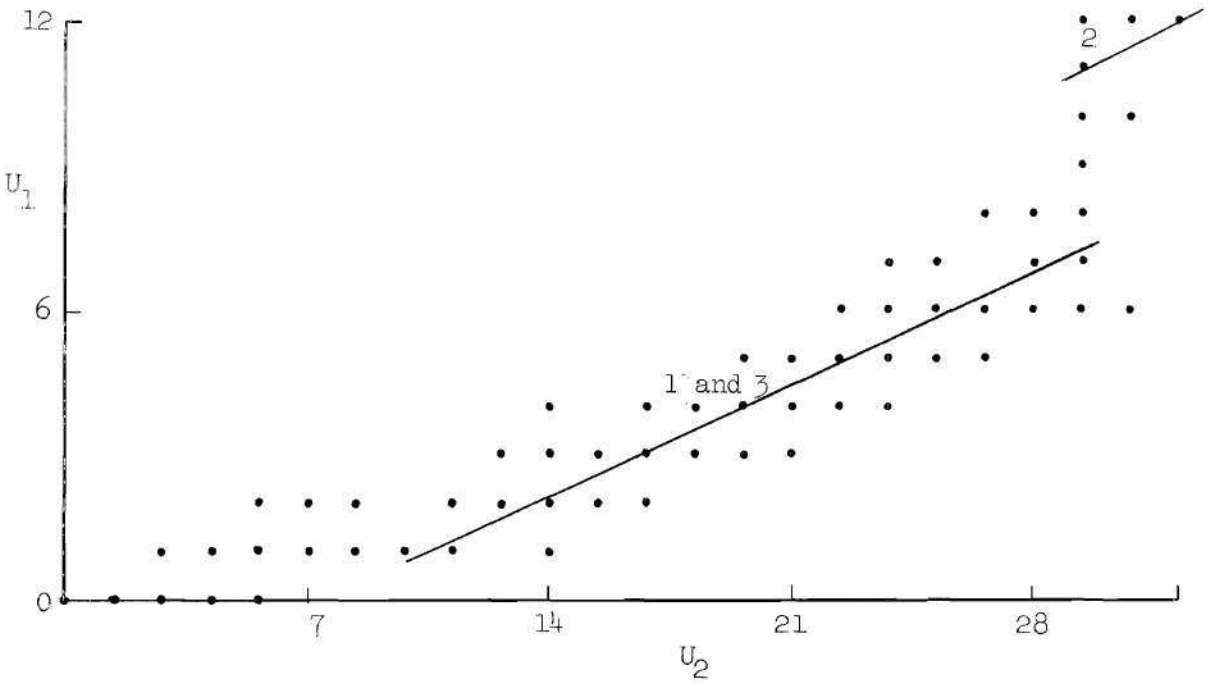

Figure 8. Relative Plot of the Antenna Output Signals.

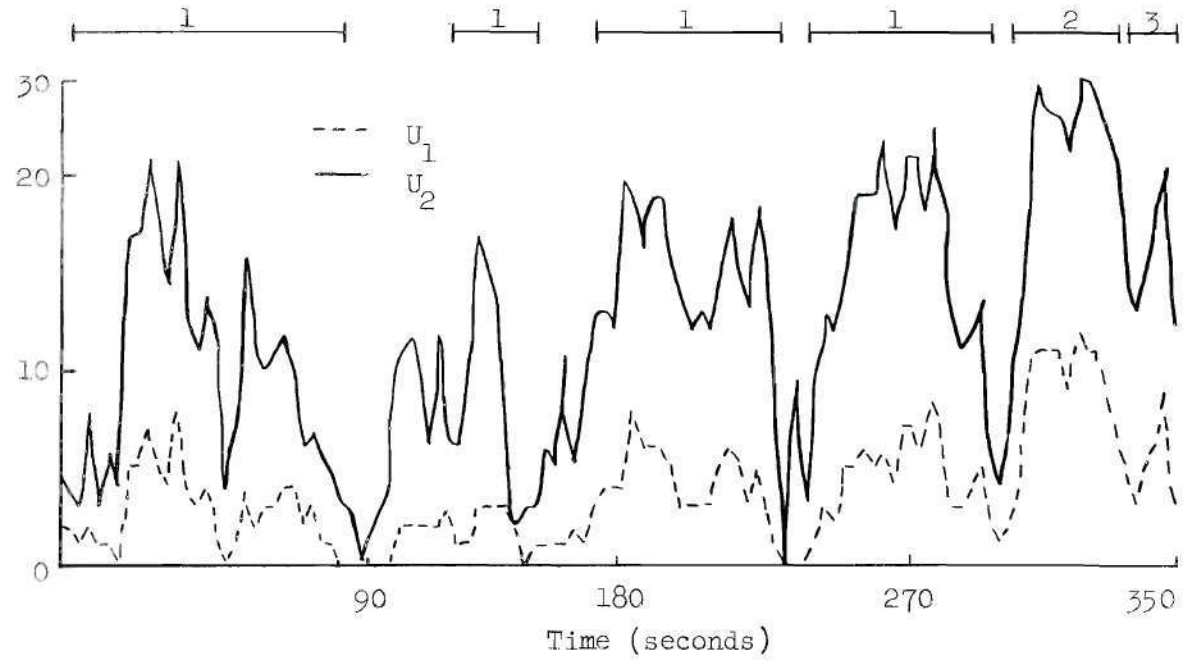

Figure 9. Time Plot of the Antenna Output Signals.

on the time plot of Figure 9.

The results of a time plot similar to Figure 9 may be utilized to define a time weighing function T_W which indicates the decimal portion of the test period during which relative reciprocity exists. If the portion of the test period during which relative reciprocity exists is defined as T_R and the period during which non-reciprocity exists is defined as T_N, the time weighing function T_W may be expressed as

$$T_W = \frac{T_R}{T_R + T_N} \tag{53}$$

Application of equation (53) to a set of experimental data will yield approximate results in terms of a time weighing factor which may be used to compare experimental reciprocity data obtained over a period of time in light of the existence or non-existence of relative reciprocity.

CHAPTER VI

APPLICATION OF THE RELATIVE RECIPROCITY THEOREM

The mathematical validity of the "relative reciprocity theorem" was established in Chapter IV. The purpose of the present discussion is to demonstrate the practical validity and application of the theorem. Although no experimental tests were conducted during the present study, some recent experimental reciprocity data was available to the author for reduction. The experimental work from which this reciprocity data was derived was financed by the Lincoln Laboratory of the Massachusetts Institute of Technology under subcontract No. 92 to prime contract AF 19 (604)-5200. Experimental work was performed through the facilities of and by personnel of the Communications Branch of the Engineering Experiment Station, Georgia Institute of Technology.

Comparison of the Theoretical and Experimental Test Conditions

Prior to any reduction and interpretation of the experimental reciprocity data, the conditions existing during the actual experimental tests must be examined in comparison with the optimum test conditions specified in Chapter V. The purpose of this comparison is to establish the procedures by which the relative reciprocity theorem is to be applied to the data and to facilitate an interpretation of the results obtained through utilization of the theorem.

The experimental data was obtained over a two-way transmission

link existing between Ipswich, Massachusetts and Fairburn, Georgia (a great circle path length of approximately 1556.5 kilometers). Tests were conducted during a period beginning February, 1959 and ending September, 1959. Only two operational sites were involved in the experiments, therefore the vertical incidence ionosonde data, required by the theoretical test specifications, was not available during these experimental tests. A lack of this type of ionosonde data makes it more difficult to relate the oblique incidence data to the composition of the ionosphere during periods of either reciprocal or non-reciprocal transmission.

Orientation of the principle axes of the major lobes of the rhombic antennas utilized in the tests were such that the horizontal azimuth pointing of the transmission path from Fairburn to Ipswich was approximately 45 degrees east of magnetic north and the vertical pointing was approximately 10 degrees above the tangent to the earth's surface. The antennas, transmitting and receiving equipments were as nearly identical as is practically possible, thereby conforming to these theoretical test specifications.

The experimental synchronization technique did not conform to the general specifications of the technique described in Chapter V, since the experimental technique depended upon the composition of the ionosphere to a much greater extent than the theoretical technique. Prior to each experimental run the two transmitters involved in the tests were manually pulled into synchronization by observing received pulses on the scope presentation of the receiver output network. Once this has been accomplished, time synchronization was accomplished by the utilization of an

uncalibrated secondary frequency standard. The inherent disadvantage of such a technique is that the original step in synchronization depends upon the mode of propagation via the ionosphere, a condition which was not established in many of the tests for several days or possibly a longer period of time after the test had been performed. In addition the fact that the secondary frequency standards were not in continuous calibration against a standard time station, coupled with the preceding condition, could easily contribute time differences in synchronization in the order of 100 microseconds. This does not mean that the reciprocity data is not useful data, but it does indicate that the overall time accuracies specified by Falcon (25) are doubtful.

Although the transmitting and receiving equipments at both of the tests sites were identical, the test procedures used during the tests deviated from the theoretical specifications. Neither of the receivers was calibrated for sensitivity or threshold level. In addition there was no correlation between the individual gain settings at the different sites. Each site operator independently set his receiver gains prior to each test run and maintained these particular gain settings throughout the run. Unfortunately the gain settings were not recorded along with the other pertinent test data. Figure 10 shows a block diagram of the receiver and the unknown gain constants. Referencing Figure 10, the receiver input and output signals may be related by

$$V_M = B_M \log_{10}(A_M U_M) \quad \text{and} \tag{54}$$

$$V_G = B_G \log_{10}(A_G U_G) \quad .$$

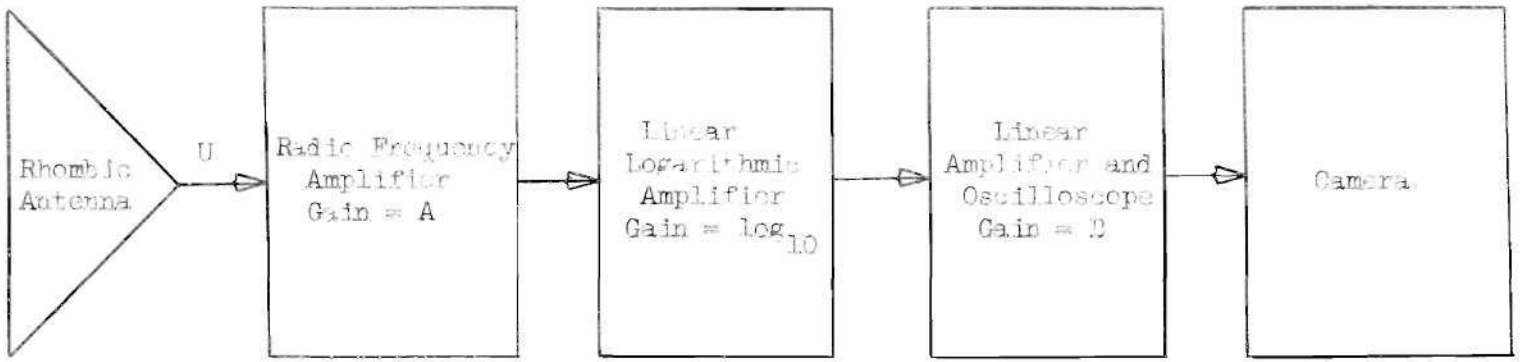

Figure 10. The Receiving System Block Diagram.

The subscripts M and G denote the received signals at the Massachusetts and the Georgia sites respectively. The receiver output signals V_M and V_G were recorded photographically on film at each site and were superimposed in composite form on a single film strip on a time synchronized basis at a later time. Only oblique incidence ionograms were recorded prior to each reciprocity run, so no N(h) profiles were computed. Classification of the pulse data as to the region of reflection and mode of propagation was based on these ionograms and the transmission time delays obtained from the recorded pulse data. No attempt was made to classify the experimental data as to wave components, i.e. ordinary or extraordinary waves.

The interpretation of the reciprocity data in terms of a sample correlation coefficient is questionable in view of the relationship between the receiver input and output signals as given by equation (54). Any interpretation of the significance of a sample correlation coefficient is predicated on the basis that a linear regression line exists when the data is plotted on a scattergram (40). Since the receiver gains are unknown, the output data cannot be converted to receiver input data form. Therefore any interpretation of a sample correlation coefficient, derived from the output data, in terms of the input data violates the general mathematical precepts of the theory involved. However it may be shown that such an interpretation is possible for one special case. During periods in which relative reciprocity exists between the receiver input signals, equation (54) may be reduced to

$$V_G = (B_G/B_M)\, V_M + B_G \log_{10} (bA_G/A_M) \qquad (55)$$

by substitution of the relationship $U_G = bU_M$. This equation is a straight line in the V_G, V_M plane if b is a constant. For this one case a linear regression line does exist in the U_G, U_M plane and a sample correlation coefficient computation based on receiver output data would be one, indicating correlation between receiver input signals.

An Interpretation of Some Experimental Data in Terms of Relative Reciprocity

In order to apply the relative reciprocity theorem of Chapter IV, a relationship between the receiver input and output signals must be established in terms of the unknown receiver gain constants. Equation (54) may be rearranged to give

$$U_G = (A_M/A_G)\left[10^{(V_G/B_G - V_M/B_M)}\right]U_M . \qquad (56)$$

Equation (56) may be simplified during the periods in which relative reciprocity exists between U_G and U_M by substitution of the relationship ($U_G = bU_M$) yielding equation (55). An interpretation of equations (55) and (56) in terms of the relative reciprocity theorem now provides a means of interpreting the receiver output data and commenting on the variation of the receiver input data, which is the data of interest.

During periods in which relative reciprocity exists between the two receiver input signals U_M and U_G, equation (55) represents the equation of a family of straight lines in the V_G,V_M plane. Since A, B, and b are positive, these straight lines have positive slopes equal to (B_G/B_M) and V_G intercepts equal to $B_G \log_{10}(bA_G/A_M)$. During periods of non-reciprocity, equation (56) indicates that the locus on the V_G, V_M plane

will be a logarithmic curve.

Another factor affecting the interpretation of the test data is the linearity of the receiver characteristics. Since the characteristics of the linear logarithmic amplifier utilized in the tests are not available, the following comments are based on a set of linear logarithmic receiver characteristics presented by Chambers and Page (41). Figure 11 shows the amplitude response characteristics of two such logarithmic receivers. The amplitude characteristics of the receivers experience a deviation from linearity at both the upper and lower ends of the curves. This condition will be reflected in the reciprocity data when the amplitude of either of the signals is near the threshold level or the saturation level of the receivers. During periods in which relative reciprocity exists, this effect will appear as a deviation of the data from a straight line approximation when the signal amplitudes are very small or very large. Several cases in which this condition exists are noted in succeeding paragraphs.

Table 5 contains the pertinent information concerning some representative experimental reciprocity data which was reduced and interpreted in terms of the relative reciprocity theorem.

Table 5. Classification of Data

Figure No.	Test Date	Test Time(EST)	Frequency(Mc)	Mode	Tw
12	3/10/59	1150	16.95	1E	0.85
14	3/5/59	1405	16.95	1E	0.69
16	3/5/59	1420	16.95	1E	0.61
18	9/10/59	1044	16.95	1E	0.61
20	4/21/59	1422	16.55	1E	0.46
22	4/21/59	1434	16.55	1E	0.46

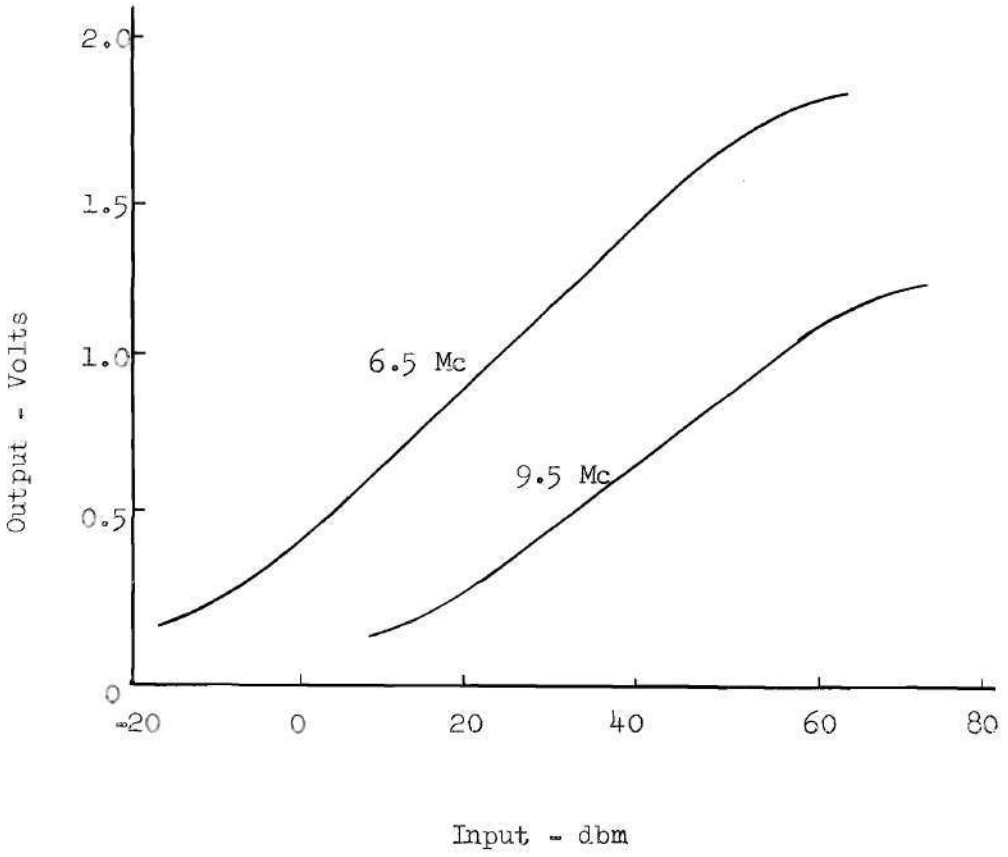

Figure 11. Amplitude Response of Broad-Band Logarithmic Receivers.

Figures 12 through 23 show the corresponding relative and time plots of the reciprocity data. A comparison of the time weighing factors and computed sample correlation coefficients for Figures 20 and 22 illustrates one of the disadvantages of trying to interpret reciprocity in terms of such a correlation coefficient. The two sets of data were obtained in tests performed on the same day in a twelve minute interval. The time plots of the two sets of data (Figures 21 and 23), indicate a striking similarity in the shapes of the two curves, a condition to be expected for normal atmospheric conditions. This same condition is reflected by a comparison of the time weighing factors for the two sets of data (Table 5). A comparison of computed correlation coefficients based on this same data shows one coefficient equal to 0.67 (Figure 20) and the other equal to 0.90 (Figure 22).

Another interesting feature of the relative plots of the data is the fact that the slopes of the straight line approximations indicate that the gains of both receiver output stages were the same for a majority of the experimental runs considered in this study. This is evident since the slopes of the straight line approximations for most of the experimental runs, during periods of relative reciprocity, are approximately one based on a graphical computation. Comparison of this value of m with the theoretical slope $m = (B_G/B_M)$ shows that B_G and B_M are of the same magnitudes. Figure 12 contains an exception to this case. The slope for this case is approximately one half indicating that B_M is approximately twice B_G. Figures 12, 16, 18 and 22 illustrate the nonlinearity of the receiver gains near the threshold level.

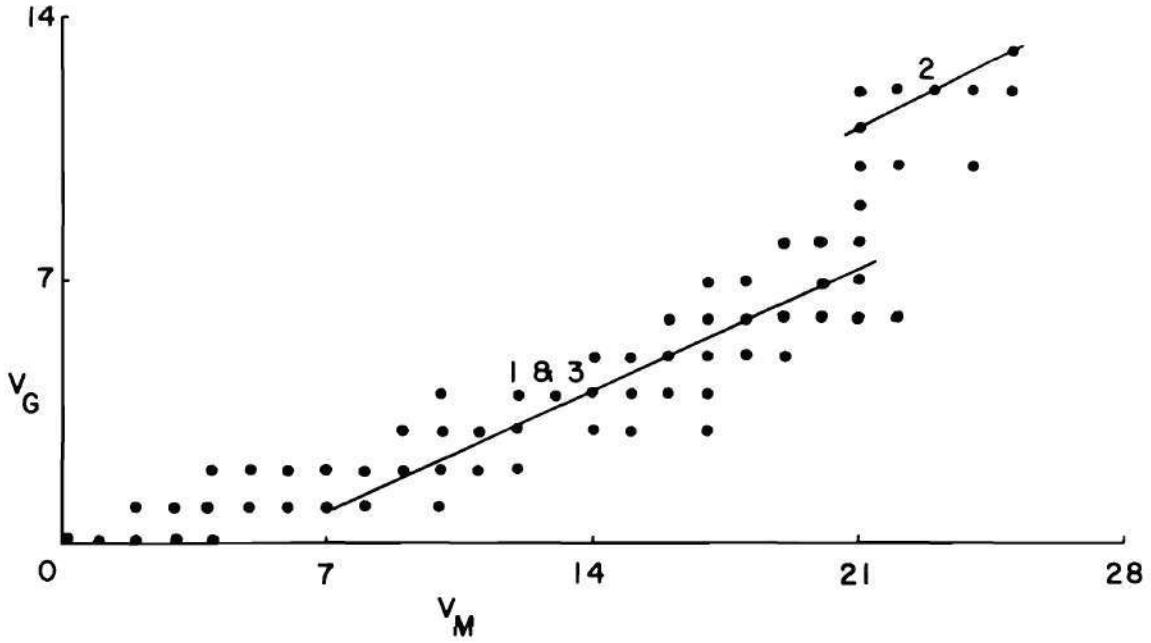

Figure 12. Relative Plot of Experimental 1E Data, f = 16.95 Mc.

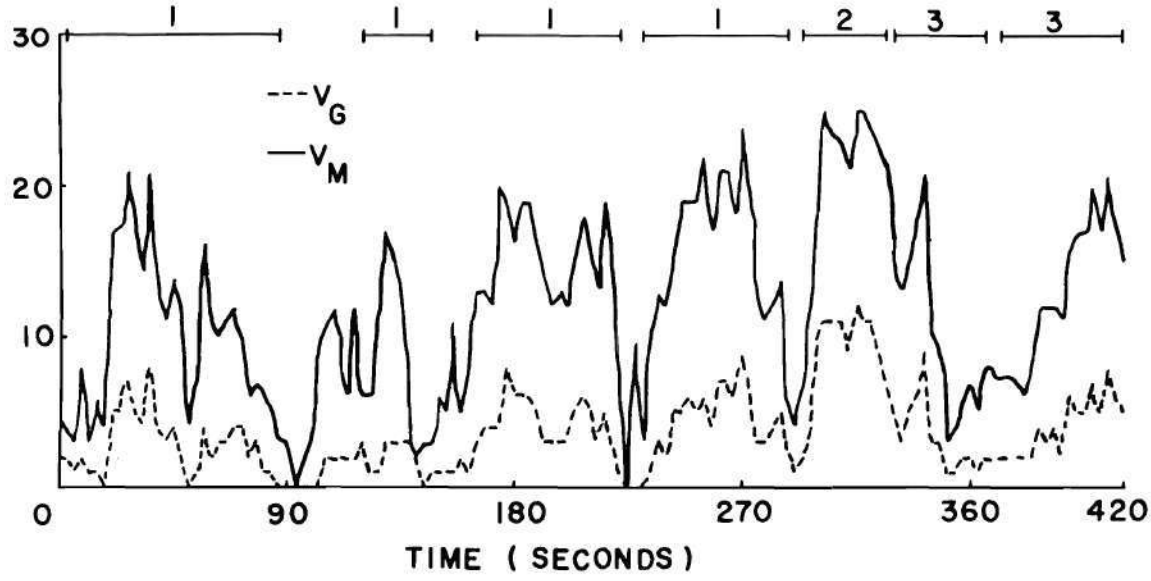

Figure 13. Time Plot of Experimental 1E Data, f = 16.95 Mc.

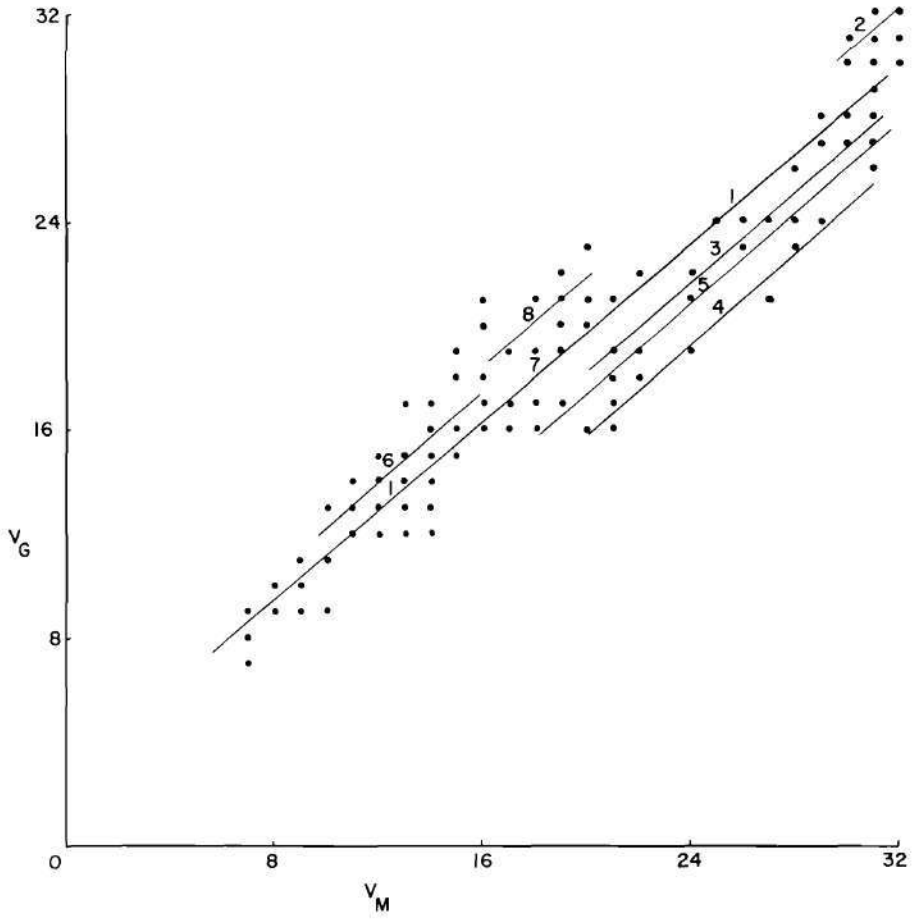

Figure 14. Relative Plot of Experimental 1E Data, f = 16.95 Mc.

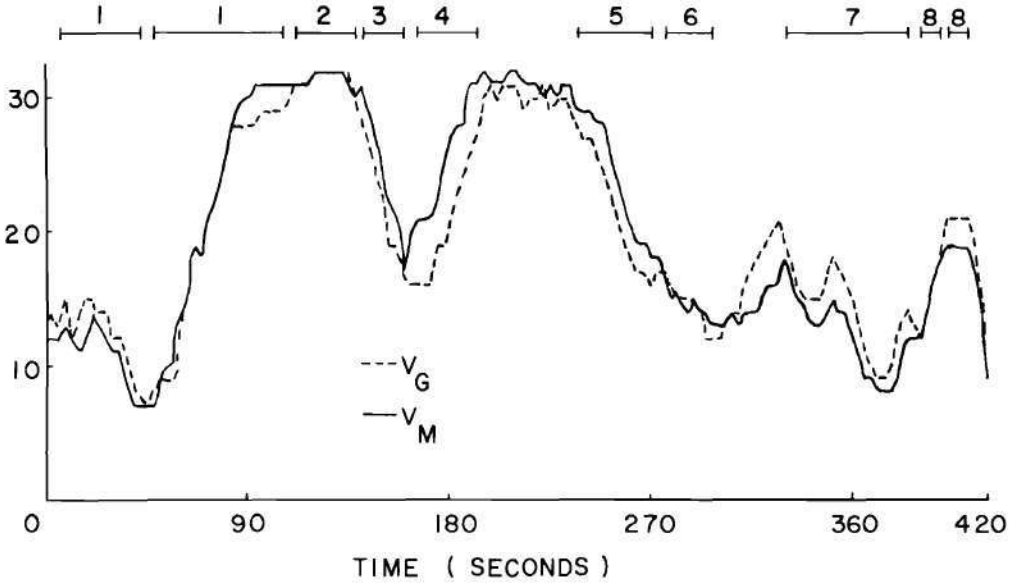

Figure 15. Time Plot of Experimental 1E Data, f = 16.95 Mc.

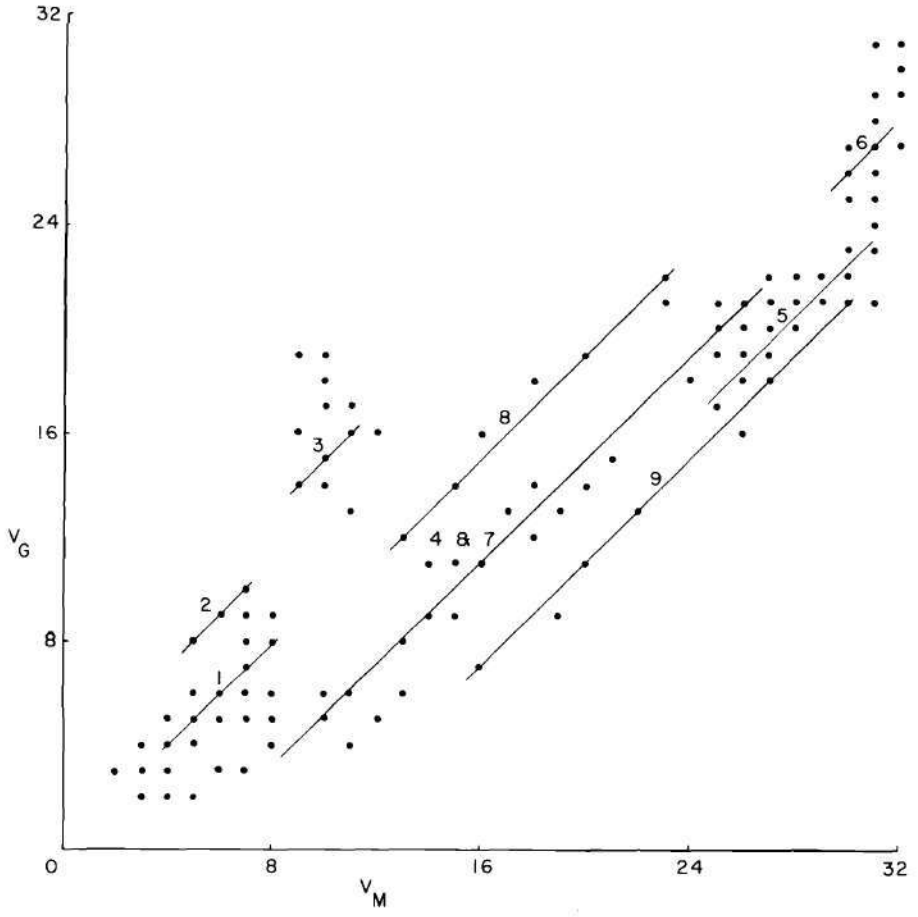

Figure 16. Relative Plot of Experimental 1E Data, f = 16.95 Mc.

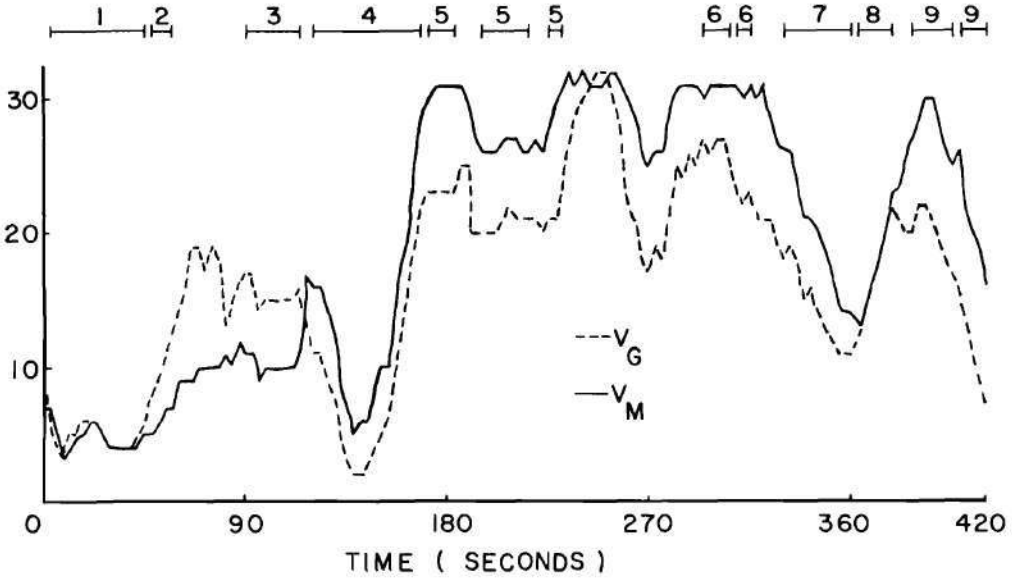

Figure 17. Time Plot of Experimental 1E Data, f = 16.95 Mc.

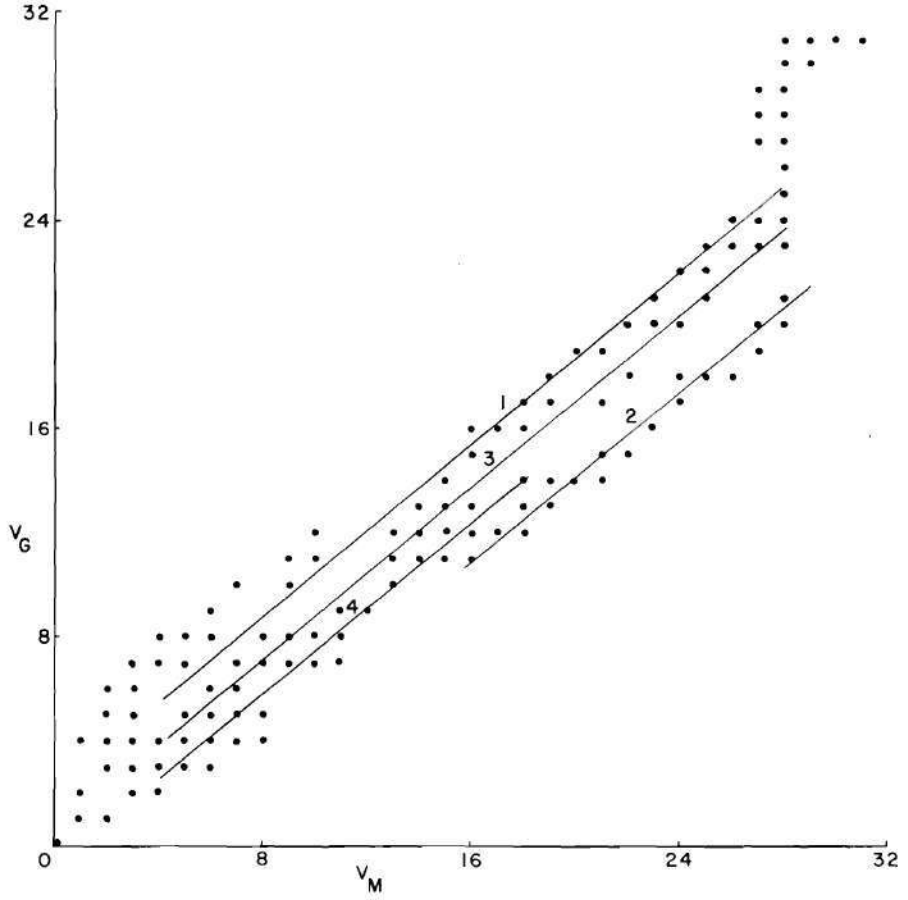

Figure 18. Relative Plot of Experimental 1E Data, f = 16.95 Mc.

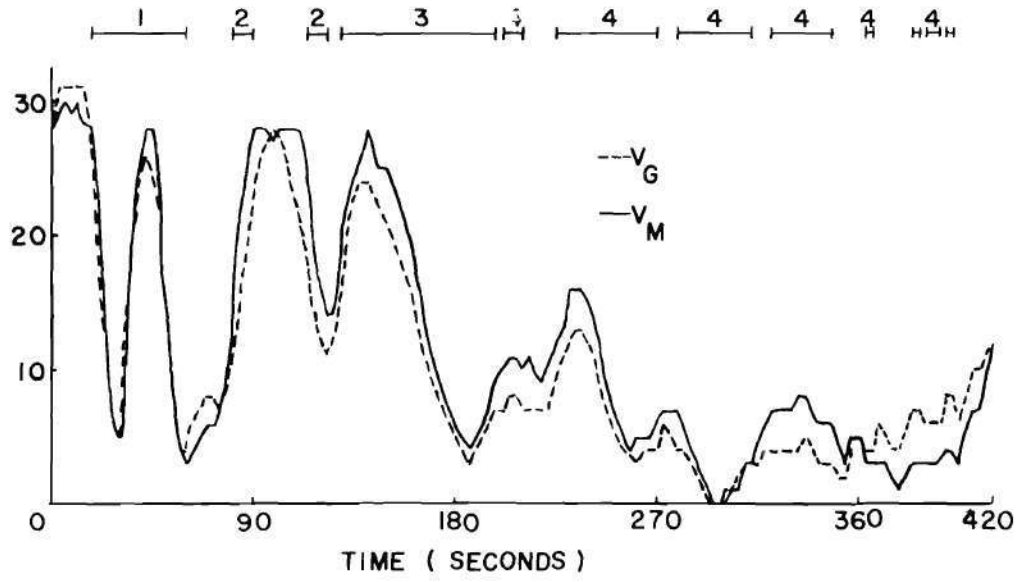

Figure 19. Time Plot of Experimental 1E Data, f = 16.95 Mc.

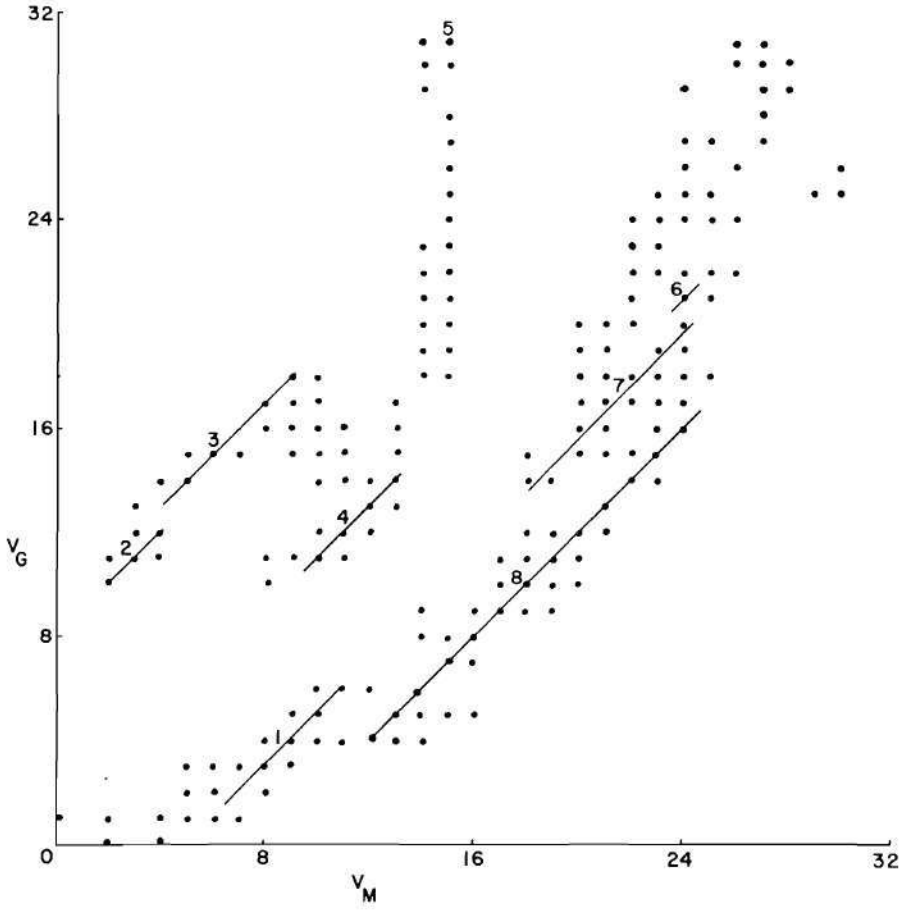

Figure 20. Relative Plot of Experimental 1E Data, f = 16.55 Mc.

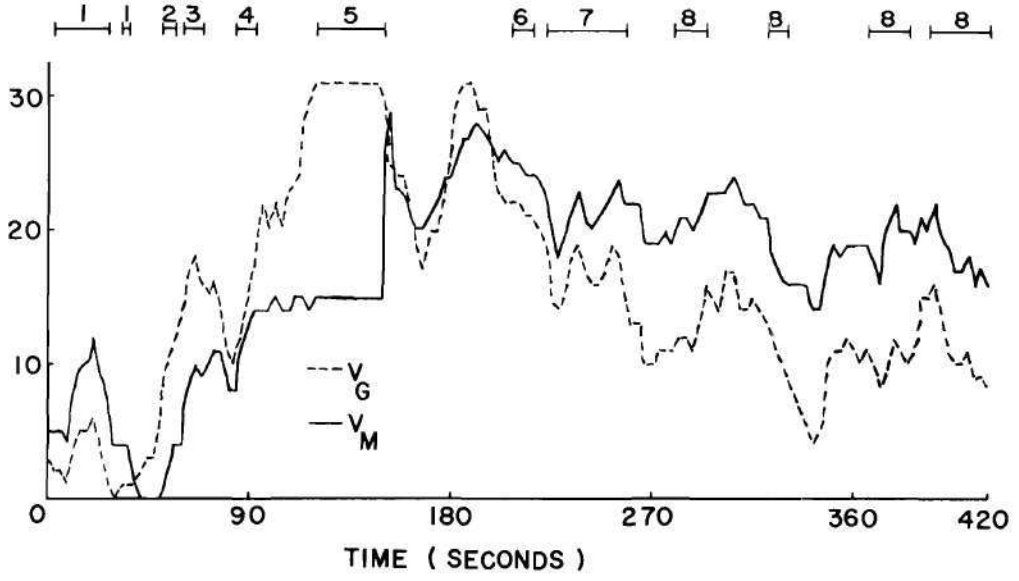

Figure 21. Time Plot of Experimental 1E Data, f = 16.55 Mc.

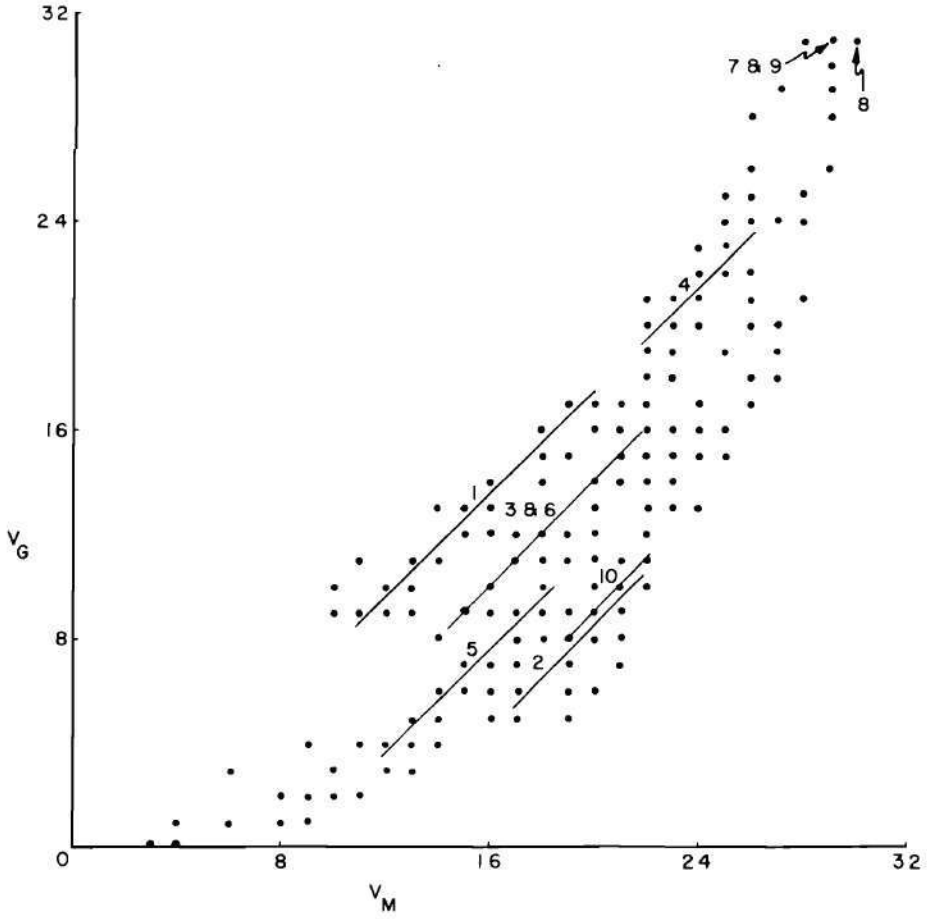

Figure 22. Relative Plot of Experimental 1E Data, f = 16.55 Mc.

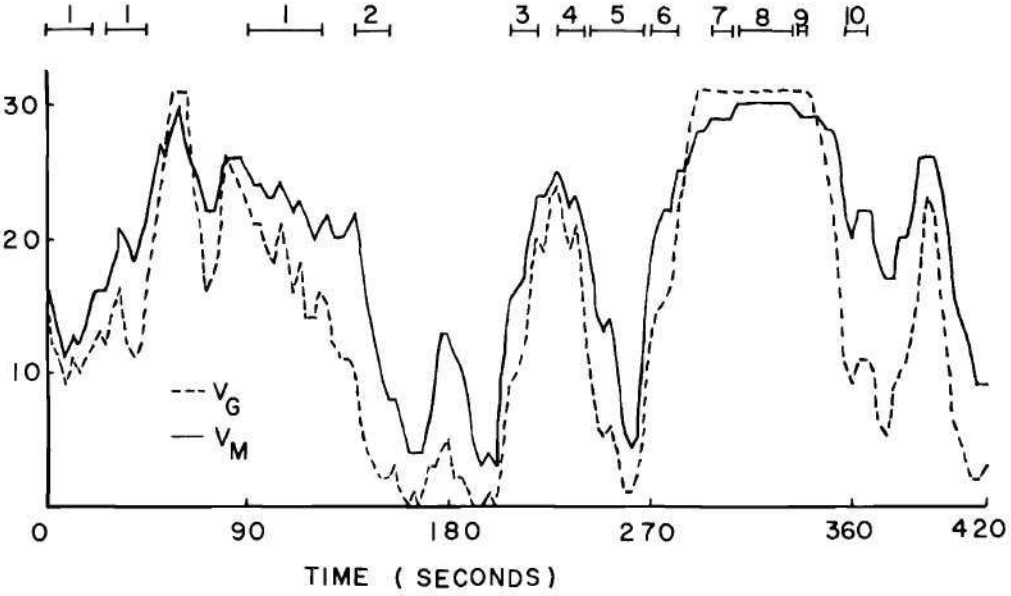

Figure 23. Time Plot of Experimental 1E Data, f = 16.55 Mc.

The preceding computations and results clearly demonstrate the practical value and the versatility of the "relative reciprocity theorem." A set of experimental data (obtained under less than optimum conditions) has been reduced and interpreted in light of this theorem and the test specifications formulated in Chapter V in a manner which provides a technique for cataloging and comparing the "reciprocity" of experimental propagation data.

CHAPTER VII

AN INVESTIGATION OF FACTORS CONTRIBUTING TO NON-RECIPROCAL TRANSMISSION

During the process of reducing and interpreting the experimental data discussed in Chapter VI, a question arose concerning factors which contributed or possibly caused the periods of non-reciprocal transmission observed in the data. In order to provide in some measure answers to this question the magneto-ionic wave equations (Booker's equations) were programmed for solution on a digital computer for the conditions existing over the Fairburn-Ipswich transmission link. The following discussion is based upon an interpretation of the results obtained from the digital computer solutions of equations (25) and (33).

Since Booker's equations do not take into account the penetration of more than a single ionospheric region, the following remarks are applicable to the one-hop, E-region mode of reflection (the only type of reciprocity data reduced in terms of the relative reciprocity theorem). In following the wave packet along its propagation path in the ionosphere, it must be noted that the wave packet does not remain in the original plane of incidence. It experiences a lateral deviation in a plane perpendicular to the original plane of incidence on both the upgoing and the downcoming portions of its path in the ionosphere. As a matter of fact, the upgoing and downcoming portions of the propagation path are not symmetrical. A vertical through the apex of the actual path does not in general bisect or even intersect the line joining the points where the

wave packet enters and leaves the ionosphere. However, the direction of the motion of a wave packet forms the same angle with respect to a downwardly directed vertical after leaving the ionosphere as is formed with an upwardly directed vertical prior to entering the ionosphere. After leaving the ionosphere, the wave packet moves in a vertical plane which is parallel to, although in general not coincident with, the original plane of incidence. This means that the two propagation paths, directed in opposite directions over the transmission link, are not coincident with one another since they are laterally displaced in space at the path mid-point. The physical structure of the ionosphere is known to contain irregularities or blobs in which the ionization level may be quite different from the adjacent or surrounding regions, a fact which in itself produces varying degrees of non-reciprocal two-way transmissions. It is also known that disturbances or large irregularities in the structure of the ionosphere move or advance laterally under the influence of the currents existing in the various ionospheric regions. These currents may also cause a transport in the sense that the levels of ionizations produced by the disturbances may tend to move upward in the ionosphere. It is therefore apparent that the lateral deviation of the wave packet during its stay in the ionosphere is one of the factors which must be examined in terms of its effect upon periods of non-reciprocal transmission.

Computation of the Lateral Deviation Curves

Identical rhombic antennas were utilized at both the Fairburn and Ipswich test stations. The antennas had fan shaped patterns approximately 10 degrees in width in a horizontal plane and 20 degrees in width in a vertical plane. Both beam width measurements were referenced to the half

power points of the antenna patterns. The axis of the Fairburn antenna pointed approximately 45 degrees east of the horizontal component of magnetic north and the axis of the Ipswich antenna pointed approximately 135 degrees southwest of the horizontal component of magnetic north. Assuming the earth to be a perfect sphere, the axes of both antennas pointed approximately 69 degrees to a midpoint vertical reference line.

A number of conditions will now be investigated to provide a means of determining ways in which the variations in the composition of the ionosphere contributed to the periods of non-reciprocal transmission. The first condition which must be established is the correlation of the q, α relationships for transmission from Fairburn to Ipswich and from Ipswich to Fairburn. Figure 24 shows a comparison of these curves for the two different directions of propagation for the extraordinary wave. The curves were computed assuming an angle of incidence θ equal tc 69 degrees and a magnetic field strength of 5.74×10^{-5} webers per square meter at a dip angle of 70 degrees for the earth's magnetic field $\underline{B}_o$. This value for $\underline{B}_o$ compares favorably with the value specified for the E-region at Cheltenham, Maryland (33) a location which is displaced slightly northeast from the midpoint of the transmission link. In Figure 24 the solid curve represents wave propagation from Fairburn to Ipswich while the dashed curve represents wave propagation from Ipswich to Fairburn. A careful comparison of the two curves reveals that they are the mirror images of one another. It may also be shown that the similar curves for the ordinary wave are mirror images of one another for the two directions of propagation. In view of the relationship existing for the two pairs of curves, only a single propagation direction (Fairburn to Ipswich) has

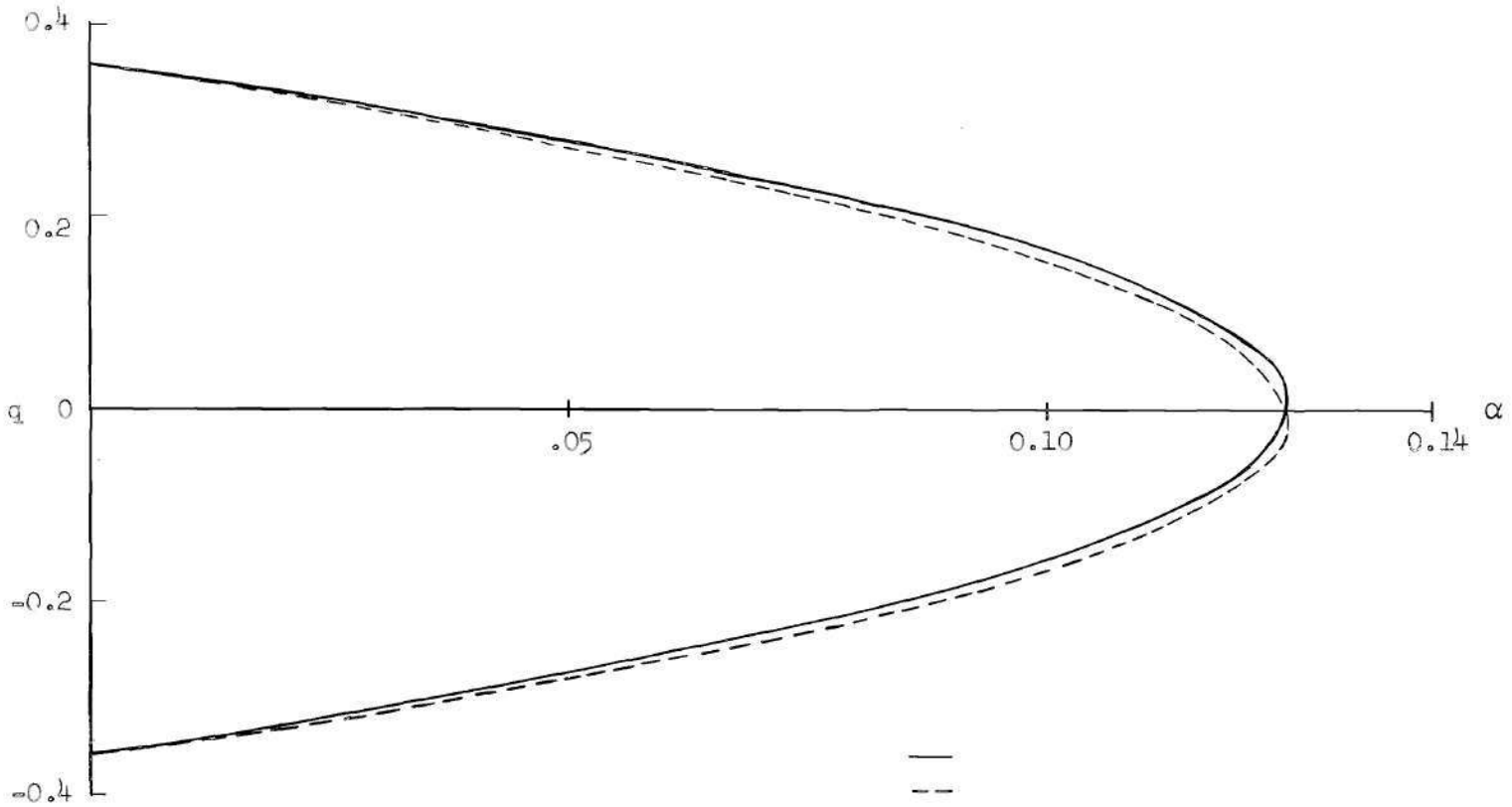

Figure 24. Comparison of the q,α Curves for Opposite Directions of Propagation.

been utilized in the following computations.

One propagation condition of interest is a comparison of the Fairburn-Ipswich transmission link with the special cases of transverse and longitudinal propagation. Figure 25 contains a plot of the q, α curves (Figure 4, p. 25) for these two special cases and the Fairburn-Ipswich link. The curves were computed for the same conditions as for Figure 24, that is an angle of incidence equal to 69 degrees and a magnetic field strength of 5.74×10^{-5} webers per square meter at a dip angle of 70 degrees. The figure shows that both the upgoing ordinary and extra-ordinary waves closely approximate the special case of transverse propagation for values of α up to approximately 0.10. The maximum deviation between the transmission link and the transverse curves occurs at the points of reflection of the two waves (R_1 for the extra-ordinary wave and R_2 for the ordinary wave). It is obvious that the experimental case, even at the points of maximum deviation, tends to approximate the transverse case over the entire range of values of q and α; a condition which is to be expected in view of the large angle of incidence and magnetic dip angle.

In view of the preceding conclusions, it is to be anticipated that rays representing transmitted and received wave packets which emanate and terminate over the entire horizontal antenna beam width would be reflected at approximately the same heights and experience approximately the same lateral deviations on both their upgoing and downcoming paths. In order to compute the lateral deviation of a particular wave packet as a function of height, it is necessary to compute the N(h) profiles for the corresponding periods of signal transmission and reception. Unfortunately

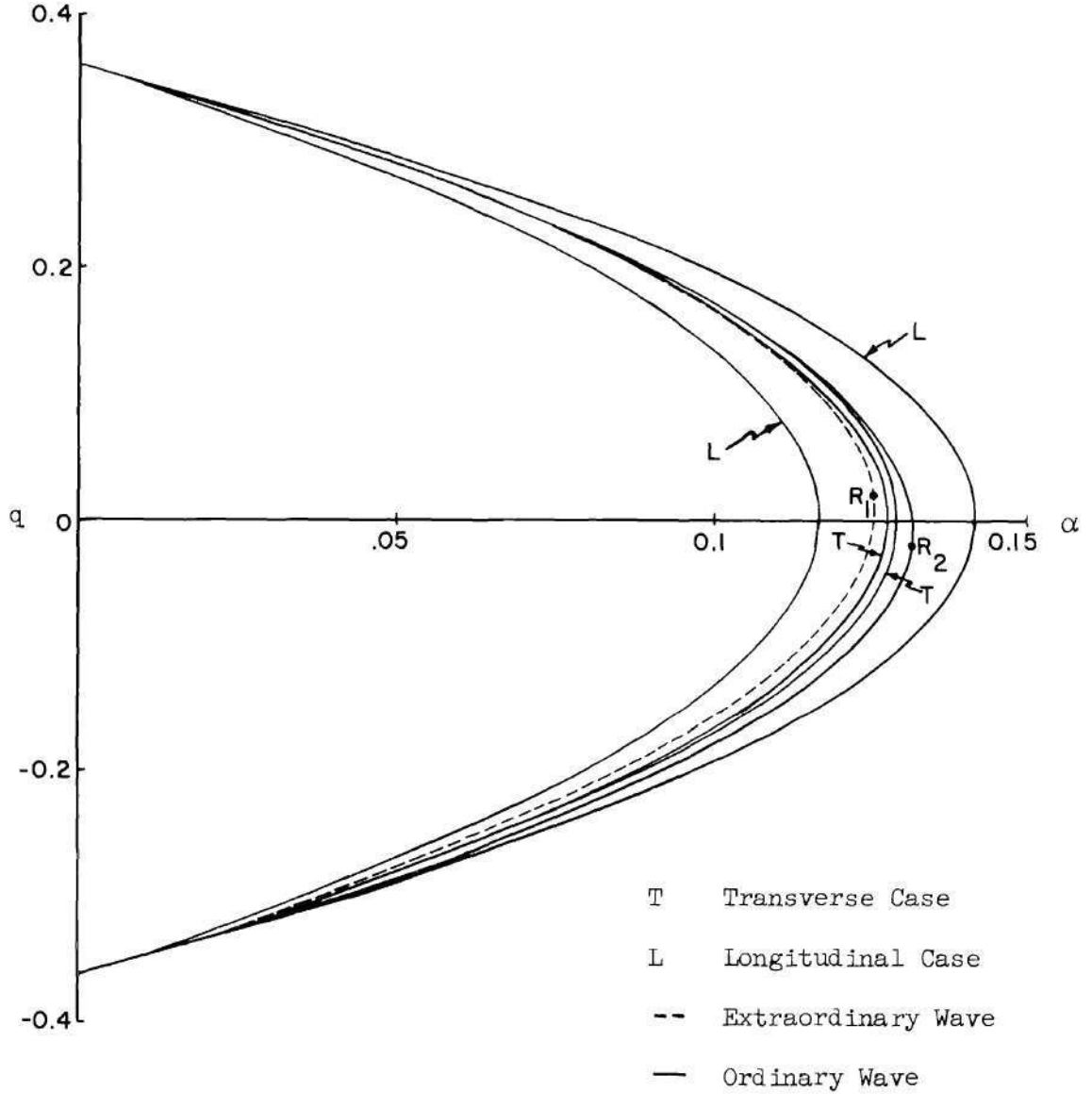

Figure 25. Comparison of the Fairburn-Ipswich Link with the Transverse and the Longitudinal Modes of Propagation.

the experimental ionograms, which would have provided the basis for the computation of the N(h) profiles, were not available to the author. However a computation of the rate of change of the lateral deviation of the wave packet per unit change in height provides the desired information and these computations may be made without the use of the experimental ionograms. Figures 26 and 27 show a comparison of the computed q, α and dx/dz, α curves for a fixed angle of incidence of 69 degrees and $\underline{B}_o$ equal to 5.74×10^{-5} webers per square meter at a dip angle of 70 degrees and three planes of incidence oriented 40, 45 and 50 degrees east of the horizontal component of $\underline{B}_o$. Since the y,z plane was chosen as the plane of incidence, the rate of change of x with respect to z represents the rate of change of the lateral deviation per unit change in the height of the wave packet perpendicular to the plane of incidence. Figures 26 and 27 confirm the fact that small horizontal variations in the plane of incidence relative to a fixed value of θ and $\underline{B}_o$ will result in negligible variations in the height at which the waves are reflected and in the lateral deviation experienced by the wave packet.

A detailed examination of Figure 27 reveals that the ordinary wave experiences a deviation toward magnetic north over the first portion of its upward propagation path ($0 < \alpha \leq .069$, $0.240 \leq q \leq 0.359$). When α reaches an approximate value of .069, the wave packet is traveling in a vertical plane parallel to, but not coincident with the original plane of incidence. On the remaining portion of the upgoing path, the wave packet experiences a lateral deviation away from magnetic north. After reflection the ordinary wave experiences a lateral deviation back towards magnetic north on its downward path to the base of the ionosphere.

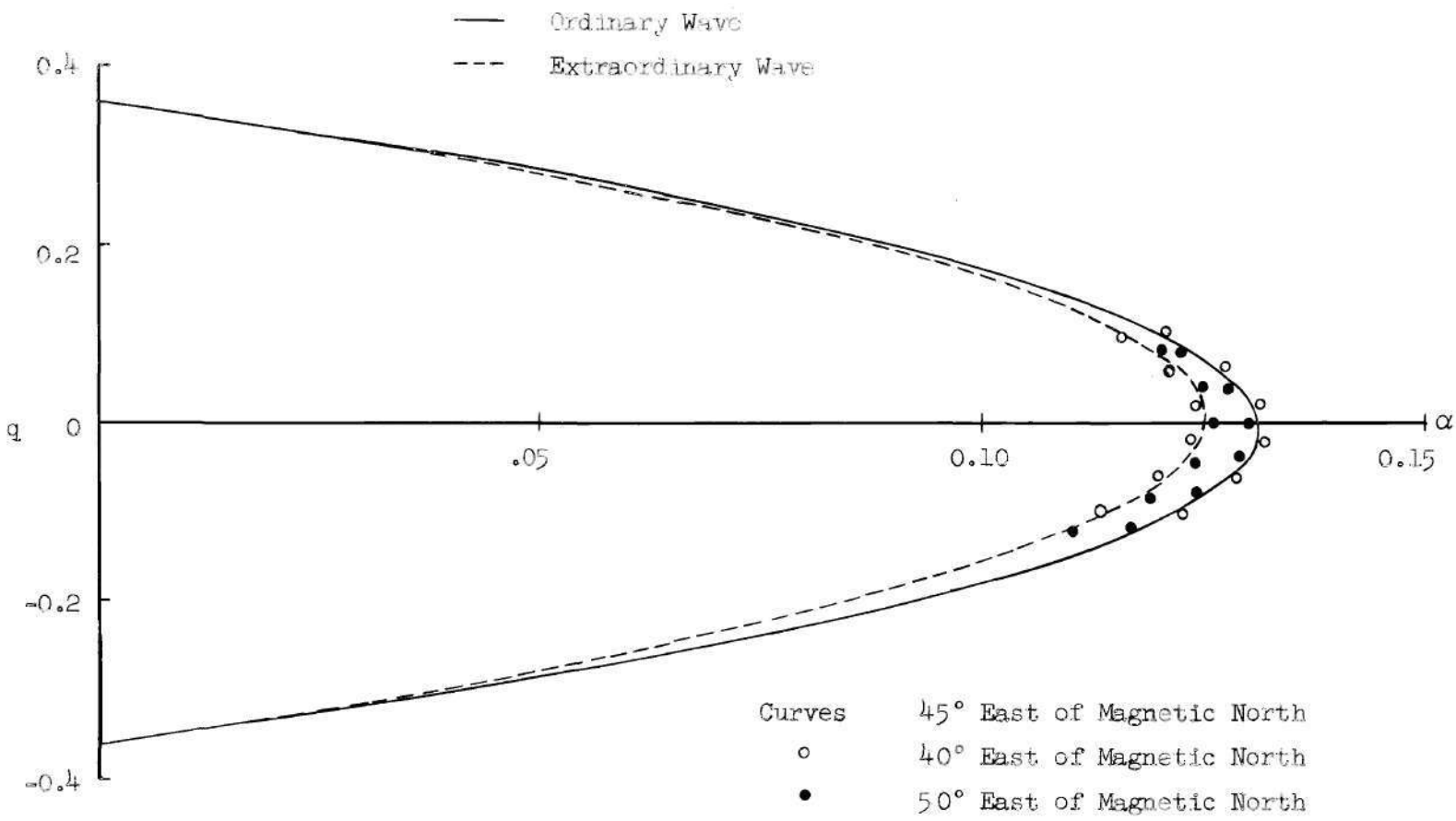

Figure 26. q,α Curves for θ_i Fixed and the Direction of Propagation Variable.

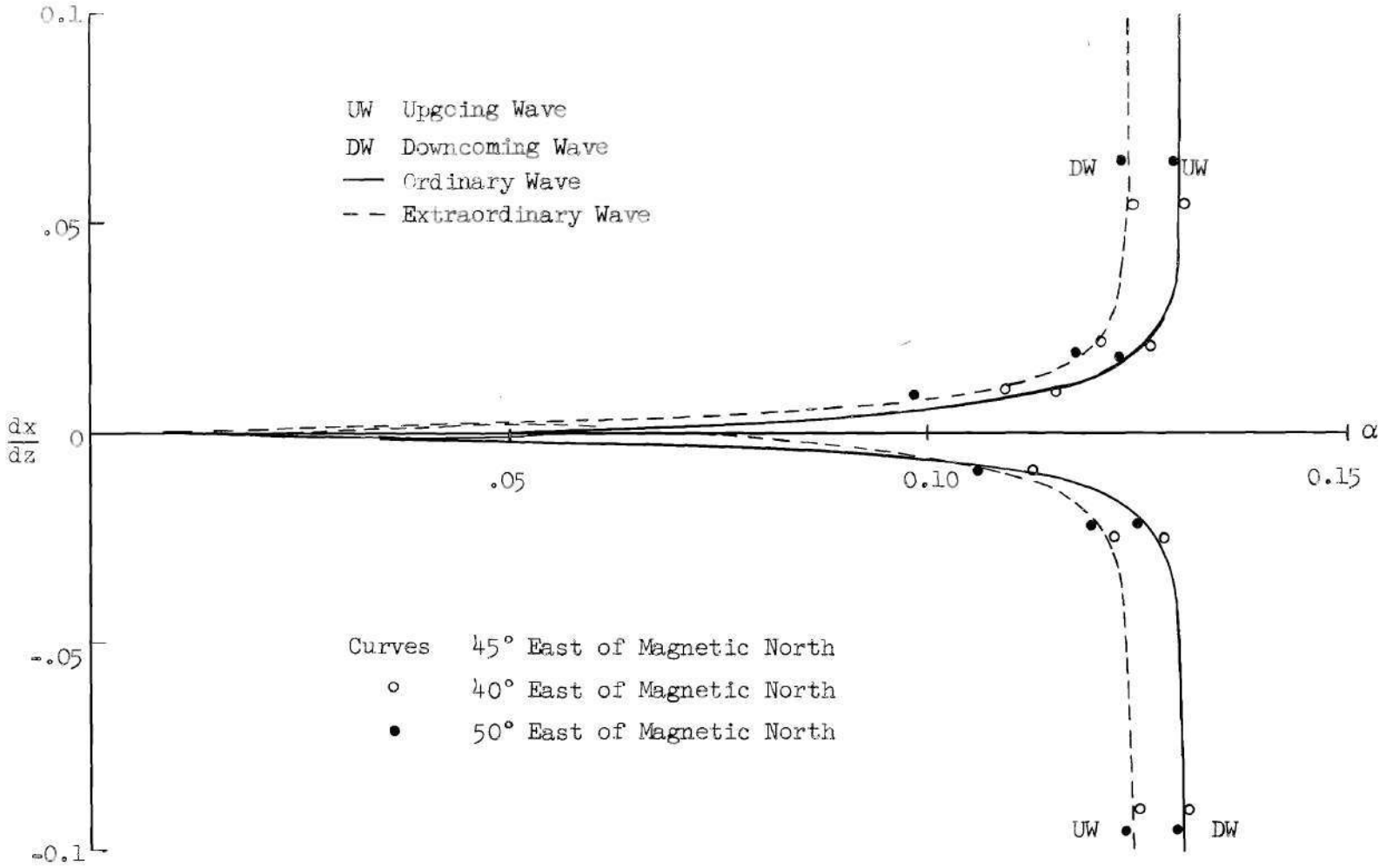

Figure 27. dx/dz, α Curves for θ_i Fixed and the Direction of Propagation Variable.

The extraordinary wave experiences a lateral deviation away from magnetic north on the first portion of its upward path ($0 \leq \alpha \leq .066$, $0.245 \leq q \leq 0.359$). At the point where α is approximately .066, the wave moves laterally toward magnetic north until it reaches the point of reflection. Lateral deviation away from magnetic north occurs over the entire downward path of the extra-ordinary wave.

The last of the propagation conditions to be considered is the case of the angle of incidence θ varying while the plane of incidence and $\underline{B}_o$ remain fixed. In Figures 28 and 29, the variation in the level of reflection and the rate of change of lateral deviation per unit change in height have been computed for $\underline{B}_o$ equal to 5.74×10^{-5} webers per square meter at a dip angle of 70 degrees, the plane of incidence oriented 45 degrees east of magnetic north and the angle of incidence θ_i equal to 59, 69 and 79 degrees respectively. These curves show that a large variation occurs in both the level of reflection and the rate of change of lateral deviation per unit change in height with a change in ray orientation from the upper to the lower sections of the vertical pattern of the antenna. Care must be exercised in an interpretation of these curves when comparing them to the transverse case of propagation. Computations show that the condition where θ_i is equal to 69 degrees more closely approximates the transverse case of propagation than either of the other two cases considered. The large change in the value of dx/dz experienced by the wave packet for the 59 and 79 degree cases is primarily due to the different heights of reflection and the different time periods associated with the wave's stay in the ionosphere. When θ_i equals 79 degrees, the wave packet enters the ionosphere with the ray vector $\underline{n}$

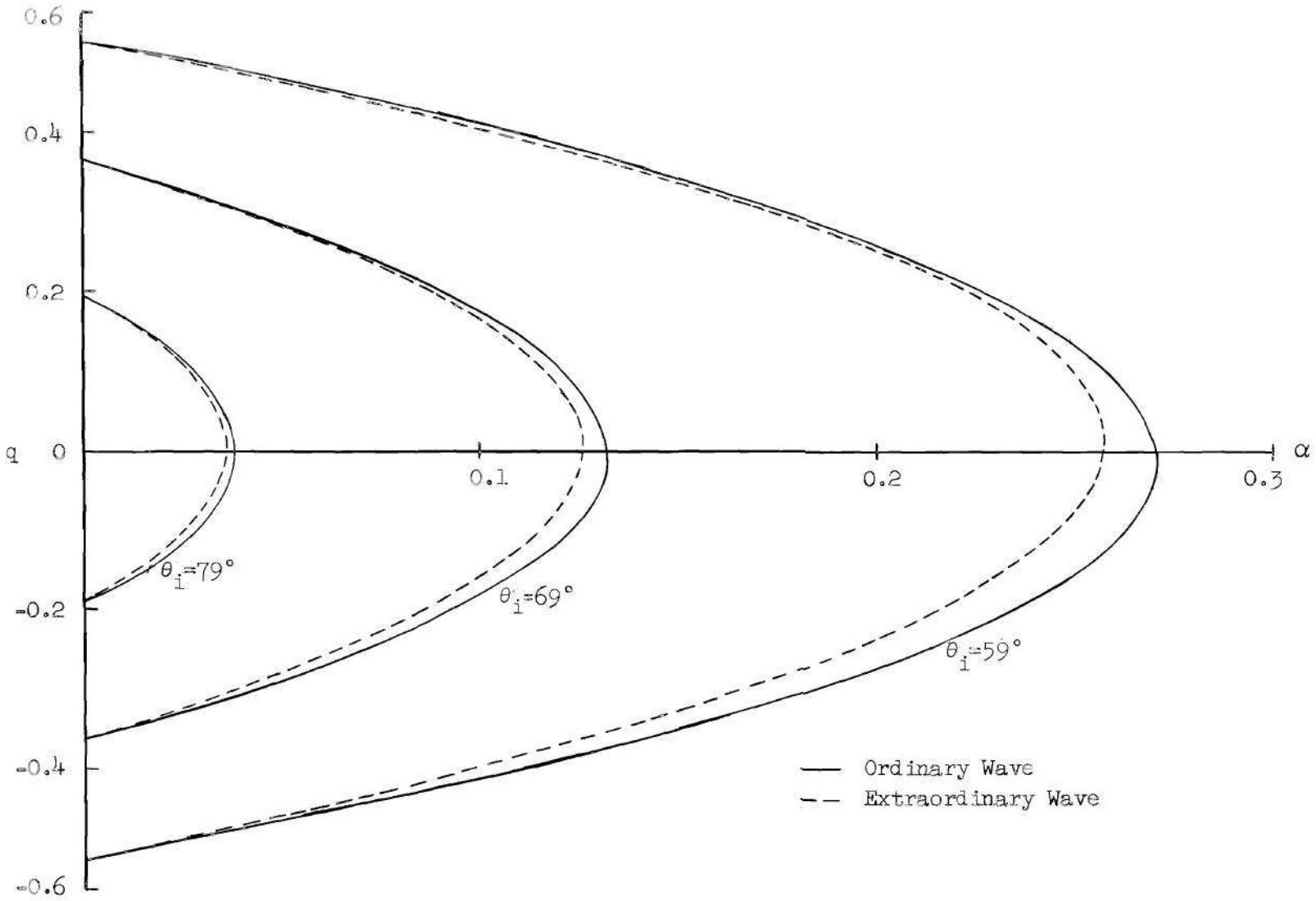

Figure 28. q,α Curves for θ_i Variable and the Direction of Propagation Fixed.

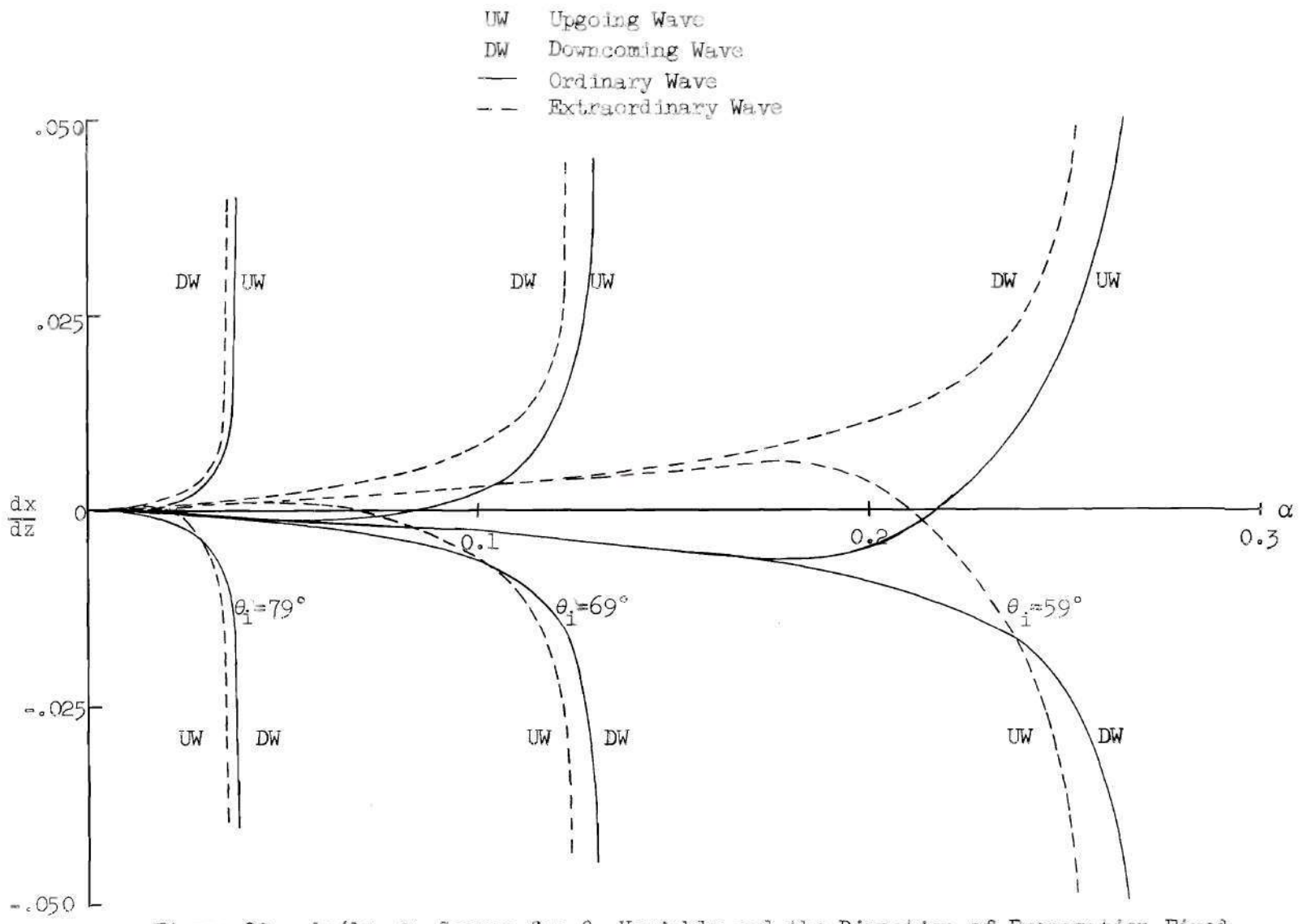

Figure 29. dx/dz, α Curves for θ_j Variable and the Direction of Propagation Fixed.

almost parallel to the lower boundary of the ionosphere (the vertical component of $\underline{n}$ is equal to 0.191 n) while $\underline{n}$ has a vertical component which is 0.515 n when θ = 59 degrees. It is apparent that the wave packet with the larger vertical component of $\underline{n}$ will stay in the ionosphere for the longer period, thereby attaining a greater height prior to reflection and subsequently experiencing a greater lateral deviation.

Factors Contributing to Non-Reciprocal Transmission

On the basis of the preceding computations and observations, it is now possible to interpret the effect of the variations in the composition of the ionosphere in terms of their contributions to the periods of non-reciprocal transmission. As noted earlier in this section, the levels of ionization in the ionosphere experiences a transport in both the horizontal and vertical directions. If this condition occurs during a given test run, relative reciprocity will exist whenever the changes are uniform in the sense that the wave packets traveling in opposite directions experience the relative change in the ionization along their respective paths during the same instant of time. This would be true whether the transport occurs in a horizontal or vertical direction. Complete reciprocity, as defined earlier in this study, would not exist during these periods since a comparison of the ray paths during the transport period shows ray orientations located at various points of the antenna patterns, thereby producing variations in the overall transmission link gain. This condition further enhances the utilization of the relative reciprocity theorem as an aid in interpreting experimental reciprocity data. A second type of ionospheric irregularity which may occur is the appearance of a sharp variation in adjacent levels of ionization. If the wave packet

traveling in one direction encounters this disturbance as it enters the ionosphere and the wave traveling in the opposite direction does not, the height of reflection and the lateral deviation experienced by the two waves will be quite different thereby producing non-reciprocal transmission.

At times the lower boundary of the ionosphere may be tilted. If tilt of the lower boundary lies in a plane perpendicular to the transmission paths of both waves, Figures 26 and 27 show that each of the oppositely traveling waves would experience very little change in either their height of reflection or lateral deviation. Therefore this condition would still produce reasonably reciprocal signal transmission when considered in terms of relative reciprocity. If the tilt of the lower boundary of the ionosphere lies in a plane parallel to the transmission paths of both waves, Figures 28 and 29 indicate that both waves would experience appreciable changes in their height of reflection and lateral deviation during their stay in the ionosphere. This condition would in general produce non-reciprocal transmission.

Figures 28 and 29 may also be utilized to offer an explanation of another phenomenon observed in the time plots of the experimental data (Figures 13, 15, 17, 19, 21 and 23). These figures indicate an almost periodic variation in the amplitudes of the received signals which could occur in the following manner. Recognizing that the E-region of the ionosphere does not present a smooth lower boundary to the incident waves and further that the irregularities in this boundary tend to be transported horizontally, the incident waves impinge on a boundary which is slowly varying in height. If the transport conditions are such that waves

traveling in opposite directions experience the same boundary height variations, the angle of incidence will vary producing continuous changes in the heights of reflection and the lateral deviations of the waves which are in time phase with the corresponding variations in the boundary height. These changes in the wave's angle of incidence at the boundary correspond to signal transmissions and receptions over different sections of the antenna's vertical pattern. This condition produces time variations in the overall gain of the transmission link which are in time phase with the changes in boundary height. During these periods relative reciprocity will exist. If the transport occurs so that the waves traveling in opposite directions encounter a different boundary height, non-reciprocal transmission will occur.

A further examination of the q, α curves reveals that the extraordinary wave is reflected at a lower height than the ordinary wave for the E-region. This condition will exist whenever the N(h) profiles vary smoothly from a minimum to a maximum value of ionization. If the layer under consideration has a sharp discontinuity in the ionization level of its lower boundary and the minimum value at the discontinuity exceeds the value of α required at the lower level of extraordinary wave reflection, the ordinary wave may be reflected at the lower height and the extraordinary wave at a higher value of α (see Figure 4, p. 25).

CHAPTER VIII

CONCLUSIONS AND RECOMMENDATIONS

Prior to a presentation of the conclusions which evolved from the present study, a brief summary of the work performed is presented in the succeeding paragraphs. Reciprocity has been defined in a relative sense which is applicable to the case of oblique reflections of electromagnetic waves from the ionosphere. This definition has been stated in the form of a relative reciprocity theorem and represents a theoretical extension of Goubau's reciprocal antenna theorem. Theoretical test specifications have been formulated to provide a sound basis for future reciprocity tests. Some available experimental reciprocity data has been reduced in light of the relative reciprocity theorem and the theoretical test specifications. The results of this analysis confirm the validity and practicality of the theorem.

The ray approximation for the magneto-ionic wave equations was solved on a high speed digital computer. These solutions provided a basis for an interpretation of the effects of ionospheric irregularities on the non-reciprocal, simultaneous, two-way transmission and reception of electromagnetic waves obliquely incident upon the ionosphere. In addition these calculations pointed up the important role played by the transmitting and receiving antennas in any practical interpretation of experimental reciprocity data. This fact in itself further enhances the utilization of the relative reciprocity theorem as an aid in the interpretation of experimental reciprocity data.

Conclusions

The conclusions which evolved from the present study are:

1. The mathematical validity and practical application of "the relative reciprocity theorem" have been established. This theorem provides a method for cataloging and comparing experimental propagation data in terms of reciprocal or non-reciprocal transmission characteristics.

2. Test procedures have been formulated which define one optimum technique for obtaining valid experimental relative reciprocity data.

3. Non-reciprocal effects of the lateral deviation of wave packets transmitted over an experimental two-way propagation link (Fairburn-Ipswich link) have been established for the one-hop E-region mode of propagation.

Recommendations

Although beyond the scope of the present study, two extensions of the general reciprocity problem present merit insofar as future studies are concerned.

1. The possibilities of utilizing a photo-reader in conjunction with a digital computer to compute the time weighing factor T_W from the original photographs of the experimental reciprocity data should be investigated. Such a program would minimize the labor presently involved in reducing the experimental data.

2. An investigation involving the prediction of reciprocal or non-reciprocal propagation characteristics for a number of different transmission link orientations and conditions via digital computer solutions of Booker's equations could be conducted. A tabulation of the

results of this investigation would aid in the refinement of experimental test procedures prior to actual tests, thereby insuring the production of the best possible reciprocity test data.

APPENDIX

ELECTRON DENSITY PROFILES

Chapman (42) and (43) made an important contribution to the problem of ionospheric reflections by deriving a law for the variation of electron density N with height. The general theory of the formation of the ionosphere has been refined and extended by Chapman and others. Only an introductory version of the Chapman theory is presented in the following discussion.

The air density δ at a height z above the earth's surface may be expressed as

$$\delta = \delta_o \exp(-z/H) \tag{57}$$

if the earth's atmosphere is assumed to be constant in composition and at a constant temperature. In equation (57) δ_o is the density of the air at ground level and

$$H = RT/Mg \tag{58}$$

where R is the gas constant, M is the mean molecular weight, T is the absolute temperature and g is the gravitational acceleration which is assumed to be constant. H is in effect a scale height for the atmosphere and is approximately 10 kilometers at the surface of the earth.

Consider a beam of monochromatic radiation from the sun passing through the atmospheric layers at an angle of inclination χ referenced to the zenith. Let the flux of energy in the incident radiation outside

the earth's atmosphere be W_o. The energy flux W decreases as the beams penetrate the atmosphere. This decrease may be written in differential form as

$$dW = \left[W \tau \delta \sec \chi\right] dz \tag{59}$$

where W is the energy flux at the height z and τ is the mass absorption coefficient of the air for the radiation. Substitution of equation (57) into (59) yields after integration

$$W = W_o \exp\left[- \tau \delta_o H \exp(-z/H) \sec \chi\right] . \tag{60}$$

Equation (60) may be simplified by defining

$$z_o = H \log(\tau \delta_o H) . \tag{61}$$

With this substitution, equation (60) becomes

$$W = W_o \exp\left\{- \sec \chi \exp\left[-(z - z_o)/H\right]\right\} . \tag{62}$$

Assuming that the rate of production of electrons P is proportional to the rate of absorption of radiation per unit volume and noting that the rate of absorption of energy at a height z is given by $\cos \chi \, (dW/dz)$, we may express P as

$$P = P_o \exp\left\{\left[(z_o - z)/H\right] - \sec \chi \exp\left[(z_o - z)/H\right]\right\} . \tag{63}$$

The maximum rate of production of electrons for an arbitrary angle of incidence of the sun's rays is $(P_o \cos \chi)/2.718$ and occurs when $z = z_o - H \log(\cos \chi)$. This function yields an absolute maximum for P when $\chi = 0$ (the sun is directly overhead).

The electron removal process is very complex in the practical case, but the overall effect of such removals is the same as the case where all of the electrons simply recombine with positive ions. Denoting the density of both electrons and positive ions per unit volume as N (this assumes an equal number of each), the rate of removal of electrons is a function of a recombination coefficient Γ. The variation of N with time may now be expressed as

$$dN/dt = P - \Gamma N^2 . \qquad (64)$$

Whenever Γ is very large, dN/dt may be neglected in comparison with the term ΓN^2. For this case the process of formation and removal of electrons arrives at an equilibrium condition in a negligibly small time giving as a first approximation

$$N = (P/\Gamma)^{1/2} . \qquad (65)$$

If the layer involved experiences a removal of electrons by attachment, equation (65) may or may not be a good approximation to the actual conditions existing in the layer.

Assuming the recombination coefficient Γ is independent of height, a simultaneous solution of equations (63) and (65) yields

$$N = N_o \exp 1/2 \left\{ \left[(z_o - z)/H\right] - \sec \chi \exp \left[(z_o - z)/H\right] \right\} . \qquad (66)$$

N has a maximum value of $0.607\ N_o (\cos \chi)^{1/2}$ at the level where $z_m = z_o + H \log (\sec \chi)$. Equation (66) presents a simplified picture of the process of the formation and the removal of electrons in the ionosphere. Electron density profiles based upon equation (66) are called "Chapman

profiles." Figure 30 illustrates the general shape of the N(h) profiles where χ is a parameter. In order to simplify the computations of the profiles, a normalized electron density (N/N_o) and height $(z_o - z)/H$ were chosen as the abcissa and ordinate of the family of curves.

The lower regions of the profiles may be approximated by a linear function if a small interval of z is selected. Near the maximum value of N the linear approximation is no longer valid even for small intervals of z. However in this region the profile may be approximated by a parabolic function such as

$$N = N_m \left[1 - (z - z_m)^2/h_a^2\right] \text{ for } |z - z_m| \leq h_a \text{ and} \qquad (67)$$

$$N = 0 \text{ for } |z - z_m| \geq h_a .$$

In equation (67) the quantity h_a is the half thickness of the ionospheric layer and z_m is the value of z for which N_m occurs.

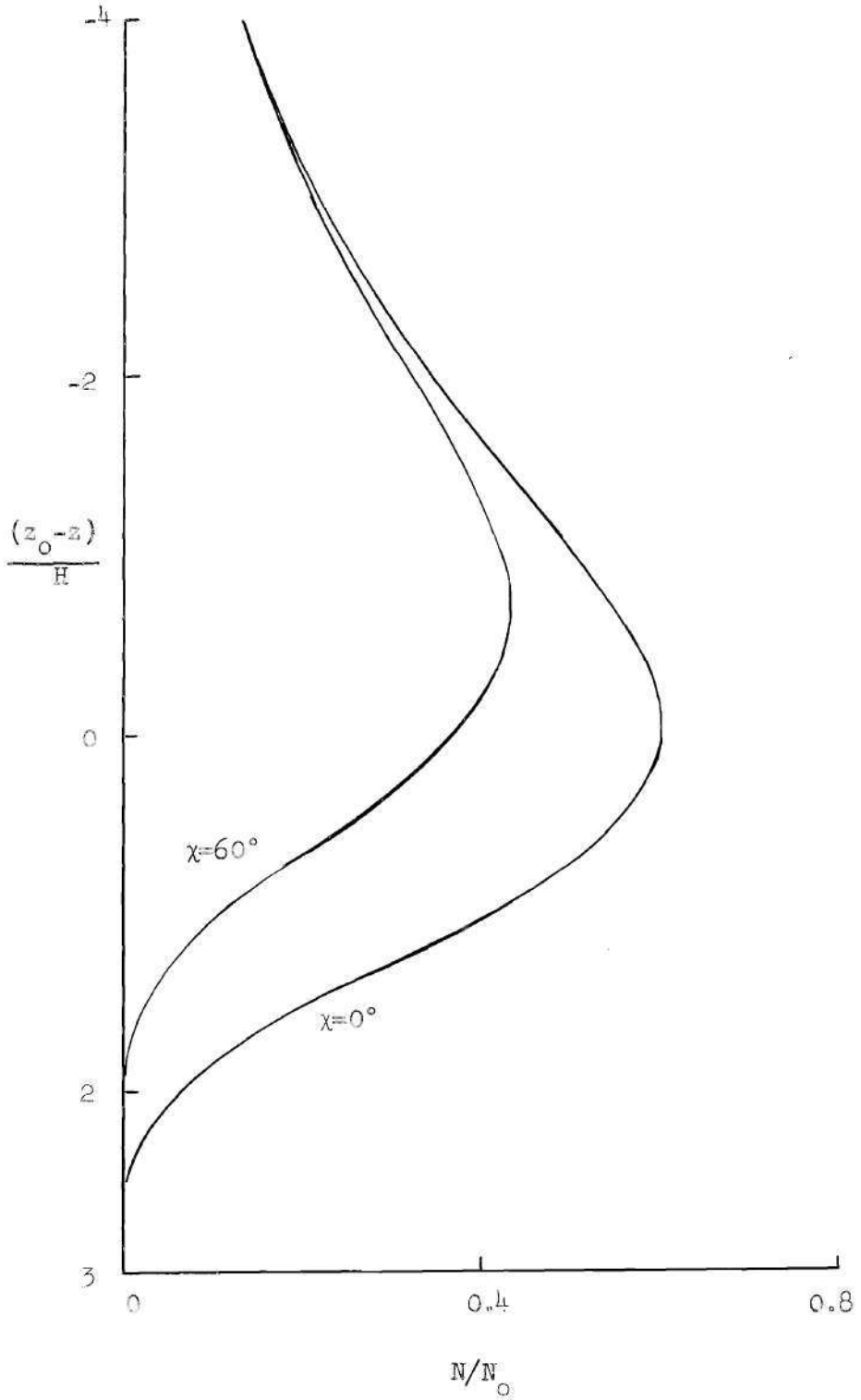

Figure 30. Chapman N(h) Profiles.

BIBLIOGRAPHY

1. Eccles, W. H., "On the Diurnal Variation of the Electric Waves Occurring in Nature, and on the Propagation of Electric Waves Round the Bend of the Earth," Proceedings of the Royal Society A, Vol. 87, 1912, p. 79.

2. Larmor, J., "Why Wireless Electric Rays Can Bend Round the Earth," Philosophical Magazine, Vol. 48, 1924, p. 1025.

3. Appleton, E. V., "Wireless Studios of the Ionosphere," Journal of the Institute of Electrical Engineers, Vol. 71, 1932, p. 642.

4. Mitra, A. P., The Upper Atmosphere, Calcutta, India, The Asiatic Society, 1952.

5. Budden, K. G., Radio Waves in the Ionosphere, Cambridge, England, The University Press, 1961.

6. Gregory, J. B., "Ionospheric Reflections from Heights Below the E-Region," Australian Journal of Physics, Vol. 9, 1956, pp. 324-342.

7. Thomas J. A. and Smith, E. K., "A Survey of the Present Knowledge of Sporadic-E Ionization," Journal of Atmospheric and Terrestrial Physics, Vol. 13-14, 1958-59, pp. 295-303.

8. Appleton, E. V., "The Normal E Region of the Ionosphere," Proceedings of the Institute of Radio Engineers, Vol. 47, 1959, p. 156.

9. Bates, D. R. and Massey, H. S. W., "The Basic Reactions in the Upper Atmosphere. Part 2 - The Theory of Recombination in the Ionized Layers," Proceedings of the Royal Society, Vol. 192, 1947, pp. 1-16.

10. Martyn, D. F., "The Normal F Region of the Ionosphere," Proceedings of the Institute of Radio Engineers, Vol. 47, 1959, p. 156.

11. Jackson, J. E. and Seddon, J. C., "Ionosphere Electron Density Measurements with the Navy Aerobee-Hi Rocket," Journal of Geophysical Research, Vol. 63, 1958, pp. 197-208.

12. Martyn, D. F., "Atmospheric Tides in the Ionosphere: Part 3 - Lunar Tidal Variations at Canberra," Proceedings of the Royal Society A, Vol. 194, 1948, pp. 429-444.

13. Allis, W. P. and Buchsbaum, S., "Unpublished Notes - Massachusetts Institute of Technology Summer Program on Plasma Dynamics," Massachusetts Institute of Technology, 1959.

14. Sitenko, A. F. and Stepanov, K. N., "On the Oscillations of an Electron Plasma in a Magnetic Field," Soviet Physics JETP, Vol. 4, 1957, pp. 512-520.

15. Booker, H. F., "Propagation of Wave-Packets Incident Obliquely Upon a Stratified Doubly Refracting Ionosphere," Philosophical Transactions of the Royal Society A, Vol. 237, 1938-39, pp. 411-451.

16. Booker, H. F., "Application of the Magneto-ionic Theory to Radio Waves Incident Obliquely Upon a Horizontally-Stratified Ionosphere," Journal of Geophysical Research, Vol. 54, 1949, pp. 243-274.

17. Allis, W. P., "Propagation of Waves in a Plasma in a Magnetic Field," Institute of Radio Engineers Transactions on Microwave Theory and Techniques, Vol. MTT-9 No. 1, January, 1961, pp. 79-82.

18. Carson, J. R., "A Generalization of the Reciprocal Theorem," Bell System Technical Journal, Vol. 3, 1924, pp. 393-399.

19. Strutt, J. W. and Baron Rayleigh, Theory of Sound (Second Edition), Vol. 1, London: Macmillan and Co., Ltd., 1929, p. 155.

20. Sommerfeld, A., "Das Reziprozitats-Theorem der drahtlosen Telegraphie," Jahrbuch drahtlosen Telegraphie, Vol. 26, 1925, p. 93.

21. Goubau, G., "Reziprozitat der Wellenausbreitung durch Magnetisch doppelbrechende Medien," Hochfrequenz Technic und Elektroakustik, Vol. 59-60, 1942, pp. 155-160.

22. Budden, K. G., "A Reciprocity Theorem on the Propagation of Radio Waves via the Ionosphere," Proceedings of the Cambridge Philosophical Society, Vol. 50, 1954, p. 611.

23. Moller, H. G., "Further Results of Sweep Frequency Oblique Incidence Experiments," Journal of Atmospheric and Terrestrial Physics, Vol. 13-14, 1958-59, p. 173.

24. Meadows, R. W., "An Experiment to Test the Reciprocal Radio Transmission Conditions over an Ionospheric Path of 740 Kilometers," Proceedings of the Institution of Electrical Engineers, Vol. 103, Part B, 1956, p. 224.

25. Falcon, G. D., An Investigation of Non-Reciprocity in Oblique Incidence Ionospheric Radio Propagation, Master's Thesis, Georgia Institute of Technology, 1960, pp. 37-43.

26. Hartke, D., "A New Clock for Improving the Accuracy of Local Frequency and Time Standards, Hewlett-Packard Journal, Vol. 11, No. 3-4, Nov. - Dec., 1959.

27. Morgan, A. H., "Precise Time Synchronization of Widely Separated Clock," National Bureau of Standards Boulder Laboratories Technical Note, No. 22, July, 1959.

28. "Granger Associates Model 902 Series Step-Frequency Ionosphere Sounder," Granger Associates Technical Bulletin, November, 1960.

29. Breit, G. and Tuve, M. A., "A Test of the Existence of the Conducting Layer," Physical Review, Vol. 28, 1926, p. 554.

30. Martyn, D. F., "Propagation of Medium Radio Waves in the Ionosphere," Proceedings of the Physical Society, Vol. 47, 1935, p. 332.

31. Appleton, E. V. and Beynon, W. J. G., "The Application of Ionospheric Data for Radio Communication Problems: Part 1," Proceedings of the Physical Society, Vol. 52, 1940, p. 518.

32. Appleton E. V. and Beynon, W. J. G., "The Application of Ionospheric Data for Radio Communication Problems: Part 2," Proceedings of the Physical Society, Vol. 59, 1947, p. 58.

33. Brown, J. N. "Automatic Sweep-Frequency Ionosphere Recorder, Model C-4," Proceedings of the Institute of Radio Engineers, Vol. 47, No. 2 1959, pp. 296-300.

34. Beynon, W. J. G. and Thomas, J. O., "The Calculations of the True Heights of Reflection of Radio Waves in the Ionosphere," Journal of Atmospheric and Terrestrial Physics, Vol. 9, 1956, p. 184.

35. Becker, W., "New Methods and Some Results Concerning True Ionospheric Height Calculations," Journal of Atmospheric and Terrestrial Physics, Vol. 16, 1959, p. 67.

36. Kelso, J. M., "A Procedure for the Determination of the Vertical Distribution of the Electron Density in the Ionosphere," Journal of Geophysical Research, Vol. 57, 1952, p. 357.

37. Kelso, J. M., "The Determination of the Electron Density Distribution of an Ionospheric Layer in the Presence of an External Magnetic Field," Journal of Atmospheric and Terrestrial Physics, Vol. 5, 1954, p. 11.

38. Kelso, J. M., "The Calculation of Ionospheric Electron Density Distributions," Journal of Atmospheric and Terrestrial Physics, Vol. 10, 1957, p. 103.

39. Titheridge, J. E., "The Calculation of Real and Virtual Heights of Reflection in the Ionosphere," Journal of Atmospheric and Terrestrial Physics, Vol. 17, 1959, p. 96.

40. Scarborough, J. B. and Wagner, R. W., Fundamentals of Statistics, Ginn and Company, 1948, p. 39.

41. Chambers, T. H. and Page, I. H., "The High-Accuracy Logarithmic Receiver," Proceedings of the Institute of Radio Engineers, Vol. 42, 1954, p. 1314.

42. Chapman, S., "The Production of Ionization by Monochromatic Radiation Incident Upon a Rotating Atmosphere," Proceedings of the Physical Society, Vol. 43, 1931, p. 26 and p. 483.

43. Chapman, S., "The Atmospheric Height Distribution of Band Absorbed Solar Radiation," Proceedings of the Physical Society, Vol. 51, 1939, p. 93.

VITA

Thomas Dewey Shockley, Jr. was born November 2, 1923 in Haynesville, Louisiana. He attended public schools in Haynesville and graduated from Haynesville High School in 1940. Mr. Shockley attended Northwestern State Teachers College, The College of William and Mary, and Louisiana State University. He received the BSEE degree in 1950 and the MSEE degree in 1952 from Louisiana State University.

Mr. Shockley served in the United States Army from 1942 to 1946 in both the American and European Theaters of Operation. He was released from active duty with the rank of Second Lieutenant, Infantry, in 1946. From 1950 through 1953 he served as a member of the engineering faculty at Louisiana State University. His industrial experience includes aircraft and missile work at Chance Vaught Aircraft Corporation, 1952 and Convair, 1953 to 1956. From 1956 to 1958 he was employed as a Research Engineer by the Engineer Experiment Station, Georgia Institute of Technology. In 1958 he accepted a position as an Assistant Professor of Electrical Engineering, Georgia Institute of Technology, a position he holds at the present time.

He is a member of the Sigma Pi Sigma national honorary physics fraternity, of the Pi Mu Epsilon national honorary mathematics fraternity, and the Institute of Electrical and Electronics Engineers. He is married to the former Willie Belle Austin of Baton Rouge, Louisiana, and has two daughters.